

**STUDY OF THE INFLUENCE OF SEA SURFACE TEMPERATURE ON
TROPICAL CYCLONE FORMED IN THE BAY OF BENGAL DURING
1981 – 2007 AD**

MASTER OF PHILOSOPHY IN PHYSICS

MD. REZAUL KARIM KHAN



**DEPARTMENT OF PHYSICS
BANGLADESH UNIVERSITY OF ENGINEERING AND TECHNOLOGY,
DHAKA-1000, BANGLADESH
December' 2010.**

**STUDY OF THE INFLUENCE OF SEA SURFACE TEMPERATURE ON
TROPICAL CYCLONE FORMED IN THE BAY OF BENGAL DURING
1981 – 2007 AD**

**A Dissertation Submitted to the Department of Physics
Bangladesh University of Engineering and Technology, Dhaka,
in Partial Fulfillment for the Requirement of the Degree of
Master of Philosophy in Physics**

Submitted by

Md. Rezaul Karim Khan

Roll No. 040514009P

MASTER OF PHILOSOPHY IN PHYSICS



**Department of Physics
BANGLADESH UNIVERSITY OF ENGINEERING AND TECHNOLOGY,
DHAKA -1000, BANGLADESH
December' 2010**

Bangladesh University of Engineering and Technology
Department of Physics



CERTIFICATION OF THESIS

The the sis title d “**Study the influence of sea surface temperature on tropical cyclone formed in the Bay of Bengal during 1981-2007 AD**” Submitted by **Md. Rezaul Karim Khan**, Roll No. 040514009P, Session: April 2005 has been accepted as satisfactory in partial fulfillment of the requirement for the degree of **Master of Philosophy (M. Phil.)** in Physics on 04 December, 2010.

BOARD OF EXAMINERS

1. _____
Dr. Md. Rafi Uddin (Supervisor) Chairman
Assistant Professor
Department of Physics, BUET, Dhaka
2. _____
Dr. A. K. M. Akther Hossain (Ex-officio) Member
Professor and Head
Department of Physics, BUET, Dhaka
3. _____
Mrs. Fahima Khanam Member
Associate Professor
Department of Physics, BUET, Dhaka
4. _____
Dr. Md. Forhad Mina Member
Assistant Professor
Department of Physics, BUET, Dhaka
5. _____
Dr. Md. Mahbub Alam Member (External)
Professor
Department of Physics
Khulna University of Engineering
and Technology, Khulna

DECLARATION

It is hereby declared that this thesis or any part of it has not been submitted elsewhere for the award of any degree or diploma.

Signature of the Candidate

Md. Rezaul Karim Khan
Candidate
Roll No. 040514009P
Session: April 2005

Table of Contents

Contents	Pages
List of Tables	viii
List of Figures	ix
Abstract	xiii
Chapter One : Introduction	1-3
1.1 Prelude	1
1.2 Objectives of the Research	3
Chapter Two : Literature Review	4-24
2.1 Introduction	4
2.2 Cyclone Activity and SST	4
2.3 Sea Surface Temperature	9
Ocean Temperature profile	9
2.3.1 Sea Surface Temperature	9
2.3.2 Vertical Structure of SST	10
2.3.3 Sea Temperature with the Time and Space	11
2.3.4 Techniques for Measuring SST	12
2.3.5 Difficulties with Satellite based Absolute SST	14
2.3.6 Sea Surface Temperature Determination	14
2.4 Tropical Cyclone	16
Historical Overview	16
2.5 Cyclone Formation Areas	16

2.6	The Birth of a Cyclone	17
2.7	Rotation of a Cyclone	19
	2.7.1 Coriolis Effect	19
2.8	Cyclone Structure	22
	2.8.1 The Eye	22
	2.8.2 The Eyewall	22
	2.8.3 The Spiral Rainbands	23
2.9	Cyclone Size	23
2.10	Death of a Cyclone	23
Chapter Three	: Data and Methods	25-27
3.1	Data used and methodology	25
Chapter Four	: Results and Discussion	28-70
4.1	Categorization of Tropical Disturbances	28
4.2	Life Snatching Cyclones	28
4.3	Statistics on Seasonal SST and Cyclones	29
4.4	Distribution of Depressions	32
4.5	Distribution of Deep Depressions	33
4.6	Distribution of Cyclonic Storms	34
4.7	Distribution of Severe Cyclonic Storms	35
4.8	Distribution of Very Severe Cyclonic Storms and Super Cyclones	36
4.9	Distribution of Cyclones	37
4.10	Distribution of Disturbances	38
4.11	Monthly and Yearly Distributions of Tropical Disturbances and SST	39

4.12	Distribution of Monthly SST Anomalies and Cyclones	40
4.13	Trends of SST and Tropical Cyclone Frequency	42
4.14	Trends of SST and Tropical Cyclone Duration	46
4.15	SST and Tropical Cyclone Intensity	49
4.16	SST Profile in the Study Area	53
4.17	Comparison of Temporal SST and Contemporaneous SST	57
4.18	Observation of Weekly SST during Cyclone Formation	58
4.19	Probability of Intensification of disturbance and SST	61
4.20	Area of Powerful Cyclone Formation	66
4.21	Area of Longest Residence Time of Cyclones	68
Chapter Five	: Conclusions	71-72
References		73-80
List of Published/Submitted Papers		81

List of Tables

Table No.	Caption	Page
Table 4.1.	Classification of cyclone develops in the Bay of Bengal.	28
Table 4.2.	Statistics of fatalities due to cyclones in Bangladesh.	29
Table 4.3.	Various types of tropical cyclones formed in the four seasons within 1981 -2007, their total number, duration, seasonal mean SST and standard deviation of seasonal mean SST.	30
Table 4.4.	Monthly and annual occurrence number of depressions in the Bay of Bengal during 1981-2007.	32
Table 4.5.	Monthly and annual occurrence number of deep depressions in the Bay of Bengal during 1981-2007.	33
Table 4.6.	Monthly and annual occurrence number of cyclonic storms in the Bay of Bengal during 1981-2007.	34
Table 4.7.	Monthly and annual occurrence number of severe cyclonic storms in the Bay of Bengal during 1981-2007.	35
Table 4.8.	Monthly and annual occurrence number of very severe cyclonic storms and super cyclones in the Bay of Bengal during 1981 -2007.	36
Table 4.9.	Monthly and annual occurrence number of cyclones in the Bay of Bengal during 1981-2007.	37
Table 4.10.	Monthly and annual occurrence number of disturbances in the Bay of Bengal during 1981-2007.	38
Table 4.11.	Comparison among the number of various types of cyclones at 0.5°C temperature bins (starting from 26°C) with the total number of weeks remaining within that temperature bin.	52
Table 4.12.	Starting point, landfall or die out point and retention time in hour of the disturbances, whose duration was more than 100 hours, in three different regions.	69

List of Figures

Figure No.	Caption	Page
Fig. 2.1.	Ocean temperature profile.	9
Fig. 2.2.	The difference between the pre-dawn temperature at 1-5m depths and temperature at varies depths during night (a) and during day (b).	12
Fig. 2.3.	Areas where cyclones form and travel paths with annual percentages of cyclones in each region.	17
Fig. 2.4.	Coriolis deflection of winds blowing eastward at different latitudes. After a few hours the winds along the 20 th , 40 th and 60 th parallels appear to veer off course. This deflection (which does not occur at the equator) is caused by Earth's rotation, which changes the orientation of the surface over which the winds are moving.	20
Fig. 2.5.	Effect of Coriolis force on wind which is moving towards low pressure centre due to air pressure force.	21
Fig. 2.6.	Details of a cyclone structure.	22
Fig. 2.7.	World map of the oceans shows sea surface temperatures by color.	23
Fig. 3.1.	Rectangular box in the regional map showing the study area.	25
Fig. 3.2.	The three rectangular boxes in the regional map showing the regions of interest.	26
Fig. 4.1.	Monthly occurrence number of tropical disturbance and SST during the period 1981-2007.	39
Fig. 4.2.	Yearly occurrence number of tropical disturbances and SST during the period 1981-2007.	40
Fig. 4.3.	Monthly distribution of SST anomalies of the Bay of Bengal during 1981-2007.	41
Fig. 4.4.	Monthly distribution of 81 cyclones formed over the Bay of Bengal during 1981-2007.	42
Fig. 4.5.	Trends of tropical cyclone frequency and SST in winter season from 1982-2007.	42

Fig. 4.6.	Trends of tropical cyclone frequency and SST in pre-monsoon season from 1982-2007.	43
Fig. 4.7.	Trends of tropical cyclone frequency and SST in monsoon season from 1982-2007.	44
Fig. 4.8.	Trends of tropical cyclone frequency and SST in post-monsoon season from 1982-2007.	44
Fig. 4.9.	Yearly trends of tropical cyclone frequency and SST from 1981-2007.	45
Fig. 4.10.	Decadal trends of tropical cyclone frequency and SST from 1981-2007.	46
Fig. 4.11.	Variation of SST and TC duration in winter season during 1982-2007.	46
Fig. 4.12.	Variation of SST and TC duration in pre-monsoon season during 1982-2007.	47
Fig. 4.13.	Variation of SST and TC duration in monsoon season during 1982-2007.	48
Fig. 4.14.	Variation of SST and TC duration in post-monsoon season during 1982-2007.	48
Fig. 4.15.	Yearly variation of SST and TC during 1981-2007.	49
Fig. 4.16.	The relationship between maximum wind speed and SST encountered prior to reaching the maximum wind speed.	50
Fig. 4.17.	Maximum wind speed and initial SST of 91 tropical cyclones.	51
Fig. 4.18.	Temporal average sea surface temperature of 272 observation points (17 latitude points for each longitude points, i.e. $17 \times 16 = 272$). Gray shade indicates the topography in meter.	53
Fig. 4.19.	Position of twelve points (a to l) taken in the Bay of Bengal to show the decadal SST variation.	54
Fig. 4.20.	Yearly SST variation at twelve points in the Bay of Bengal.	55
Fig. 4.21.	Decadal variation of SST at twelve points (a to l) in the Bay of Bengal.	56

Fig. 4.22.	Comparison of temporal average SST and contemporaneous average SST at the (a) Cyclonic Storm (CS) (b) Severe Cyclonic Storm (SCS) and (c) Very Severe Cyclonic Storm (VSCS) and Super Cyclone (SC) formation location.	57
Fig. 4.23.	Weekly SST distribution at the time of a CS formation on 14/10/2000.	58
Fig. 4.24.	Weekly SST distribution at the time of a SCS formation on 10/5/2003.	59
Fig. 4.25.	Weekly SST distribution at the time of a VSCS formation on 23/5/1989.	60
Fig. 4.26.	Weekly SST distribution at the time of a SC formation on 25/4/1991.	61
Fig. 4.27.	Probability of intensification of D into VSCS during (a) first decade (1981-1990) (b) second decade (1991-2000) and (c) third decade (2001-2007).	62
Fig. 4.28.	Probability of intensification of CS into SCS during (a) first decade (1981-1990) (b) second decade (1991-2000) and (c) third decade (2001-2007).	64
Fig. 4.29.	Probability of intensification of CS into VSCS during (a) first decade (1981-1990) (b) second decade (1991-2000) and (c) third decade (2001-2007).	65
Fig. 4.30.	Initial location of very severe cyclonic storm (triangle) and depression (circle). Gray shade indicates the topography in meter.	67
Fig. 4.31.	Variation of average temporal SST with respect to the latitude.	68
Fig. 4.32.	Variation of maximum wind speed of VSCS and SC with respect to latitude.	70

Acknowledgements

First and foremost, I would like to thank, Almighty Allah, who has helped me in everything, I did and do. No achievement in life without Allah could be true. Besides I owe any measure of success to the array of input from so many. Dr. Md. Rafi Uddin, Assistant Professor, Department of Physics, BUET my talented and excellent supervisor whose relentless pursuit of and patience with me during preparation and delivery of this thesis was a tremendous source of motivation and encouragement. To my class teacher, Dr. Md. Nazrul Islam (on leave from BUET) Professor of Meteorology, Department of Meteorology, King Abdulaziz University, Jeddah, Saudi Arabia, I am greatly grateful for his immense deal of help during this painstaking research. I am very much grateful to my employer, Bangladesh Atomic Energy Commission, for giving me permission to perform M.Phil. program.

My thanks and gratitude goes to Professor Dr. A. K. M. Akther Hossain, Head, Department of Physics, BUET for his overall compassionate deportment. I also express my thanks to Professor Dr. Mominul Huq, Professor Dr. Md. Abu Hashan Bhuiyan, Professor Dr. Nazma Zaman, Professor Dr. Jiban Podder, Professor Dr. Md. Feroz Alam Khan, Professor Dr. Md. Mostak Hossain, Associate Professor Mrs. Fahima Khanam, Associate Professor Dr. Afia Begum, Assistant Professor Dr. Md. Forhad Mina, and all other teachers of the Department of Physics for their encouragement during this work. My thanks and gratitude goes to all the staffs of Department of Physics for helping me in providing information regarding to administration that enabled me to pursue my thesis.

I would like to show my appreciation to Bangladesh Meteorological Department (BMD) and National Oceanic and Atmospheric Administration (NOAA) for allowing me the privilege of sharing data in this research. I thank at last but by no means least, to Md. Abdul Mannan, Meteorologist, BMD, Dhaka; Golam Dastagir Al-Qaderi, Assistant Professor, Department of Physics, University of Dhaka and Md. Mizanur Rahman, Scientist, Theoretical Division, SAARC (South Asian Association for Regional Cooperation) Meteorological Research Centre (SMRC) for help and co-operations they had extended. Proper thanks are due to my beloved wife and baby boy for their unwavering support.

Abstract

The influence of Sea Surface Temperature (SST) on tropical cyclone formed in the Bay of Bengal was examined, using 314 months (November 1981 • December 2007) of National Oceanic and Atmospheric Administration (NOAA) Optimum Interpolation version 2 weekly mean SST data. The study area was from 5.5-21.5°N to 80.5-95.5°E; with a total 272 grid points at $1^{\circ} \times 1^{\circ}$ grid spans were found. During the study period, 162 disturbances were formed over the Bay of Bengal. 91 were cyclones, among these cyclones 38 were cyclonic storms (CS), 23 were severe cyclonic storms (SCS), 28 were very severe cyclonic storms (VSCS) and 2 were super cyclones (SC). More than 86% cyclones are formed in the observed months having positive SST anomalies. The average of the contemporaneous SST at the formation time of CS, SCS, VSCS and SC was 28.93, 29.08, 29.27 and 29.41°C, respectively. The frequency of cyclones shows positive trend in pre-monsoon season and negative trends all other seasons with increasing SST. The duration of cyclones shows positive trends in winter and pre-monsoon seasons and negative trends in monsoon and post-monsoon seasons with increasing SST. The formation of SCS, VSCS and SC starts after 27.50°C and increases with increasing SST but discontinuously. However, the intensity of cyclone has a step-like rather than continuous relationship with SST. It is seen that the depressions which are formed in April have 100% probability of intensification to convert into VSCS or SC. The most active zone for powerful cyclone (VSCS and SC) formation is located within area-3 (7.5°N • latitude < 13.5°N) where the temporal average SST is higher (around 28.70°C) and the rate of declining temperature with increasing latitude is nearly constant (0.01°C/latitude). The retention time of the disturbances within the area-3 shows the highest value. At the initial stage, the speed of the disturbance remains less. So the consumption of heat energy from the reservoir, which has nearly constant 0.010°C/latitude and higher SST, remains lower. As the heat acts as fuel for cyclone, adequate heat energy lingers the cyclone to survive in area-3. It is found that when the disturbance moves to the higher latitudinal direction the speed gradually increases and the SST decreases. As the SST decreases the heat energy also decreases. It may be due to the augmentation of wind speed as the supplied energy does not cope with the burning up of heat energy. For this reason the highest number of cyclones die out within area-1 (within 17.5°N • latitude < 21.5°N) where the SST decrease was the highest of value 0.36°C/latitude.

Chapter One

Introduction

1.1 Prelude

Bangladesh is a densely populated country with 1099/ km². The coastal area of Bangladesh is one of the most hazardous coasts in the world in terms of the number of people who suffer from various types of environmental hazards every year. Among the diversity of environmental perils the cyclone is one of the most perilous types of disaster. Due to the scarcity of data, overall scientific research in Bangladesh particularly relating to cyclone is inadequate.

19 coastal districts, covering 32% area and about 33% of the total population of Bangladesh, are the cyclone prone area. The coastal area is flat low-lying land having altitude less than 3m from the mean sea level. The climate of Bangladesh is a part of the humid tropics with the Himalayas lying in the north and the funnel shaped coast touching the Bay of Bengal in the south. Owing to the funnel shaped coast of the Bay of Bengal, the cyclones formed in it frequently make landfall on the coastal area of Bangladesh. The cyclones formed in the Bay of Bengal also move towards the eastern coast of India, towards Myanmar and sporadically into Sri Lanka. The cyclones cause the maximum damage when they come into Bangladesh and north-eastern coast of India (Tahmeed et al. 2005). This is because of the low flat terrain, high density of population and mostly tin-shed and thatched houses.

The working and maintenance of the tropical cyclones (TCs), the most destructive of all the natural disasters, is still a puzzle. The genesis and development of this magnificent heat engine is being pondered by atmospheric scientists from many years. TC genesis is one of the few atmospheric processes that are poorly understood. The climatological conditions under which tropical cyclones occur have now been well established over decades of research. The importance of monsoon circulations in determining tropical cyclone characteristics is related to the six primary environmental factors defined by Gray (1968, 1975) to be favorable for tropical cyclone formation. These include (i) large values of low-level cyclonic relative vorticity, (ii) a location that

is at least a few degrees pole-ward of the equator, (iii) weak vertical wind shear, (iv) large values of relative humidity in the lower and middle troposphere, (v) conditional instability throughout a deep tropospheric layer, and (vi) Sea surface temperature (SST) above 26°C. The existence of such conditions is common in the tropics.

Several recent publications (Emanuel 1987, 2000, and 2005) have shown that the intensity of TC is linked with rising SST. It is well established that $SST > 26^{\circ}\text{C}$ is a requirement for TC formation in the current climate (Palmen 1948). Webster et al (2005) found an increase trend in tropical cyclone number, duration and intensity with increasing SST in North Indian Ocean basin. All these research have fueled the debate on whether warming environment is causing an increase in intensity of TC. Mark and Adam (2008) used a statistical model to disentangle the two main hurricane predictions - SST and near-surface trade wind speed. These two variables together explain about 80% of the variance observed in tropical Atlantic hurricane activity between 1965 and 2005. Their result indicates that 0.5°C increase of SST in August – September SST, an average 40% increase in hurricane activity, a measure including both number and severity of storms. Their study showed that if the SST increases by 2°C by 2100 AD, maximum wind speeds of hurricanes could increase by 63%, with damage from hurricanes rising in proportion to the cube of the wind speed. This is because the warm ocean water provides sensible heat and water vapor that fuels the intense convection of a hurricane, and assists the conversion of a depression to a cyclone.

Jadhav and Munot (2008) examined the intensity as well as duration of low pressure system (LPS) in association with the increasing SST in the Bay of Bengal. They classified LPS into two categories, viz.: (1) only low-pressure areas (LPA) and (2) more intense systems like depressions/storms (DDS). They found that the frequency and duration of LPA (DDS) during the monsoon season are positively (negatively) correlated with SSTs of the Bay of Bengal during winter, pre-monsoon and monsoon season indicating warmer SST of the Bay of Bengal may not be favorable for intensifying lows into depressions. Mandake and Bhide (2003) found decreasing trend of storm frequency on decadal scale with the increase of SST during monsoon season over Bay of Bengal.

They used monthly mean SST data which may obscure associations between tropical cyclone and the actual SST over which the storm exists.

1.2 Objectives of the Research

The objectives of this research work are to i) determine the trends of SST and cyclone frequency across the Bay of Bengal, ii) determine the variation of SST and cyclone duration, iii) determine SST anomaly, iv) determine the seasonal and yearly SST trends, v) examine the relationship between the SST and the intensity of the cyclone, vi) determine the area of powerful cyclone formation and longest residence time.

These results may have the potential to provide information to explain spatial and temporal variability characteristics of cyclone. The results also could be used to predict the intensity, frequency and duration of the tropical cyclones, which will originate in the Bay of Bengal.

Chapter Two

Literature Review

2.1 Introduction

This chapter will review relevant studies on SST and cyclone activity on global level as well as regional, sea surface temperature and tropical cyclone activities. Due to paucity of similar type of work on the Bay of Bengal area the works but related to other basins also mentioned, which have provided motivations and ideas for the researcher to conduct this study.

2.2 Cyclone activity and SST

Tropical cyclones are the most devastating of all natural disasters. One of the most interesting issues is how TC activity will change under global warming, and whether increasing sea surface temperature (SST) due to anthropogenic climate change influences both the frequency and intensity of TCs.

On global level, numerous studies based on observed records have argued for a large increase in TC intensity, linked to warming SST that may be associated with global warming (Emanuel 2005; Webster et al. 2005). Since high SST is one of the main factors for TC genesis and intensification (Gray 1968), an increase in SST could bring about an increase in TC activity. Despite this simple argument, it is still unclear whether such a relationship occurs in observations (Landsea et al. 2006; Pilke et al. 2006). It is argued that the recent increase in frequency of intense typhoons is likely a part of the large interdecadal variations in the number of intense TCs related to similar temporal fluctuations in the atmospheric environment. Furthermore, it is reported that there is a negative correlation in cyclone intensity with local tropical SSTs (Chan 2006). Quite a few pioneer works have utilized the climate models for studying the influence of greenhouse warming on the tropical storm climatology (Broccoli and Manabe 1990; Bengtsson et al. 1996, Sugi et al. 2002; Tsumui 2002; Kutson and Tuleya 2004; McDonald et al. 2005; Oouchi et al. 2006; Gualdi et al. 2008, and among others). Recent high-resolution climate models show an enhanced TC activity in terms of the storm wind or precipitation due to underlying SST increases, but show a decreased TC genesis

frequency over the globe. However, there are still large discrepancies in terms of regional changes among various model simulations. These results require thorough understanding of the relationship between TC activity and the spatial distribution of SST changes (Chauvin et al. 2006). Approximately, one-third of all TCs originate over the western North Pacific (WNP) (Elsner and Liu 2003). Over the past decades, many studies have paid attention to the relationship between TC activity in the WNP and tropical Pacific SST (i.e., El Niño and Southern Oscillation, ENSO) in terms of genesis location, track, intensity and number based on the observations (Chan 1985; Lander 1994; Chen et al. 1998, Chia and Ropelewski 2002; Wang and Chan 2002) and coupled general circulation models (CGCMs) (Iizuka and Matsuura 2008). These studies have reached in the agreement that ENSO plays a role in determining the distribution of TCs over the WNP. During El Niño the mean genesis location of TCs is shifted to the east. During La Niña, on the other hand, the mean genesis location of TCs tends to shift to the northwest (Chan 1985; Lander 1994, Chen et al. 1998; Chia and Ropelewski 2002; Wang and Chan 2002; Iizuka and Matsuura 2008). Regarding the relationship between the TC frequency over the WNP and ENSO, however, the results have not been consistent in all cases (Ramage and Hori 1981; Pan 1982; Dong 1988; Wu and Lau 1992; Lander 1993, 1994; Camargo and Sobel 2005). It has been pointed out that there is no significant linear relation between ENSO and the TC frequency, which is mainly due to differences in data and technique or due to other factors, such as quasi-biennial and interdecadal oscillation influencing TC occurrence number. Other studies have argued that there is a nonlinear relation between the number of TCs and ENSO (Chan and Shi 1996; Chen et al. 1998; Chan 2000; Wang and Chan 2002). Such results require more understanding of the relationship between the number of TCs in the WNP and the tropical Pacific SST.

For the regional level, in a study Shaji et al. (2003) discussed the seasonal cycle of the heat budget in the basins of Arabian Sea, Bay of Bengal and the Equatorial Indian Ocean. They described that the Indian Ocean is a relatively poorly studied area and data coverage of this area is also sparse. While some data sets do exist, they are predominantly on coarse space and time scales. The earlier efforts, such as the

International Indian Ocean Expedition (IIOE), the Monsoon Experiment (MONEX) and the First Global Experiment (INDEX), extensively observed the equatorial and western Indian Ocean basins (Wyrski, 1971; Schott, 1983; Swallow *et al.*, 1983; Schott *et al.*, 1988). The projects, such as the Indian Joint Global Ocean Flux Studies (JGOFS), Tropical Ocean and Global Atmosphere (TOGA) and the World Ocean Circulation Experiment (WOCE), have substantially improved the quantity of the measured data in this region. Additionally, individual studies have also contributed in recent years to the understanding of the dynamics in the Indian Ocean. There are a few atlases covering the Indian Ocean (e.g. Wyrski, 1971; Hastenrath and Lamb, 1979; Cutler and Swallow, 1984; Rao *et al.*, 1989), which contribute significantly to our understanding of the tropical Indian Ocean dynamics. However, the observations are not detailed enough to study mesoscale dynamic features. On the modeling aspects, beginning with the pioneering efforts of Cox (1970, 1976, 1979), numerous modeling studies have endeavored to explain the observed flow in the Tropical Indian Ocean. Most of these studies were concentrated on the development of barotropic/reduced gravity models or prognostic models which mainly deal with the upper ocean circulation (e.g. Hurlburt and Thompson, 1976; Luther and O'Brien, 1985; McCreary and Kundu, 1986; Kindle and Thompson, 1989; Woodbury *et al.*, 1989; Jensen, 1990; Potemra *et al.*, 1991; McCreary *et al.*, 1993). Diagnostic and semi-diagnostic modeling techniques have also been adapted to describe the climatic state of the Indian Ocean (Bahulayan and Shaji, 1996; Shaji *et al.*, 1999, 2000). Modeling has also been used to study the effect of the throughflow on remote currents. Godfrey and Golding (1981) and McCreary and Kundu (1986) found that the input from the Pacific through the Indonesian passages significantly affects, at least regionally, the sea surface temperature (SST) and surface heat flux of the Indian Ocean. Recently, the Ocean General Circulation Model (OGCM) MOM2 has also become an important tool for studies related to the seasonal and interannual variations of circulation in the Tropical Indian Ocean (Wacongne and Pacanowski, 1996; Vinayachandran and Yamagata, 1998; Vinayachandran *et al.*, 1999).

The Indian subcontinent divides the North Indian Ocean into two semi-enclosed tropical basins the Arabian Sea to the west and the Bay of Bengal to the east. These two basins merge with the Equatorial Indian Ocean at their southern boundary, where interaction with the rest of the Indian Ocean occurs. Although the Bay of Bengal and the Arabian Sea are located in the same latitudinal belt and are influenced by monsoons, oceanographically these two basins exhibit remarkable differences. Unlike the Arabian Sea, a large quantity of freshwater enters the Bay as rainfall and as river discharge (UNESCO, 1971). In the Arabian Sea, evaporation exceeds precipitation and it receives very saline water from the marginal seas, the Red Sea and the Persian Gulf. As a consequence, the western part of the North Indian Ocean is very saline in contrast to an anomalously fresh eastern part. The Bay of Bengal is favorable for the genesis and maintenance of synoptic scale disturbances such as lows, depressions and cyclones because the SST of Bay is above the threshold (26.5°C) for active generation of convection over a large part of the year (Hastenrath and Lamb, 1979). On the other hand, the Arabian Sea west of about 70°E is too cold throughout most of the year to generate such disturbances.

Some works have been done on cyclonic disturbances such as depressions and cyclonic storms in the Bay of Bengal. Koteswaram and George (1958), Rao and Jayaraman (1958), Sikka (1977), Joseph (1981) and Saha et al. (1981) and some others have extensively studied the depressions/storms during the monsoon season. Mandal (1991) studied year-to-year fluctuations in the frequency of cyclonic disturbances and found a negative trend since the 1950s. Patwardhan and Balme (2001) observed a significant negative trend in the frequency of cyclonic disturbances during the recent years. Moolley and Shukla (1987) examined some characteristic features of Low Pressure System (LPS) in terms of formation, location, movement and duration of LPS. This work was further extended by Sikka (2006), carrying out statistical analysis of the low-pressure systems. Xavier and Joseph (2000) showed that frequency of depressions/storms depends on the vertical windshear. Rajeevan et al. (2000a, b) noticed a statistically negative trend in the activity of the depressions/storms during the Indian monsoon season for the period 1951–1998 in spite of above-normal SST of the

Bay of Bengal. Singh (2001) investigated long-term trends in the frequency of cyclonic disturbances over the Bay of Bengal and the Arabian Sea using the 100-year (1890–1999) data and found significant negative trends. Jadhav (2002) studied the performance of monthly monsoon rainfall of the meteorological subdivisions with respect to the location and duration of LPS. Mandake and Bhide (2003) found decreasing storm frequency in spite of increasing SST of Bay of Bengal. Dash et al. (2004) discussed the unfavourable atmospheric conditions over the Bay of Bengal responsible for the decreasing frequency of depressions/storms during monsoon season for the recent decades. Jadhav and Munot (2004) made statistical analysis of all the total low-pressure systems that occurred during the monsoon season and showed that decadal frequency of LPS remains unchanged and only the number of LPS days has significantly increased during the period 1971–1990.

Sea Surface Temperature

2.3 Ocean Temperature Profile

The ocean can be divided into three vertical zones as shown in Fig.2.1, depending on temperature. The top layer is the surface layer, or mixed layer. This layer is the most easily influenced with solar energy (the sun's heat), wind and rain. The next layer is the thermocline. Here the water temperature drops as the depth increases. The last layer is the deep-water layer. Water temperature in this zone decreases slowly as depth increases. Water temperature in the deepest parts of the ocean averages about 36° F (2°C).

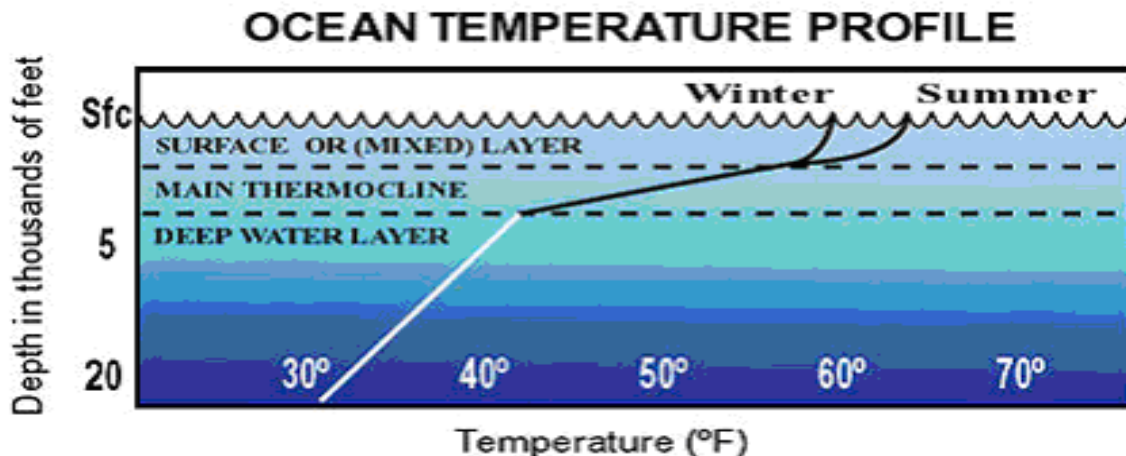


Fig 2.1. Ocean temperature profile (*Source: website*).

2.3.1 Sea Surface Temperature

The temperature structure of the upper ocean is quite complex and depends on various processes acting at the surface and on the first meters of water column. The air-sea interface is affected by processes responsible for the heat transfer between the ocean and the atmosphere: the net long wave radiation, the heat convection between the air and the sea and the heating or cooling due to moisture transfer. Within the ocean, the heat is redistributed by molecular diffusivity and turbulent diffusivity. The heating related to the light absorption is another process modifying temperature of water column. All these processes acting at different depths and depth ranges complicate the definition of the

SST and the inter comparison with different instruments and models. Every SST observation depends on the measurement technique and sensor that is used, the vertical position of the measurement within the water column, the local history of all component heat flux conditions, and the time of day the measurement was obtained (Donlon, 2002). The general definition of SST is that it is the water temperature at the surface (or at 1 meter below the sea surface). However, the exacting meaning of ‘surface’ will vary according to the measurement method used because different things are actually being measured.

2.3.2 Vertical structure of SST

The vertical structure of SST can be generally classified as follows:

a. The interface SST, SST_{int}

The interface SST, SST_{int} is the temperature of an infinitely thin layer at the exact air-sea interface. It represents the temperature at the top of the SST_{skin} layer (and hence the top of the temperature gradient in that layer) and cannot be measured using current technology.

b. The skin SST, SST_{skin}

The skin SST, SST_{skin} , is a temperature measured by a radiometer at depth. Within a thin layer ($\sim 500\mu\text{m}$) at the water side of the air-sea interface where conductive and diffusive heat transfer processes dominate (where the molecular diffusion and heat conductivity dominate).

The temperature gradient within this layer is given by the ocean atmospheric heat fluxes. The skin temperature is measured by radiometers operating in the spectral region of 3.7 to $12\mu\text{m}$ (thermal infrared).

The advanced Very High Resolution Radiometers (AVHRR) and Along Track Scanning Radiometers (ATSR) are sensors measuring in the thermal infrared (Wick, 2002). The signal of these sensors potential is a approximately $10\mu\text{m}$ into the water column.

A short temperature gradient characteristically maintained in this thin layer shows SST_{skin} varies according to depth within the layer and because the penetration depth of the emitted radiation is a function of the wavelength of the radiation, the value of

SST_{skin} varies dependant on the wavelength used to for measurement. This is the basis of measuring the skin temperature gradient using infrared interferometer at wave lengths shorter than $5 \mu m$. Consequently, SST_{skin} should always be quoted at specific wavelengths in the water column, for example, $SST_{skin10.5\mu m}$. However, over the parts of the infrared spectrum used to make the measurements of SST_{skin} presented in this study, the variation in penetration depth is very small, and the values of SST_{skin} measured by ideal infrared radiometers and expected to vary by less than 0.01 K, and wavelength dependence of SST_{skin} can be ignored.

c. The sub-skin SST, $SST_{subskin}$

The sub-skin SST, $SST_{subskin}$ represents the temperature at the base of the skin layer. Beyond the skin layer, the temperature is affected by turbulent mixing and insolation. It varies on a time scale of minutes and may be influenced by solar warming. Its depth of the sub-skin is of the order of 1mm. Sensor working a low frequency (6-10GHz) with microwave measure the sub-skin SST.

d. The bulk SST or SST_{depth}

The bulk SST or SST_{depth} is the temperature of the water column under the skin layer at a depth completely immersed in the turbulent ocean. This temperature is observed by in situ buoys, CTD and XBT measurements.

e. The Constant Temperature Layer SST, SST_{CTL}

The constant temperature layer SST, SST_{CTL} is the sea temperature at a depth where the temperature is not significantly affected by the solar radiation. The diurnal variations are less than $0.20C$. The effective position of this constant temperature layer can therefore vary from one location to another.

2.3.3 Sea temperature with the Time and Space

Since the solar radiation is an important process, the night heat distribution in the upper ocean is different from the day temperature profile which is shown in the Fig. 2.2. Due to this time and space variation, the SST should be given as a temperature measurement at a specified depth and ideally at a time of day. Several satellite swaths have been combined by taking the maximum temperature. Also day time images have been used, which reduces the information for the subsurface layers. The sea surface temperature

was assimilated at 14:00 GMT. The model sea surface temperature reaches its maximum on this diurnal cycle at this time.

The initial resolution of the SST is 1km. Despite the load of the SST is linear with respect to the number of observations; there is no interest to assimilate this huge resolution temperature in the coarse resolution model. The resolution was degraded to 10km where the high resolution information in the SST is not expected to have a significant impact on the Ligurian sea model. The SST data is therefore split into a 1km resolution SST covering mainly the provincial-basis and a 10km resolution SST of the rest of the Mediterranean.

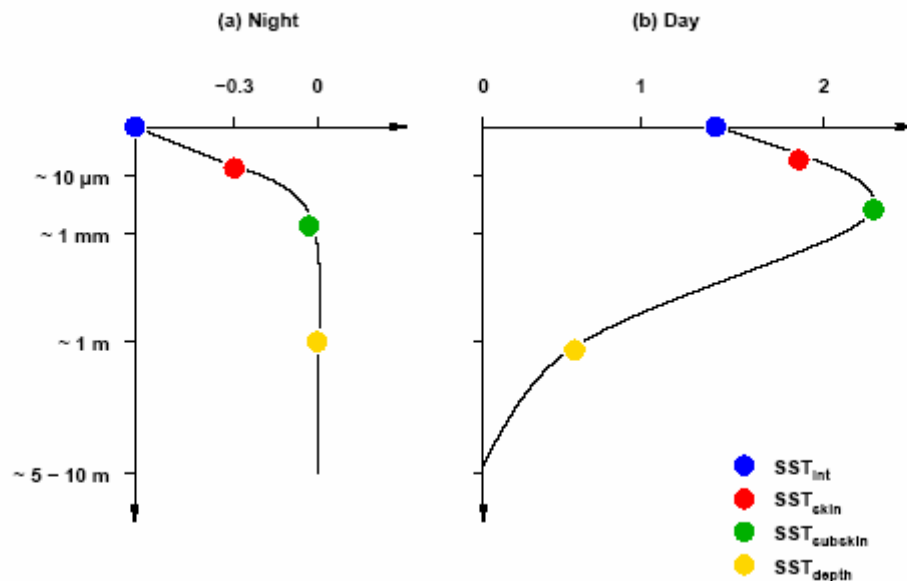


Fig 2.2. The difference between the pre-dawn temperature at 1-5m depths and temperature at various depths during night (a) and during day (b). (Adapted from Donlon (2002)) (Source: website).

2.3.4 Techniques for Measuring SST

a. Earliest Technique

A thermometer was dipped into a bucket of water manually drawn from the sea surface.

b. First automated technique

This was done by measuring the temperature of water intake port of large ships. This is not always consistent. The depth of the water intake as well as exactly where the temperature is taken can vary from vessel to vessel.

c. Fixed buoys

A thermometer attached to a moored or drifting buoy in the ocean would measure the temperature at a specific depth (example the top 1m below the sea surface). It is the most exact and repeatable measurements and the depth of water temperature is exactly 1m.

d. Satellite

Since 1980s satellites have been increasingly utilized to measure SST and have provided an enormous leap in our ability to view the spatial and temporal variation in SST. A satellite infrared radiometer measures the temperature of a very thin layer (about 10micrometer, thick) or skin of the ocean (leading to the phrase skin temperature) representing the top millimeter.

Satellite measurements of SST are far more consistent and in some cases, accurate than the in situ temperature measurements described above. The satellite measurement is made by sensing the ocean in two or more wavelengths in the infrared part of the electromagnetic spectrum, which can then be empirically related to SST.

These wavelengths are chosen because they are,

1. Within the peak of the black body radiation expected from the Earth and
2. Able to transmit well through the atmosphere

The satellite measure SST provides both a synoptic view of the ocean and a high frequency of repeat views, allowing the examination of basin-wide upper ocean dynamics not possible ships or buoys. For example, a ship traveling at 10 knots (20km/hr) would require 10 years to cover the same area a satellite covers in two minutes.

2.3.5 Difficulties with Satellite based Absolute SST

1. Because all the radiation emanates from the top “skin” of the ocean, approximately the top 0.01mm or less, it may not represent the bulk temperature of the upper meter of the ocean due primarily to effects of solar surface heating in the day time, and back radiation and sensible heat loss at night as well as from the effects of surface evaporation.
2. The satellite cannot look through clouds creating a fair weather bias in the long term trends of SST. Nonetheless, these difficulties are small compared to the benefits in understanding gained from satellite SST estimates.

2.3.6 Sea Surface Temperature Determination

In the infrared, the emissivity of the earth’s sea and land surface is near unity. As a result, in the absence of cloud or atmospheric attenuation, the brightness temperature observed with a spaceborne window radiometer is equal to surface skin temperature. However, cloud and water vapor absorption usually prohibit direct interpretation of the window channel data so that an algorithm needs to be applied to the data to alleviate the influence.

The algorithms and instrumental approach have evolved from the use of a single window channel on a polar orbiting satellite to the use of multispectral radiometer observation from both polar orbiting and geostationary satellites.

A sun synchronous polar orbiting satellite passes a given geographical location and similar local times each day, normally shortly after noon and midnight, to measure SST. In the presence of SST diurnal variation, if clouds at a location tend to appear at one of these times (say after noon), the climatology will be biased towards the other time (night SST). If clouds tend to appear at both times, the SST climatology must be estimated from other data. If the cloud diurnal variation varies seasonal, say clouds tend to appear in the afternoon in summer but not in winter, the SST will be biased towards the nighttime SST in summer but not in winter.

A weekly 1° spatial resolution optimum interpolation (OI) sea surface temperature (SST) analysis has been produced at the National Oceanic and Atmospheric

Administration (NOAA) using both in situ and satellite data. This weekly SST data has been used for the thesis work.

Tropical Cyclone

2.4 Historical Overview

The term cyclone is derived from the Greek word 'kyklos' meaning coil of snakes. The British-Indian scientist and meteorologist Henry Piddington coined the word 'Cyclone' to represent whirling storms expressing sufficiently the tendency to circular motion in his book *The Sailor's Horn-book for the Law of Storms*, published in 1848. Other meteorologists of the world immediately accepted the term and it is still current today. Satellite pictures of cyclones show that the nomenclature is very appropriate. Technically a cyclone is an area of low pressure where strong winds blow around a center in an anticlockwise direction in the Northern Hemisphere and a clockwise direction in the Southern Hemisphere. Cyclones occurring in the tropical regions are called tropical cyclones and those occurring elsewhere are called extra tropical cyclones.

Tropical Cyclone is a generic term for a low pressure system that usually forms in the tropics. All the tropical seas of the earth with the exception of south Atlantic and southeast Pacific give birth to deadly atmospheric phenomenon known as tropical cyclones. On an average, 80 tropical cyclones are formed every year all over the globe. Tropical cyclones are cyclones (area of concentration of kinetic energy which is equivalent to saying that cyclones are regions of strong winds) which form over the warm (generally tropical) ocean water and draw their energy from evaporation and condensation. They are characterized by a strong area of low pressure in the center of which strong winds swirl in a counter-clockwise direction in the northern hemisphere. Tropical cyclones are associated with strong thunderstorms, high winds and flooding.

2.5 Cyclone Formation Areas

Cyclones commonly develop in areas near, but not at the equator, as shown in the Fig. 2.3. Observations show that no cyclones form within 5 degrees latitude of the equator. Because the Coriolis force is too weak there to get air to rotate around a low pressure rather than flow from high to low pressure, which it does initially. If there is no rotation of air there is no storm. This is a reason why cyclone formation does not occur at low latitudes. As they move across the oceans their paths are steered by the presence of

existing low and high pressure systems, as well as the Coriolis force. The latter force causes the storms to eventually start turning to the right in the northern hemisphere and to the left in the southern hemisphere.

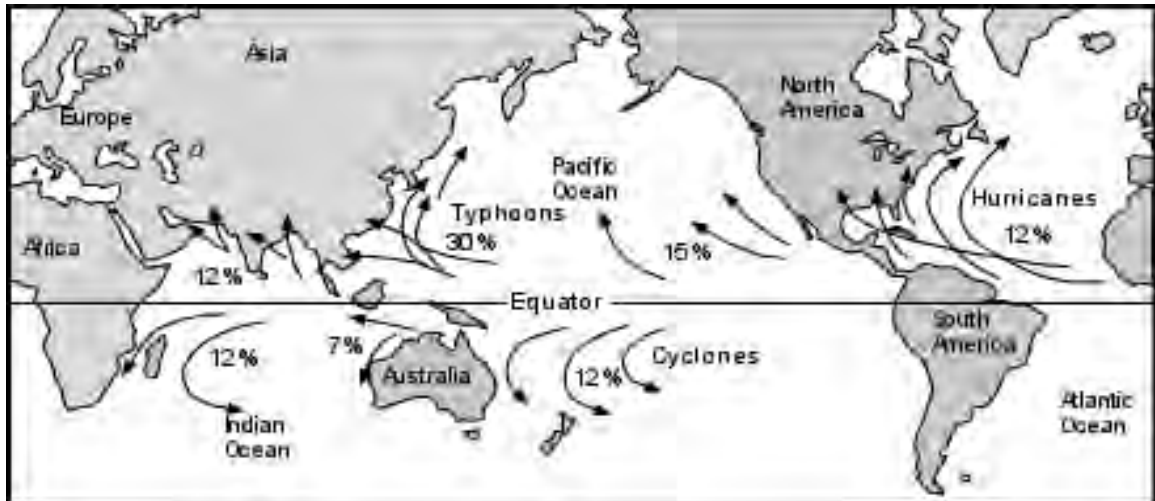


Fig.2.3. Areas where cyclones form and travel paths with annual percentages of cyclones in each region. (Source: website)

It is seen that about 12% of all tropical cyclones develop in the Atlantic Ocean. Those that begin to form near the coast of Africa are often referred to as "Cape Verde" hurricanes, because the area in which they develop is near the Cape Verde Islands. 15% of all tropical cyclones develop in the eastern Pacific Ocean, 30% develop in the western Pacific Ocean, 24% in the Indian Ocean both north and south of the equator, and 12% develop in the southern Pacific Ocean. It is notable that essentially no tropical cyclones develop south of the Equator in the Atlantic Ocean.

2.6 The Birth of a Cyclone

To understand tropical cyclone formation, there are several favorable precursor environmental conditions that must be in place (Gray 1968, 1979):

1. Warm ocean waters (of at least 26.5°C) throughout a sufficient depth (at least on the order of 50 m). Warm waters are necessary to fuel the heat engine of the tropical cyclone.

2. An atmosphere which cools fast enough with height such that it is potentially unstable to moist convection. It is the thunderstorm activity which allows the heat stored in the ocean waters to be liberated for the tropical cyclone development.
3. Relatively moist layers near the mid-troposphere (5 km). Dry mid levels are not conducive for allowing the continuing development of widespread thunderstorm activity.
4. A minimum distance of at least 500 km from the equator. For tropical cyclogenesis to occur, there is a requirement for non-negligible amounts of the Coriolis force to provide for near gradient wind balance to occur. Without the Coriolis force, the low pressure of the disturbance cannot be maintained.
5. A pre-existing near-surface disturbance with sufficient vorticity and convergence. Tropical cyclones cannot be generated spontaneously. To develop, they require a weakly organized system with sizable spin and low level inflow.
6. Low values (less than about 10 m/s) of vertical wind shear between the surface and the upper troposphere. Vertical wind shear is the magnitude of wind change with height. Large values of vertical wind shear disrupt the incipient tropical cyclone and can prevent genesis, or, if a tropical cyclone has already formed, large vertical shear can weaken or destroy the tropical cyclone by interfering with the organization of deep convection around the cyclone center.

Having these conditions met is necessary, but not sufficient as many disturbances that appear to have favorable conditions do not develop. Recent work (Velasco and Fritsch 1987, Chen and Frank 1993, Emanuel 1993) has identified that large thunderstorm systems (called mesoscale convective complexes [MCC]) often produce an inertially stable, warm core vortex in the trailing altostratus decks of the MCC. These mesovortices have a horizontal scale of approximately 100 to 200 km, are strongest in the mid-troposphere (5 km) and have no appreciable signature at the surface. Zehr (1992) hypothesizes that genesis of the tropical cyclones occurs in two stages: stage 1 occurs when the MCC produces a mesoscale vortex and stage 2 occurs when a second blow up of convection at the mesoscale vortex initiates the intensification process of lowering central pressure and increasing swirling winds.

2.7 Rotation of a Cyclone

Cyclonic rotation is a term used to describe the rotating movement of a tropical storm. In the Northern Hemisphere, tropical storms rotate counterclockwise. In the Southern Hemisphere, tropical cyclones rotate clockwise. Both directions of rotation are due to the Coriolis Effect.

2.7.1 Coriolis Effect

Coriolis Effect arises due to Coriolis force. This pseudo-force was named after Gaspard-Gustave Coriolis, a French scientist who published a paper on circular motion in 1835. The Coriolis is seen in rotating systems when objects on them move in that rotating system. It first became obvious when armies started using long range artillery. Gunners realised that their shells were landing to the right of their intended targets (this was in the Northern Hemisphere as far fewer wars were fought in the Southern Hemisphere; there the shells would have landed to the left of the intended target).

All free-moving objects, including wind, are deflected to the *right* of their path of motion in the Northern Hemisphere.

The reason for this deflection is the Coriolis force:

$$F_{coriolis} = m(2\boldsymbol{\Omega} \times \mathbf{u})$$

where m is the mass and \mathbf{u} is the velocity vector of a fluid parcel, and $\boldsymbol{\Omega}$ is the rotation vector of the Earth.

The magnitude of the Coriolis force is:

$$\begin{aligned} F_{coriolis} &= m 2\boldsymbol{\Omega} \cdot u \sin\phi \\ &= mfu \end{aligned}$$

where ϕ is the latitude, $f = 2\Omega \sin\phi$ is called the Coriolis parameter, and u is the magnitude of the velocity.

The Coriolis force written in vector form clearly indicates that

- It is directed at right angles to the direction of air flow.
- It affects only wind direction, not the wind speed.

- Its magnitude is affected by wind speed (the stronger the wind, the greater the deflecting force).
- Its magnitude increases from zero at the Equator to a maximum at the poles.

The Coriolis force thus has the effect of deflecting air flow as shown in Fig. 2.4. It also has the effect of deflecting ocean currents.

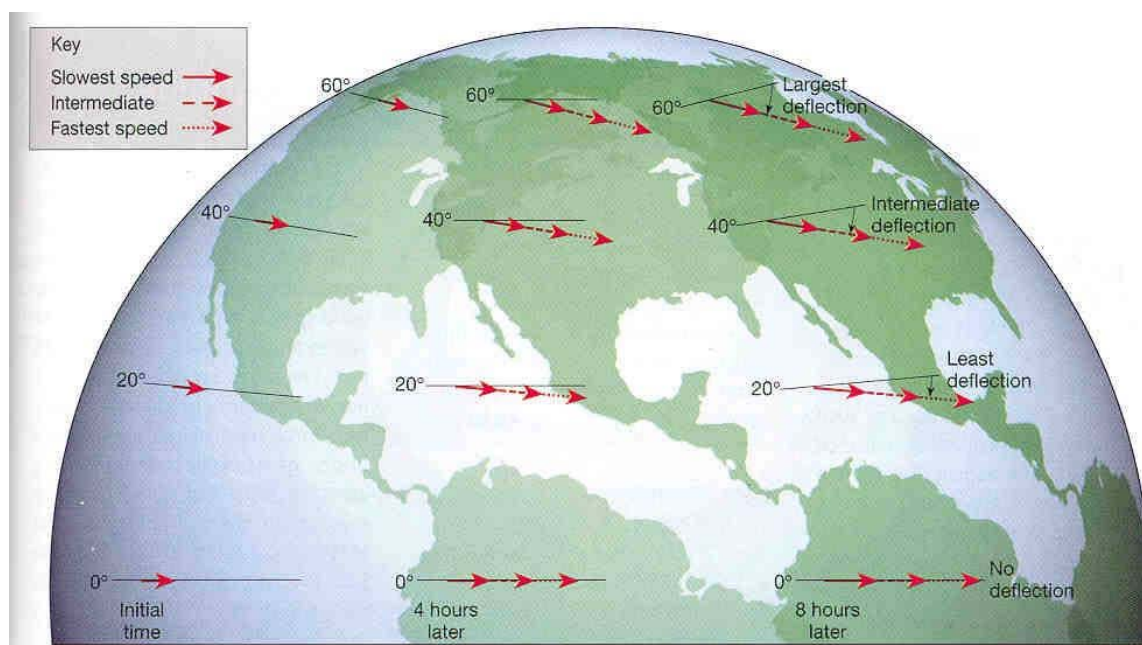


Fig.2.4. Coriolis deflection of winds blowing eastward at different latitudes. After a few hours the winds along the 20th, 40th and 60th parallels appear to veer off course. This deflection (which does not occur at the equator) is caused by Earth's rotation, which changes the orientation of the surface over which the winds are moving. (Source: website)

If a single packet of air moves towards an area of low pressure, in the Northern Hemisphere, the pressure difference, created due to different heating effect of the sun, will always push the air packet directly towards the centre of the low pressure but that the Coriolis force will seem to apply a force at 90° to its path (in this case to the right). Also the size of the Coriolis force increases as the speed of the air packet increases.

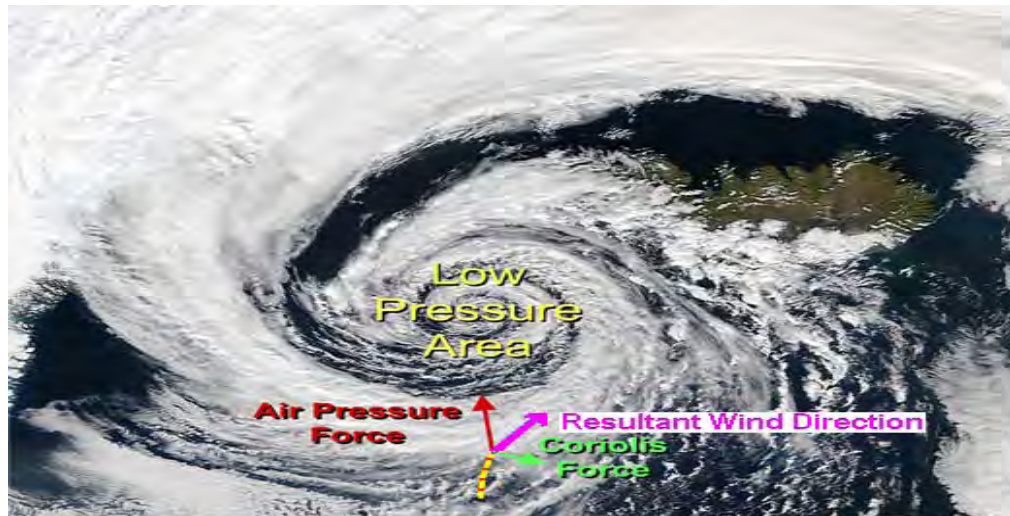


Fig.2.5. Effect of Coriolis force on wind which is moving towards low pressure centre due to air pressure force. (Source: website)

The packet of air starts to move directly towards the area of low pressure (Fig. 2.5). Its velocity is low and so the Coriolis force is also small. However combined effect of Coriolis force and pressure force deflect the flow of air slightly towards the right along the resultant force direction. Meanwhile the speed of packet of air is increasing due to the pressure gradient so the Coriolis force also increasing and simultaneously the air deflection increases.

This net force is sufficient to provide the centripetal force needed to keep the body of air rotating around the area of low pressure. The air cannot flow in rapidly and so the area of low pressure can survive for days or even weeks, travelling across the globe and influencing the weather as it does. This deflecting air ultimately rotates the water in counter-clock wise around the low pressure area.

So finally, if there were a low pressure area on a non-rotating planet then the surrounding high pressure air would rapidly flood in to fill it; only on rotating planets can sustained weather systems exist.

2.8 Cyclone Structure

The main parts, as shown in Fig.2.6, of a cyclone are the rainbands on its outer edges, the eye, and the eyewall. Air spirals in toward the center in a counter-clockwise pattern, and out the top in the opposite direction. In the very center of the storm, air sinks, forming the cloud-free eye.

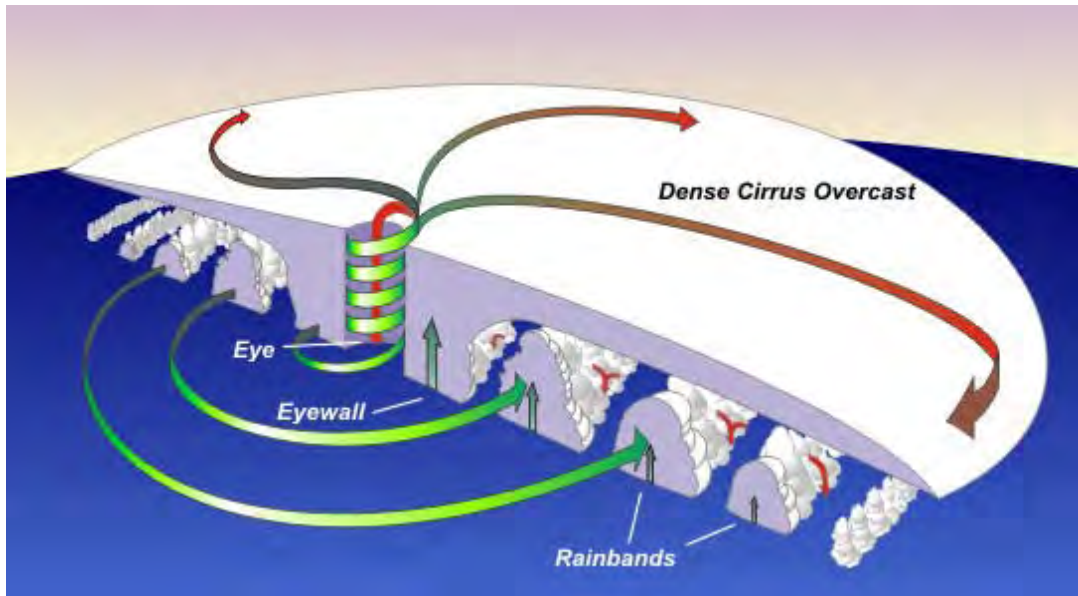


Fig.2.6. Details of a cyclone structure. (Source: website)

2.8.1 The Eye

The cyclone's center is a relatively calm, clear area usually 20-40 miles across. People in the midst of a cyclone are often amazed at how the incredibly fierce winds and rain can suddenly stop and the sky clear when the eye comes over them. Then, just as quickly, the winds and rain begin again, but this time from the opposite direction.

2.8.2 The Eyewall

The dense wall of thunderstorms surrounding the eye has the strongest winds within the storm. Changes in the structure of the eye and eyewall can cause changes in the wind speed, which is an indicator of the storm's intensity. The eye can grow or shrink in size, and double (concentric) eyewalls can form.

2.8.3 The Spiral Rainbands

The storm's outer rainbands (often with cyclone or tropical storm-force winds) can extend a few hundred miles from the center. These dense bands of thunderstorms, which spiral slowly counterclockwise, range in width from a few miles to tens of miles and are 50 to 300 miles long. Sometimes the bands and the eye are obscured by higher level clouds, making it difficult for forecasters to use satellite imagery to monitor the storm.

2.9 Cyclone Size

Typical cyclones are about 300 miles wide although they can vary considerably. Size is not necessarily a indication of cyclone intensity. Cyclone-force winds can extend outward to about 25 miles from the storm center of a small cyclone and to more than 150 miles for a large one. The area over which tropical storm-force winds occur is even greater, ranging as far out as almost 300 miles from the eye of a large cyclone.

2.10 Death of a Cyclone

One very common way that hurricanes die is by moving over cool water. The Fig.2.7 shows the average sea surface temperatures in the world during the month of November. The warmest seas are colored red. Tropical cyclones can survive in tropical areas with warm seas, but when they move out over cooler waters such as the yellow and green areas they quickly start to lose their power.

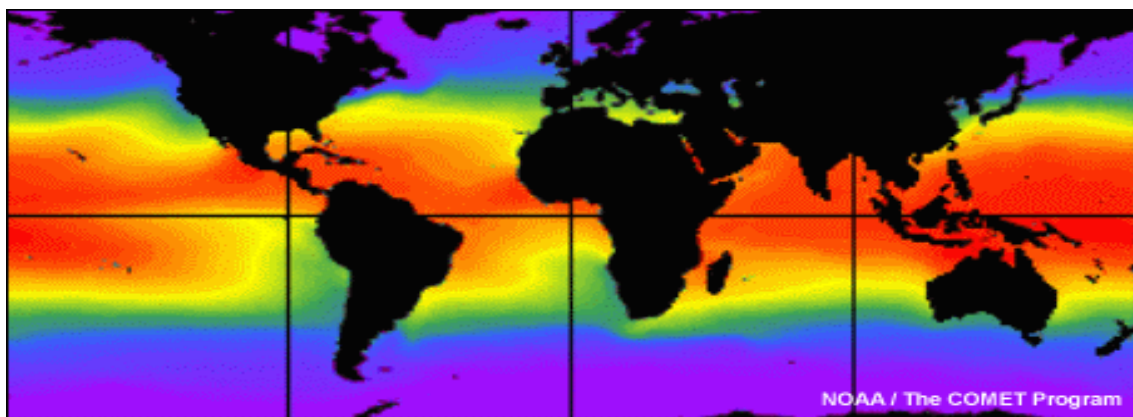


Fig.2.7. World map of the oceans shows sea surface temperatures by color. (Source: website)

In the equatorial zone, shading is bright red and orange, indicating warm temperatures. In the midlatitudes, shading goes to yellow and green, indicating cooler sea surface temperatures. Cooler seas are found along the North and South American west coasts, and the Southwest African coast. In the higher latitudes, shading goes from blue to purple, indicating much colder sea surfaces.

Chapter Three

Data and Methods

3.1 Data used and methodology

In this study the tropical cyclone data during 1981 -2007 have been taken from Bangladesh Meteorological Department (BMD) to assess the variability of tropical cyclone intensity, frequency and duration. Initial location coordinates (latitude/longitude) for all the tropical disturbances developed in the Bay of Bengal during the above mentioned period are tabulated. The data of tropical disturbances as well as the SST are tabulated season wise, namely pre-monsoon (March, April and May), monsoon (June, July, August and September), post-monsoon (October and November) and winter (December, January and February). The weekly mean SST dataset are collected from the National Oceanic and Atmospheric Administration Climate Data Center. SST has taken by matching the year, month, week and position (latitude and longitude) of the cyclone.

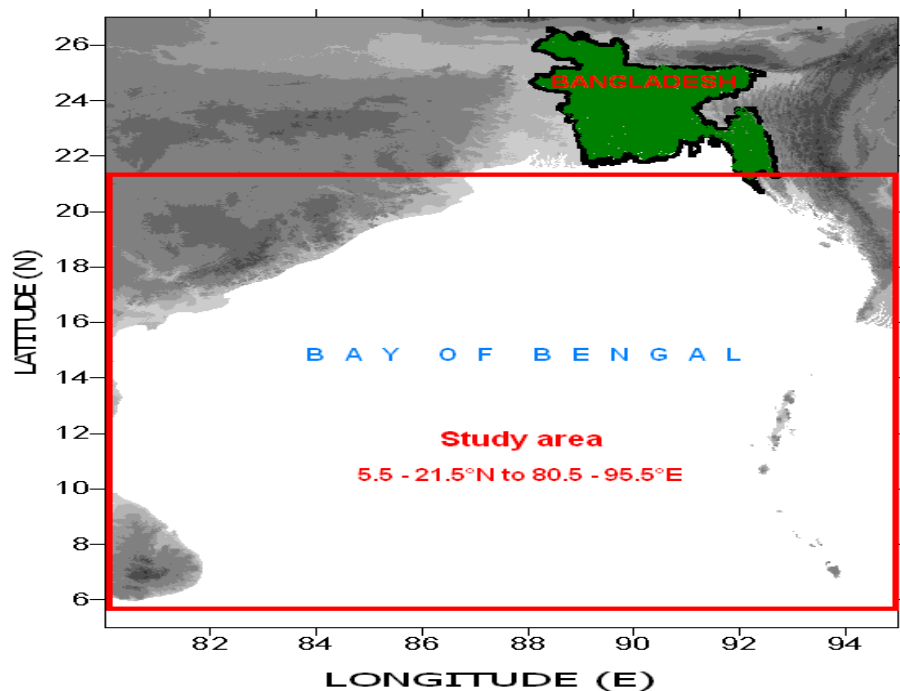


Fig. 3.1. Rectangular box in the regional map showing the study area.

The study area have been taken from 5.5-21.5°N and 80.5-95.5°E which is shown in the Fig. 3.1; from that area at 1° interval of latitude and longitude total 272 observation grid points for SST are obtained. Spatial and temporal averages of the SST data are prepared. To find SST anomaly, long term spatio-temporal average SST has deducted from contemporaneous (during the formation of cyclone) SST.

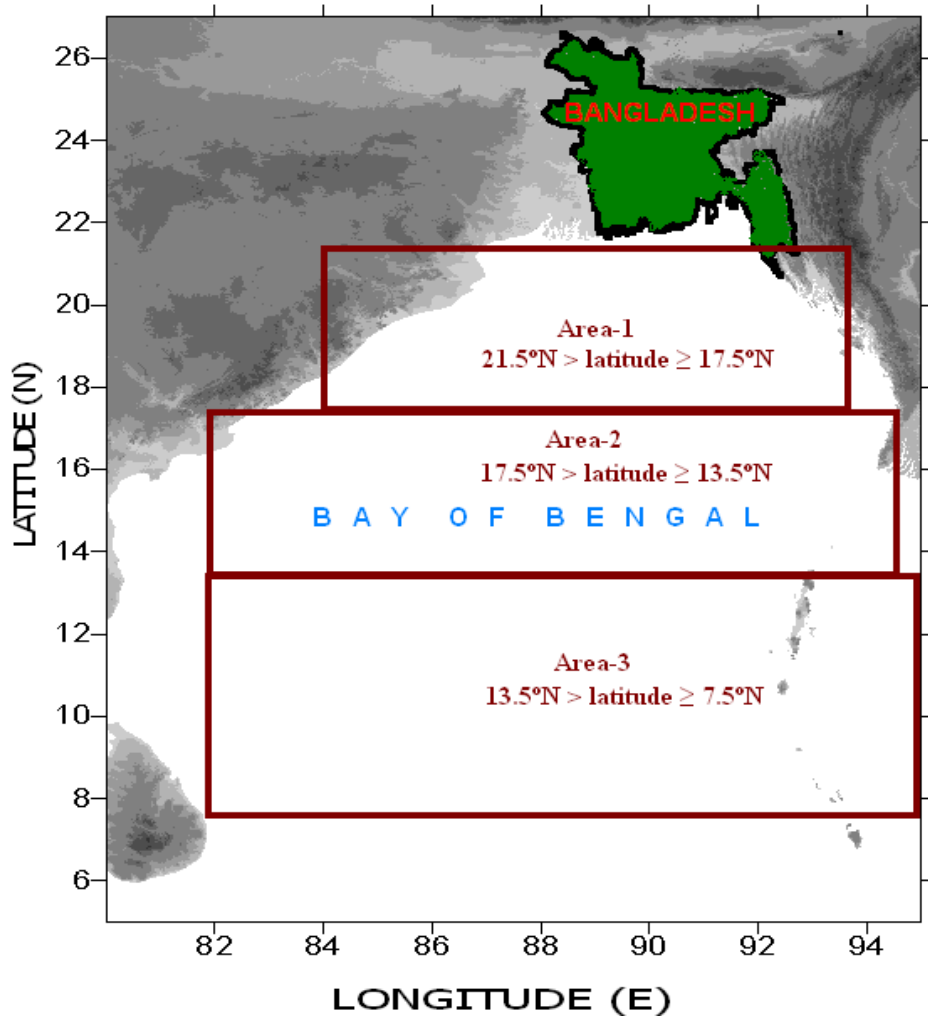


Fig. 3.2. The three rectangular boxes in the regional map showing the regions of interest.

For analysis purpose the study area has been subdivided into 3 areas (Fig. 3.2), namely, area-1 ($17.5^{\circ}\text{N} < \text{latitude} < 21.5^{\circ}\text{N}$), area-2 ($13.5^{\circ}\text{N} < \text{latitude} < 17.5^{\circ}\text{N}$) and area-3 ($7.5^{\circ}\text{N} < \text{latitude} < 13.5^{\circ}\text{N}$).

Chapter Four

Results and Discussion

4.1 Categorization of Tropical Disturbances

The intensity of tropical disturbances is defined depending on the maximum wind speed. The tropical disturbances are subdivided and categorized as shown in Table 4.1 below.

Table 4.1. Classification of cyclone develop in the Bay of Bengal.

Sl. No.	Name of disturbances	Maximum sustained wind speed (km/h)
1	Low	<31
2	Well marked low (WML)	31 – 40
3	Depression (D)	41 – 50
4	Deep depression (DD)	51 – 61
5	Cyclonic storm (CS)	62 – 88
6	Severe cyclonic storm (SCS)	89 – 117
7	Very severe cyclonic storm (VSCS)	118 – 220
8	Super cyclone (SC)	>220

4.2 Life Snatching Cyclones

During the study period (1981-2007), 91 cyclones formed in the Bay of Bengal among them 16 (18%) cyclones made landfall in the coastal region of Bangladesh. 12 (75%) of them were life snatching. A brief statistics of SST and decrease due to cyclones in Bangladesh are shown in Table 4.2. Fatality figure caused by the killer cyclone on 29-30 in April 1991 was the highest 138882.

The highest (lowest) SST was 30.33°C (26.18°C) at the land falling location of VSCS (CS) on May 20, 1998 (December 10, 1981). The SST at the land falling location of the killer cyclone was 29.24°C.

Table 4.2. Statistics of fatalities due to cyclones in Bangladesh.

Serial No.	Date of Landfall	Nature of the phenomena	SST at land falling location (°C)	Fatality
1	December 10, 1981	CS	26.18	72
2	October 15, 1983	CS	28.70	43
3	May 24, 1985	SCS	28.83	4364
4	November 29, 1988	VSCS	27.37	6133 ^a
5	April 29, 1991	SC	29.24	138882
6	May 02, 1994	VSCS	28.89	188
7	May 19, 1997	VSCS	29.25	155
8	September 27, 1997	VSCS	29.58	78
9	May 20, 1998	VSCS	30.33	14
10	October 28, 2000	CS	29.93	3
11	November 12, 2002	CS	28.75	2
12	November 15, 2007	SC	28.54	3363

^aboth Bangladesh and India,

4.3 Statistics on Seasonal SST and Cyclones

Table 4.3 shows the seasonal distribution of tropical cyclones, their duration and average spatial SST. From this Table it is clear that the formation of SCS and VSCS were dominated during the pre-monsoon and post-monsoon periods. The SST was 28.85°C (28.79°C) with standard deviation 0.21°C (0.22°C) in the pre-monsoon (post-monsoon) period. During pre-monsoon period 17 cyclones were formed, 3 of them were CS, 5

were SCS, 8 were VSCS and the rest 1 was SC. In the post-monsoon period 46 cyclones were formed, 17 of them were CS, 12 were SCS, 16 were VSCS and 1 was SC. The SST was the highest (lowest), 28.93°C (27.17°C) with standard deviation 0.26°C (0.25°C), in the monsoon (winter) season. During the monsoon period the number of total cyclones was 16, among them 13 were CS, 2 was SCS and 1 was VSCS. The number of tropical cyclone was the lowest in the winter season, 12 out of 91. In this season the number of CS was 5, SCS was 4 and VSCS was 3. The number of VSCS was the lowest, 4% (1 out of 28), during the monsoon period. From the Table 4.3 it is also found that the total cyclonic hours during the period 1981-2007 was 4858. In the post-monsoon period there were 53% (2909 hours out of 5449 hours) of the total cyclonic hours.

Table 4.3. Various types of tropical cyclones formed in the four seasons within 1981-2007, their total number, duration, seasonal mean SST and standard deviation of seasonal mean SST.

		Seasons					Total
		Winter	Pre-monsoon	Monsoon	Post-monsoon		
Cyclones	CS	Number	5	3	13	17	38
		Duration (hour)	255	105	324	1042	1756
	SCS	Number	4	5	2	12	23
		Duration (hour)	201	351	150	615	1317
	VSCS	Number	3	8	1	16	28
		Duration (hour)	264	680	65	1147	2156
	SC	Number	0	1	0	1	2
		Duration (hour)	0	115	0	105	220
Total	Cyclone	12	17	16	46	91	
	Duration (hour)	720	1251	569	2909	5449	
SST (°C)		27.17	28.85	28.93	28.79		
Standard deviation of SST (°C)		0.25	0.21	0.26	0.22		

It is found that the formation of SCS, VSCS and SC were lower at the lowest (27.17°C in winter) and highest (28.93°C in monsoon) SST, than that of SST in between

(28.85°C in pre-monsoon and 28.79°C in post-monsoon). Although SST was the highest in the monsoon period, tropical cyclones generally were less observed. This is due to the fact that the monsoon trough is generally located to the north over land during summer (Frank 1987). Hence, the required dynamical conditions, relative vorticity and vertical wind shear, for tropical cyclone formation (Gray 1979) are not satisfied.

4.4 Distribution of Depressions

The monthly and annual distributions of depressions which were formed in the Bay of Bengal are shown in the Table 4.4. 46 depressions formed during the study period and the percentage of occurrence was highest (21.7%) in the month of August and October. The yearly average formation of depression was 1.7 and the highest number (6) of depression was formed in the year of 1991 and 2006.

Table 4.4. Monthly and annual occurrence number of depressions in the Bay of Bengal during 1981-2007.

Year	J	F	M	A	M	J	J	A	S	O	N	D	Annual
1981	0	0	0	0	0	0	0	0	0	0	0	0	0
1982	0	0	0	0	0	0	0	0	0	0	0	0	0
1983	0	0	0	0	0	0	0	0	0	0	0	0	0
1984	0	0	0	0	0	0	0	0	0	0	0	0	0
1985	0	0	0	0	0	0	0	0	0	0	0	0	0
1986	0	0	0	0	0	0	0	0	0	0	0	0	0
1987	0	0	0	0	0	0	0	0	0	0	0	0	0
1988	0	0	0	0	0	0	0	0	0	0	0	0	0
1989	0	0	0	0	1	0	0	0	0	0	0	0	1
1990	0	0	0	0	0	0	0	3	0	0	0	0	3
1991	0	0	0	0	0	1	1	1	1	2	0	0	6
1992	0	0	0	0	0	0	1	0	0	0	0	0	1
1993	0	0	0	0	0	2	0	0	1	0	0	0	3
1994	0	0	1	0	0	0	0	0	0	0	0	0	1
1995	0	0	0	0	2	0	0	0	0	0	0	0	2
1996	0	0	0	0	0	0	0	0	0	0	0	0	0
1997	0	0	0	0	0	1	2	2	0	0	0	0	5
1998	0	0	0	0	0	1	0	0	0	2	0	0	3
1999	0	0	0	0	0	0	0	0	0	0	0	0	0
2000	0	0	0	0	0	0	0	0	0	0	0	0	0
2001	0	0	0	0	0	1	1	0	0	1	0	0	4
2002	0	0	0	0	1	0	0	0	0	1	0	0	2
2003	0	0	0	0	0	0	1	0	0	1	0	0	2
2004	0	0	0	0	0	0	0	0	0	1	0	0	1
2005	0	0	0	0	0	0	0	0	1	0	0	0	2
2006	0	0	0	0	0	0	0	3	2	1	0	0	6
2007	0	0	0	0	1	1	0	1	0	1	0	0	4
Total	0	0	1	0	5	7	6	10	5	10	0	0	46
Mean	0.0	0.0	0.0	0.0	0.2	0.3	0.2	0.4	0.2	0.4	0.0	0.0	1.7
% of Annual	0.0	0.0	2.2	0.0	10.9	15.2	13.0	21.7	10.9	21.7	0.0	0.0	100.0

4.5 Distribution of Deep Depressions

The monthly and annual distributions of deep depressions which were formed in the Bay of Bengal are shown in the Table 4.5. 25 deep depressions formed during the study period and the percentage of occurrence was highest (36%) in the month of October. The yearly average formation of deep depression was 0.9 and the highest number (5) of disturbance was formed in the year of 1989.

Table 4.5. Monthly and annual occurrence number of deep depressions in the Bay of Bengal during 1981-2007.

Year	J	F	M	A	M	J	J	A	S	O	N	D	Annual
1981	0	0	0	0	0	0	0	0	0	0	0	0	0
1982	0	0	0	0	0	0	0	0	0	0	0	0	0
1983	0	0	0	0	0	0	0	0	0	0	0	0	0
1984	0	0	0	0	0	0	0	0	0	0	0	0	0
1985	0	0	0	0	0	0	0	0	0	0	0	0	0
1986	0	0	0	0	1	0	0	1	1	0	0	0	3
1987	0	0	0	0	0	0	0	0	0	0	0	0	0
1988	0	0	0	0	0	0	0	0	0	0	0	0	0
1989	0	0	0	0	0	1	1	0	0	2	1	0	5
1990	0	0	0	0	0	0	0	0	0	1	0	0	1
1991	0	0	0	0	0	0	0	0	0	0	0	0	0
1992	0	0	0	0	0	0	0	0	0	2	0	0	2
1993	0	0	0	0	0	0	0	0	0	0	0	0	0
1994	0	0	0	0	0	0	0	0	0	1	0	0	1
1995	0	0	0	0	0	0	0	0	0	0	0	0	0
1996	0	0	0	0	1	0	0	0	1	1	0	0	3
1997	0	0	0	0	0	0	0	1	0	0	0	0	1
1998	0	0	0	0	0	0	0	0	0	0	0	0	0
1999	0	1	0	0	0	0	0	0	0	0	0	0	1
2000	0	0	0	0	0	0	0	0	0	1	0	1	2
2001	0	0	0	0	0	0	0	0	0	0	0	0	0
2002	0	0	0	0	0	0	0	0	0	0	0	0	0
2003	0	0	0	0	0	0	0	0	0	1	0	0	1
2004	0	0	0	0	0	0	0	0	0	0	0	0	0
2005	0	0	0	0	0	0	0	0	1	0	0	1	2
2006	0	0	0	0	0	0	0	1	0	0	0	0	1
2007	0	0	0	0	0	1	0	0	1	0	0	0	2
Total	0	1	0	0	2	2	1	3	4	9	1	2	25
Mean	0.0	0.0	0.0	0.0	0.1	0.1	0.0	0.1	0.1	0.3	0.0	0.1	0.9
% of Annual	0.0	4.0	0.0	0.0	8.0	8.0	4.0	12.0	16.0	36.0	4.0	8.0	100.0

4.6 Distribution of Cyclonic Storms

The monthly and annual distributions of cyclonic storms which were formed in the Bay of Bengal are shown in the Table 4.6. 44 cyclonic storms formed during the study period and the percentage of occurrence was highest (27.3%) in the month of November. The yearly average formation of cyclonic storm was 1.6 and the highest number (10) of cyclonic storm was formed in the year of 1981.

Table 4.6. Monthly and annual occurrence number of cyclonic storms in the Bay of Bengal during 1981-2007.

Year	J	F	M	A	M	J	J	A	S	O	N	D	Annual
1981	0	0	0	0	0	0	1	2	2	1	4	0	10
1982	0	0	0	0	0	1	1	3	1	0	0	0	6
1983	0	0	0	0	0	1	0	0	0	1	1	1	4
1984	0	0	0	0	0	0	1	1	0	0	0	0	2
1985	0	0	0	0	0	0	0	0	1	0	0	0	1
1986	0	0	0	0	0	0	0	0	0	0	0	0	0
1987	0	0	0	0	0	1	0	0	0	0	0	1	2
1988	0	0	0	0	0	0	0	0	0	0	0	1	1
1989	0	0	0	0	0	1	0	0	0	0	0	0	1
1990	0	0	0	0	0	0	0	0	0	0	1	0	1
1991	0	0	0	0	0	0	0	0	0	0	0	0	0
1992	0	0	0	0	0	0	0	0	0	0	1	0	1
1993	0	0	0	0	0	0	0	0	0	0	0	0	0
1994	0	0	0	0	0	0	0	0	0	0	0	0	0
1995	0	0	0	0	0	1	0	0	0	0	0	0	1
1996	0	0	0	0	0	0	0	0	0	1	0	0	1
1997	0	0	0	0	0	0	0	0	0	0	1	0	1
1998	0	0	0	0	0	0	0	0	0	0	1	0	1
1999	0	0	0	0	0	0	0	0	0	0	0	0	0
2000	0	0	1	0	0	0	0	0	0	1	0	0	2
2001	0	0	0	0	0	0	0	0	0	1	0	0	1
2002	0	0	0	0	0	0	0	0	0	0	2	0	2
2003	0	0	0	0	1	0	0	0	0	0	0	0	1
2004	0	0	0	0	0	0	0	0	0	0	0	0	0
2005	1	0	0	0	0	0	0	0	0	1	1	1	4
2006	0	0	0	0	0	0	0	0	0	0	0	0	0
2007	0	0	0	0	1	0	0	0	0	0	0	0	1
Total	1	0	1	0	2	5	3	6	4	6	12	4	44
Mean	0.0	0.0	0.0	0.0	0.1	0.2	0.1	0.2	0.1	0.2	0.4	0.1	1.6
% of Annual	2.3	0.0	2.3	0.0	4.5	11.4	6.8	13.6	9.1	13.6	27.3	9.1	100.0

4.7 Distribution of Severe Cyclonic Storms

The monthly and annual distributions of severe cyclonic storms which were formed in the Bay of Bengal are shown in the Table 4.7. 23 severe cyclonic storms were formed in the months of May, June, October, November and December during the study period and the percentage of occurrence was highest (30.4%) in the month of October. The yearly average formation of severe cyclonic storm was 0.9 and the highest number (4) of severe cyclonic storm was formed in the year of 1985.

Table 4.7. Monthly and annual occurrence number of severe cyclonic storms in the Bay of Bengal during 1981-2007.

Year	J	F	M	A	M	J	J	A	S	O	N	D	Annual
1981	0	0	0	0	0	0	0	0	0	0	0	0	0
1982	0	0	0	0	0	1	0	0	0	2	0	0	3
1983	0	0	0	0	0	0	0	0	0	2	0	0	2
1984	0	0	0	0	0	0	0	0	0	0	0	0	0
1985	0	0	0	0	0	0	0	0	0	2	1	1	4
1986	0	0	0	0	0	0	0	0	0	0	1	0	1
1987	0	0	0	0	0	0	0	0	0	1	0	0	1
1988	0	0	0	0	0	0	0	0	0	0	0	0	0
1989	0	0	0	0	0	0	0	0	0	0	0	0	0
1990	0	0	0	0	0	0	0	0	0	0	0	1	1
1991	0	0	0	0	1	0	0	0	0	0	1	0	2
1992	0	0	0	0	1	0	0	0	0	0	0	0	1
1993	0	0	0	0	0	0	0	0	0	0	0	1	1
1994	0	0	0	0	0	0	0	0	0	0	0	0	0
1995	0	0	0	0	0	0	0	0	0	0	1	0	1
1996	0	0	0	0	1	1	0	0	0	0	1	0	3
1997	0	0	0	0	0	0	0	0	0	0	0	0	0
1998	0	0	0	0	0	0	0	0	0	0	0	0	0
1999	0	0	0	0	0	0	0	0	0	0	0	0	0
2000	0	0	0	0	0	0	0	0	0	0	0	0	0
2001	0	0	0	0	0	0	0	0	0	0	0	0	0
2002	0	0	0	0	0	0	0	0	0	0	0	0	0
2003	0	0	0	0	1	0	0	0	0	0	0	1	2
2004	0	0	0	0	1	0	0	0	0	0	0	0	1
2005	0	0	0	0	0	0	0	0	0	0	0	0	0
2006	0	0	0	0	0	0	0	0	0	0	0	0	0
2007	0	0	0	0	0	0	0	0	0	0	0	0	0
Total	0	0	0	0	5	2	0	0	0	7	5	4	23
Mean	0.0	0.0	0.0	0.0	0.2	0.1	0.0	0.0	0.0	0.3	0.2	0.1	0.9
% of Annual	0.0	0.0	0.0	0.0	21.7	8.7	0.0	0.0	0.0	30.4	21.7	17.4	100.0

4.8 Distribution of Very Severe Cyclonic Storms and Super Cyclones

The monthly and annual distributions of very severe cyclonic storms and super cyclones which were formed in the Bay of Bengal are shown in the Table 4.8. 30 very severe cyclonic storms and super cyclones were formed during the study period and the percentage of occurrence was highest (43.3%) in the month of November. The yearly average formation of very severe cyclonic storms and super cyclones was 1.1 and the highest number (3) of very severe cyclonic storms and super cyclones was formed in the year of 1984 and 1987.

Table 4.8. Monthly and annual occurrence number of very severe cyclonic storms and super cyclones in the Bay of Bengal during 1981-2007.

Year	J	F	M	A	M	J	J	A	S	O	N	D	Annual
1981	0	0	0	0	0	0	0	0	0	0	0	1	1
1982	0	0	0	0	1	0	0	0	0	0	0	0	1
1983	0	0	0	0	0	0	0	0	0	0	1	0	1
1984	0	0	0	0	0	0	0	0	0	1	2	0	3
1985	0	0	0	0	1	0	0	0	0	0	0	0	1
1986	0	0	0	0	0	0	0	0	0	0	0	0	0
1987	0	1	0	0	0	0	0	0	0	1	1	0	3
1988	0	0	0	0	0	0	0	0	0	0	2	0	2
1989	0	0	0	0	1	0	0	0	0	0	1	0	2
1990	0	0	0	0	1	0	0	0	0	0	0	0	1
1991	0	0	0	1	0	0	0	0	0	0	0	0	1
1992	0	0	0	0	0	0	0	0	0	0	1	0	1
1993	0	0	0	0	0	0	0	0	0	0	0	0	0
1994	0	0	0	1	0	0	0	0	0	0	0	0	1
1995	0	0	0	0	0	0	0	0	0	0	1	0	1
1996	0	0	0	0	0	0	0	0	0	0	1	1	2
1997	0	0	0	0	1	0	0	0	1	0	0	0	2
1998	0	0	0	0	1	0	0	0	0	0	1	0	2
1999	0	0	0	0	0	0	0	0	0	2	0	0	2
2000	0	0	0	0	0	0	0	0	0	0	1	0	1
2001	0	0	0	0	0	0	0	0	0	0	0	0	0
2002	0	0	0	0	0	0	0	0	0	0	0	0	0
2003	0	0	0	0	0	0	0	0	0	0	0	0	0
2004	0	0	0	0	0	0	0	0	0	0	0	0	0
2005	0	0	0	0	0	0	0	0	0	0	0	0	0
2006	0	0	0	1	0	0	0	0	0	0	0	0	1
2007	0	0	0	0	0	0	0	0	0	0	1	0	1
Total	0	1	0	3	6	0	0	0	1	4	13	2	30
Mean	0.0	0.0	0.0	0.1	0.2	0.0	0.0	0.0	0.0	0.1	0.5	0.1	1.1
% of Annual	0.0	3.3	0.0	10.0	20.0	0.0	0.0	0.0	3.3	13.3	43.3	6.7	100.0

4.9 Distribution of Cyclones

The monthly and annual distributions of cyclones (including cyclonic storms, severe cyclonic storms, very severe cyclonic storms and super cyclones) which were formed in the Bay of Bengal are shown in the Table 4.9. Total 97 cyclones formed during the study period and the percentage of occurrence was highest (30.9%) in the month of November. The yearly average formation of cyclones was 3.6 and the highest number (11) of cyclones was formed in the year of 1981.

Table 4.9. Monthly and annual occurrence number of cyclones in the Bay of Bengal during 1981-2007.

Year	J	F	M	A	M	J	J	A	S	O	N	D	Annual
1981	0	0	0	0	0	0	1	2	2	1	4	1	11
1982	0	0	0	0	1	2	1	3	1	2	0	0	10
1983	0	0	0	0	0	1	0	0	0	3	2	1	7
1984	0	0	0	0	0	0	1	1	0	1	2	0	5
1985	0	0	0	0	1	0	0	0	1	2	1	1	6
1986	0	0	0	0	0	0	0	0	0	0	1	0	1
1987	0	1	0	0	0	1	0	0	0	2	1	1	6
1988	0	0	0	0	0	0	0	0	0	0	2	1	3
1989	0	0	0	0	1	1	0	0	0	0	1	0	3
1990	0	0	0	0	1	0	0	0	0	0	1	1	3
1991	0	0	0	1	1	0	0	0	0	0	1	0	3
1992	0	0	0	0	1	0	0	0	0	0	2	0	3
1993	0	0	0	0	0	0	0	0	0	0	0	1	1
1994	0	0	0	1	0	0	0	0	0	0	0	0	1
1995	0	0	0	0	0	1	0	0	0	0	2	0	3
1996	0	0	0	0	1	1	0	0	0	1	2	1	6
1997	0	0	0	0	1	0	0	0	1	0	1	0	3
1998	0	0	0	0	1	0	0	0	0	0	2	0	3
1999	0	0	0	0	0	0	0	0	0	2	0	0	2
2000	0	0	1	0	0	0	0	0	0	1	1	0	3
2001	0	0	0	0	0	0	0	0	0	1	0	0	1
2002	0	0	0	0	0	0	0	0	0	0	2	0	2
2003	0	0	0	0	2	0	0	0	0	0	0	1	3
2004	0	0	0	0	1	0	0	0	0	0	0	0	1
2005	1	0	0	0	0	0	0	0	0	1	1	1	4
2006	0	0	0	1	0	0	0	0	0	0	0	0	1
2007	0	0	0	0	1	0	0	0	0	0	1	0	2
Total	1	1	1	3	13	7	3	6	5	17	30	10	97
Mean	0.0	0.0	0.0	0.1	0.5	0.3	0.1	0.2	0.2	0.6	1.1	0.4	3.6
% of Annual	1.0	1.0	1.0	3.1	13.4	7.2	3.1	6.2	5.2	17.5	30.9	10.3	100.0

4.10 Distribution of Disturbances

The monthly and annual distributions of disturbances (including depressions, deep depressions, cyclonic storms, severe cyclonic storms, very severe cyclonic storms and super cyclones) which were formed in the Bay of Bengal are shown in the Table 4.10.

Table 4.10. Monthly and annual occurrence number of disturbances in the Bay of Bengal during 1981-2007.

Year	J	F	M	A	M	J	J	A	S	O	N	D	Annual
1981	0	0	0	0	0	0	1	2	2	1	4	1	11
1982	0	0	0	0	1	2	1	3	1	2	0	0	10
1983	0	0	0	0	0	1	0	0	0	3	2	1	7
1984	0	0	0	0	0	0	1	1	0	1	2	0	5
1985	0	0	0	0	1	0	0	0	1	2	1	1	6
1986	0	0	0	0	1	0	0	1	1	0	1	0	4
1987	0	1	0	0	0	1	0	0	0	2	1	1	6
1988	0	0	0	0	0	0	0	0	0	0	2	1	3
1989	0	0	0	0	2	2	1	0	0	2	2	0	9
1990	0	0	0	0	1	0	0	3	0	1	1	1	7
1991	0	0	0	1	1	1	1	1	1	2	1	0	9
1992	0	0	0	0	1	0	1	0	0	2	2	0	6
1993	0	0	0	0	0	2	0	0	1	0	0	1	4
1994	0	0	1	1	0	0	0	0	0	1	0	0	3
1995	0	0	0	0	2	1	0	0	0	0	2	0	5
1996	0	0	0	0	2	1	0	0	1	2	2	1	9
1997	0	0	0	0	1	1	2	3	1	0	1	0	9
1998	0	0	0	0	1	1	0	0	0	2	2	0	6
1999	0	1	0	0	0	0	0	0	0	2	0	0	3
2000	0	0	1	0	0	0	0	0	0	2	1	1	5
2001	0	0	0	0	0	1	1	0	0	2	1	0	5
2002	0	0	0	0	1	0	0	0	0	1	2	0	4
2003	0	0	0	0	2	0	1	0	0	2	0	1	6
2004	0	0	0	0	1	0	0	0	0	1	0	0	2
2005	1	0	0	0	0	0	0	0	2	1	2	2	8
2006	0	0	0	1	0	0	0	4	2	1	0	0	8
2007	0	0	0	0	2	2	0	1	1	1	1	0	8
Total	1	2	2	3	20	16	10	19	14	36	33	12	168
Mean	0.0	0.1	0.1	0.1	0.7	0.6	0.4	0.7	0.5	1.3	1.2	0.4	6.2
% of Annual	0.6	1.2	1.2	1.8	11.9	9.5	6.0	11.3	8.3	21.4	19.6	7.1	100.0

168 disturbances formed during the study period and the percentage of occurrence was highest (21.4%) in the month of October. The yearly average formation of

disturbances was 6.2 and the highest number (11) of disturbances was formed in the year of 1981. There were 3 disturbances which were formed on 14/6/1990, 12/9/2000 and 1/10/2000 but their latitude and longitude were not mentioned in the BMD's Log Book, so these were excluded.

4.11 Monthly and Yearly Distributions of Tropical Disturbances and SST

Within the study period the total number of formation of disturbance (including depression, deep depression, cyclonic storm, severe cyclonic storm, very severe cyclonic storm and super cyclone) were 168 as shown in Figure 4.1, 54% (91 out of 168) of them were cyclone. Maximum occurrence number (13) of VSCS and SC was in the month of November, whereas the most active month for the formation of SCS was in October. Maximum number (12) of CS was formed in the month of November. In the month of October maximum number (9) of DD was also formed. The most active months for the formation of D were in August and October and the number was 10.

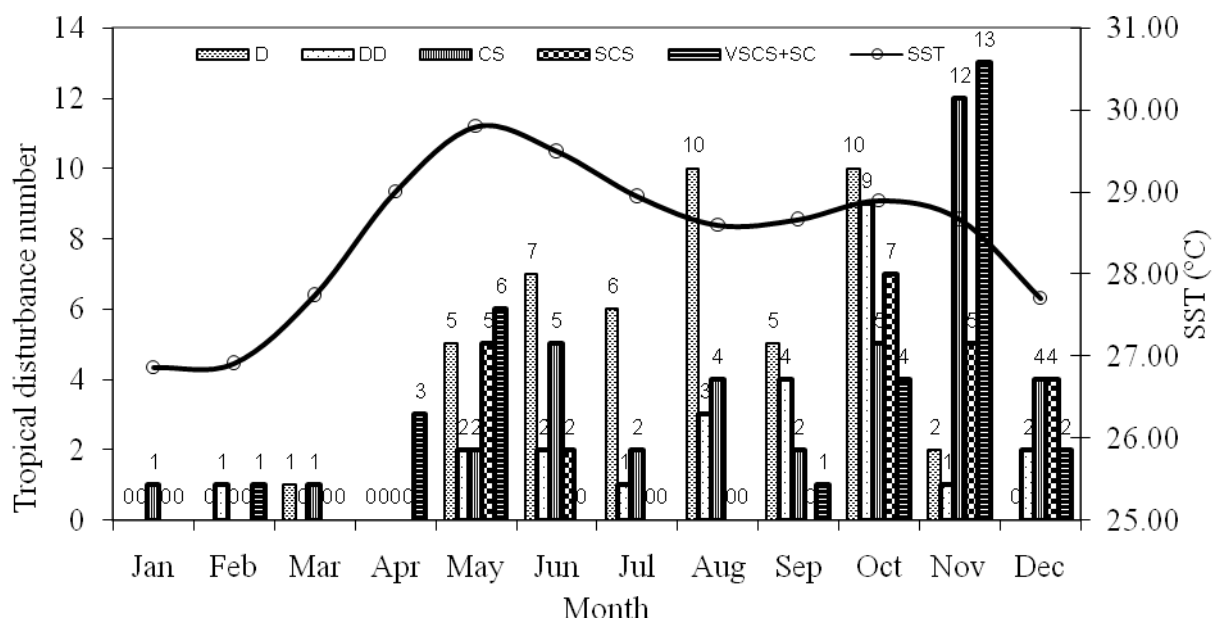


Fig.4.1. Monthly occurrence number of tropical disturbance and SST during the period 1981-2007

The Figure 4.2 shows the yearly number of disturbances and corresponding SST. The warmest year was 1998; in this year 6 disturbances were formed. In the coolest year, 1984, the formation of disturbances was 5 and the maximum frequency of cyclone was in the year of 1982.

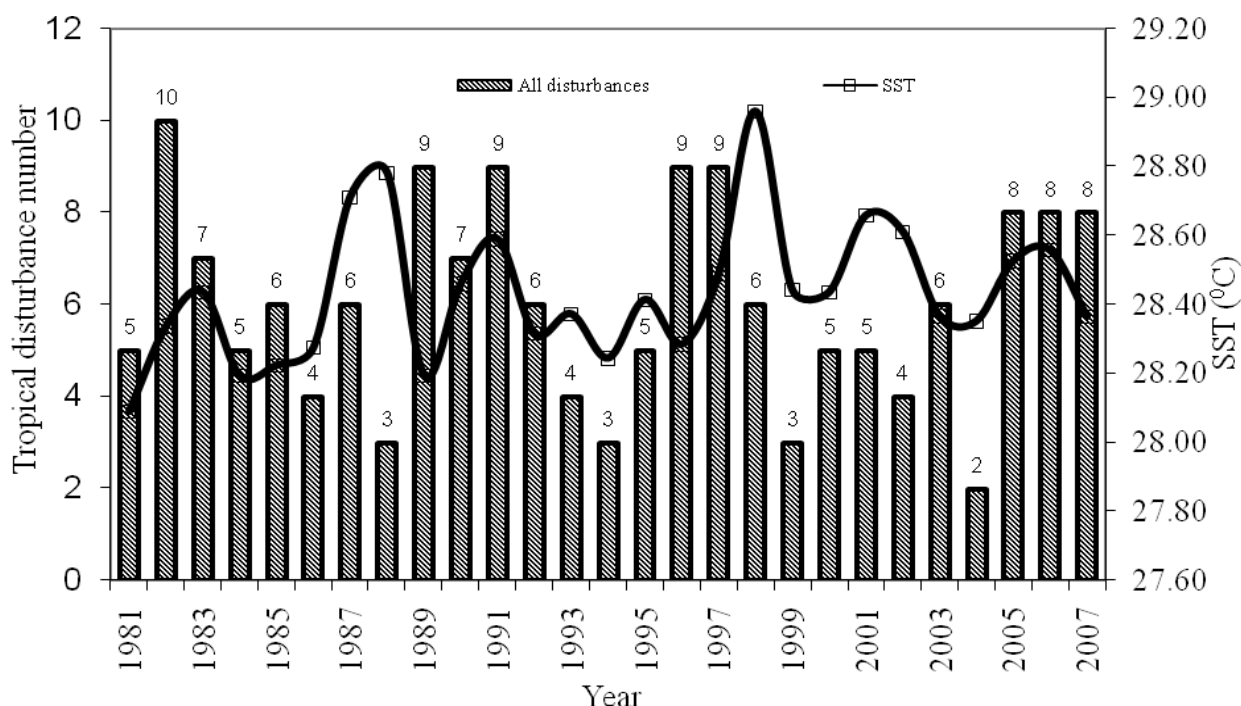


Fig.4.2. Yearly occurrence number of tropical disturbances and SST during the period 1981-2007.

4.12 Distribution of Monthly SST Anomalies and Cyclones

Figure 4.3 shows the monthly distribution of SST anomalies of the Bay of Bengal. The positive anomalies were in the months from April to November. On the other hand, negative anomalies were in the months from December to March. In the positive anomalies there were two peaks, one major peak was in the month of May and another minor peak in October. In May and October the SST were 5% and 1% more than the average spatial SST, respectively. The highest negative anomaly was found in January. The value of SST was 6% less than the average spatial SST.

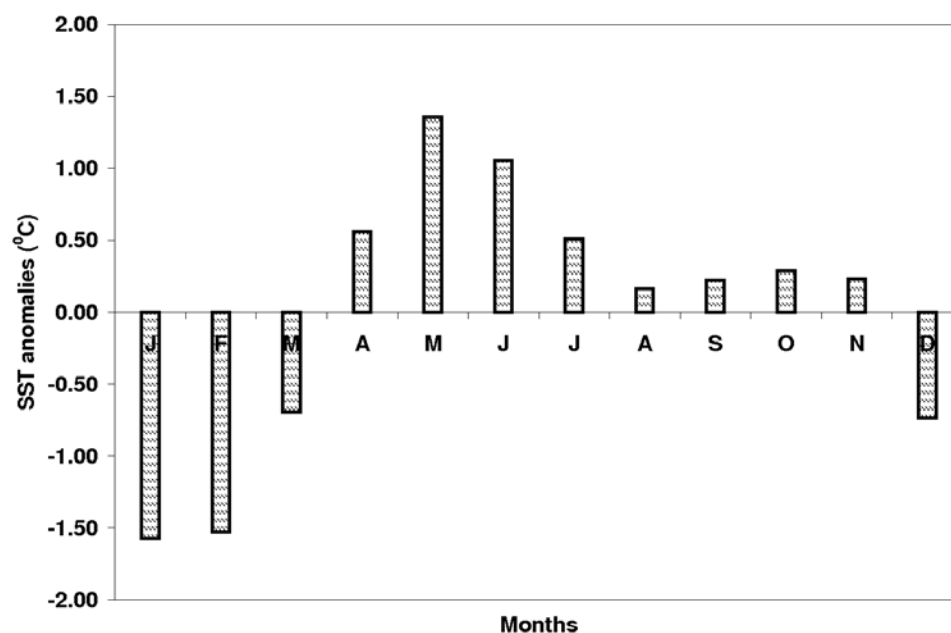


Fig. 4.3. Monthly distribution of SST anomalies of the Bay of Bengal during 1981-2007.

From Figure 4.4 it is found that the highest occurrence of cyclones was in the month of November. In this month cyclone formation was 33% (30 out of 91) of the total cyclones. From Figure 4.4 it is clear that occurrence of cyclones show two peaks, one major peak was in the month of November and the other minor peak was in May.

From Figure 4.3 and Figure 4.4 it is found the percentage of cyclone formation in the month of minor positive peak SST anomaly (Figure 4.3) was 18% (16 out of 91) whereas 14% (13 out of 91) cyclones formed on the month of highest positive peak SST anomaly (Figure 4.3). On the other hand in the highest negative SST anomaly month which was in January, the number of cyclones formation was 1% (1 out of 91) of the total cyclones. There were 4 months (December, January, February and March) having negative SST anomalies. During that 4 months 14% (13 out of 91) of the total cyclones were formed and in last 3 months (January, February and March) only 3% (3 out of 91) cyclones were found.

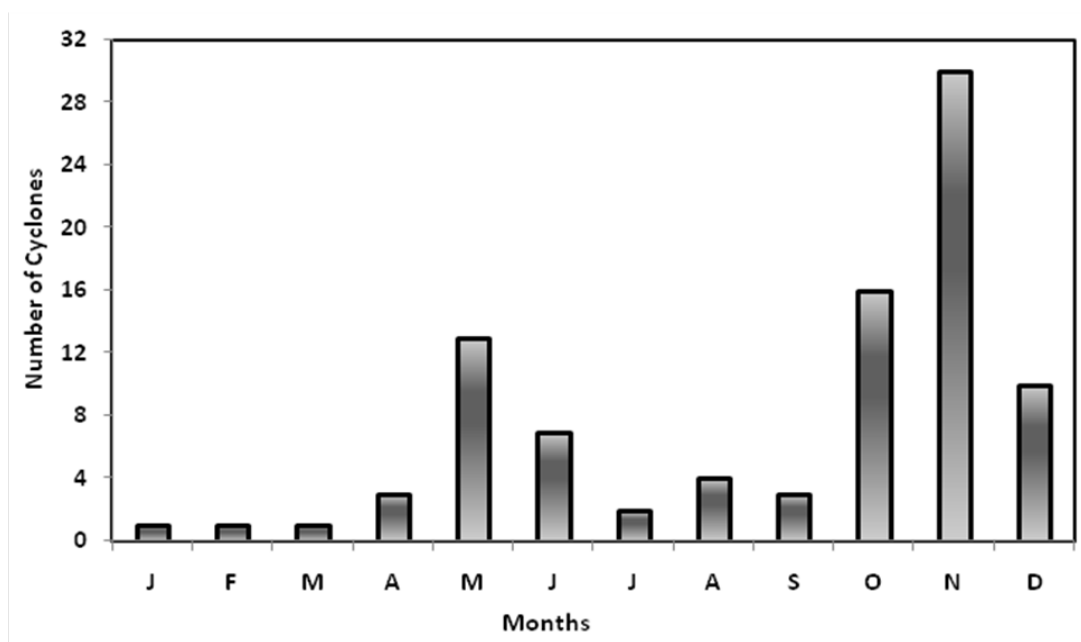


Fig. 4.4. Monthly distribution of 91 cyclones formed over the Bay of Bengal during 1981-2007.

4.13 Trends of SST and Tropical Cyclone Frequency

The SST shows positive trend in the winter season (Figure 4.5). In each winter season the increment of SST was 0.011°C . The tropical cyclone formation shows negative trend (Figure 4.5). In each winter season the decreasing rate of cyclone formation was 0.012 .

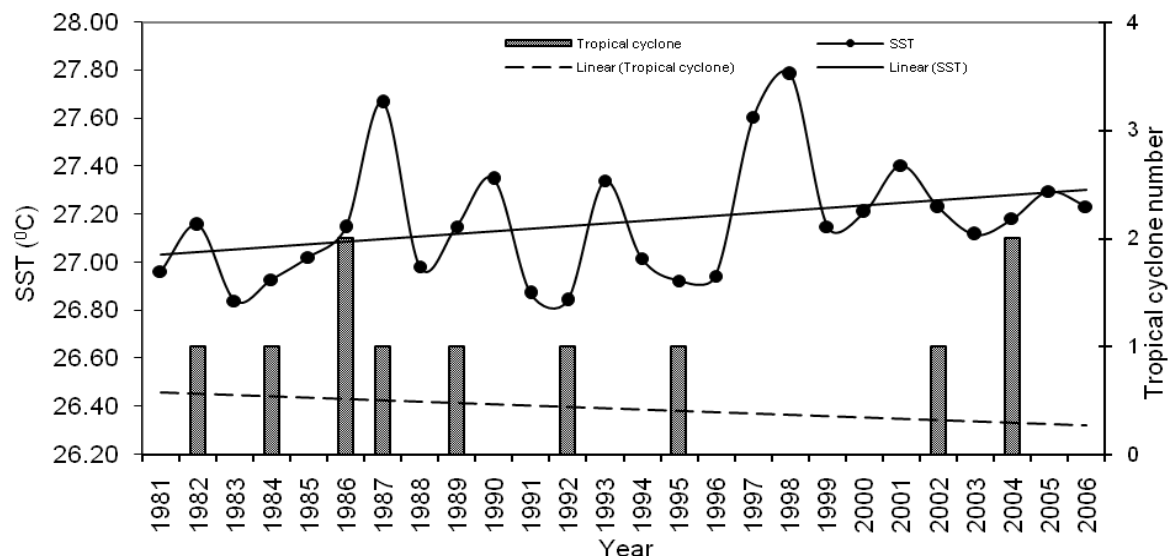


Fig.4.5. Trends of tropical cyclone frequency and SST in winter season from 1982-2007.

The SST shows positive trend in pre-monsoon season (Figure 4.6). In each pre-monsoon season the increment of SST was 0.003°C . The tropical cyclone formation also shows positive trend (Figure 4.6). In each pre-monsoon season the increasing rate of cyclone formation was 0.014.

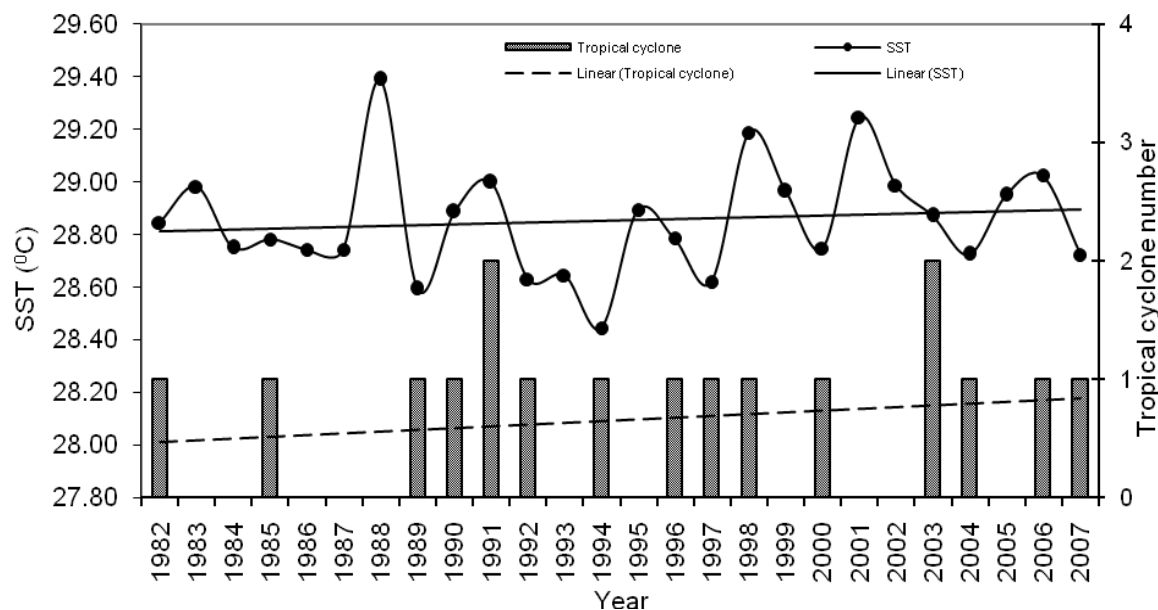


Fig.4.6. Trends of tropical cyclone frequency and SST in pre-monsoon season from 1982-2007.

The SST shows positive trend in monsoon season (Figure 4.7). In each monsoon season the increment of SST was 0.003°C . The tropical cyclone formation shows negative trend (Figure 4.7). In each monsoon season the decreasing rate of cyclone formation was 0.094.

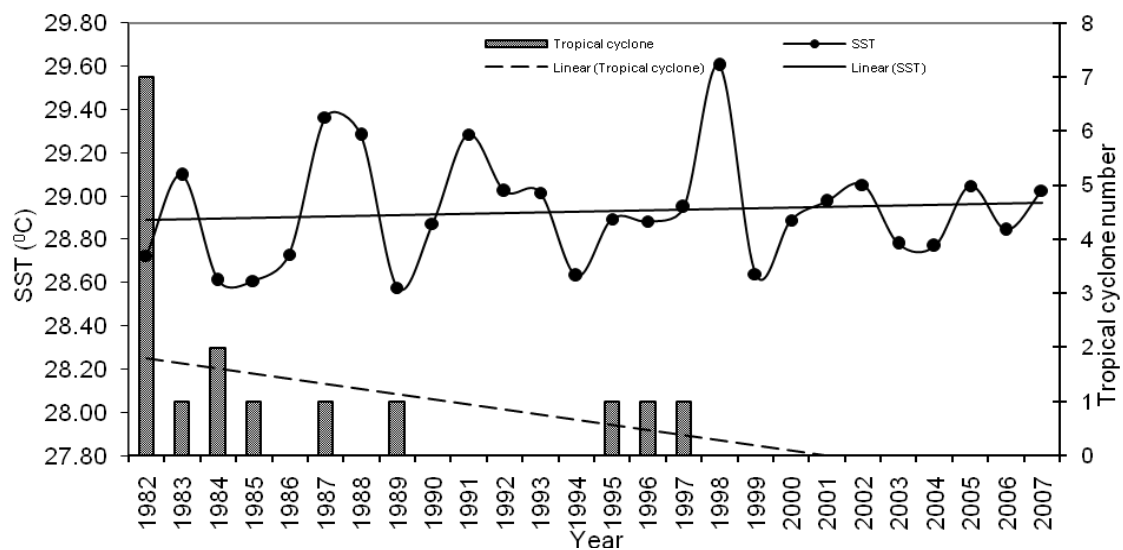


Fig.4.7. Trends of tropical cyclone frequency and SST in monsoon season from 1982-2007.

The SST shows positive trend in post-monsoon season (Figure 4.8). In each post-monsoon the increment of SST was 0.01°C . The tropical cyclone formation shows negative trend (Figure 4.8). In each post-monsoon season the decreasing rate of cyclone formation was 0.089 .

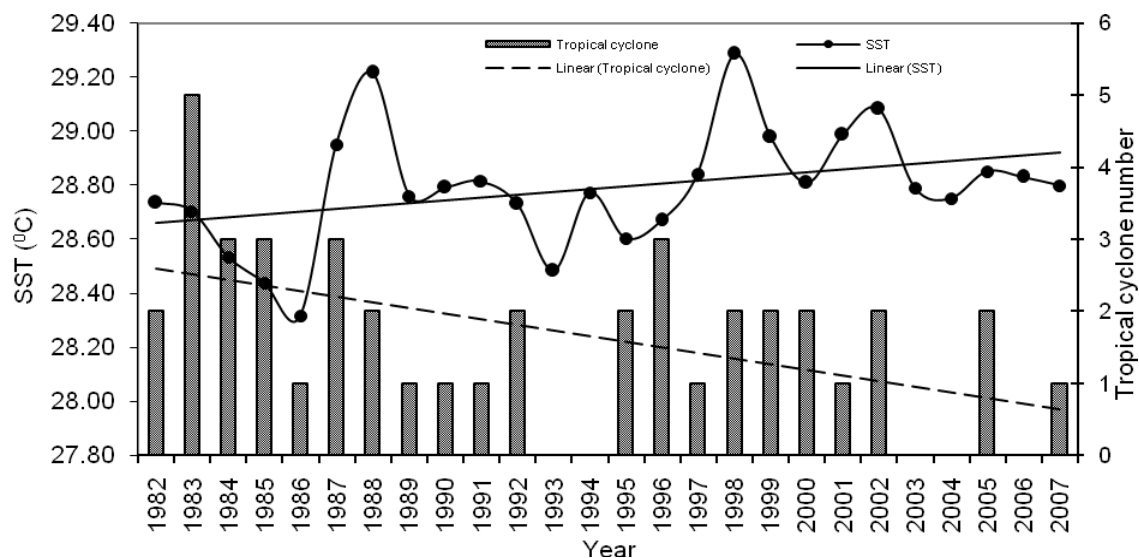


Fig.4.8. Trends of tropical cyclone frequency and SST in post-monsoon season from 1982-2007.

Figure 4.9 shows yearly trend of SST which was positive throughout the study period. The yearly increment of SST was 0.008°C . The tropical cyclone formation shows negative trend (Figure 4.9). The decreasing rate of cyclone formation per year was 0.170.

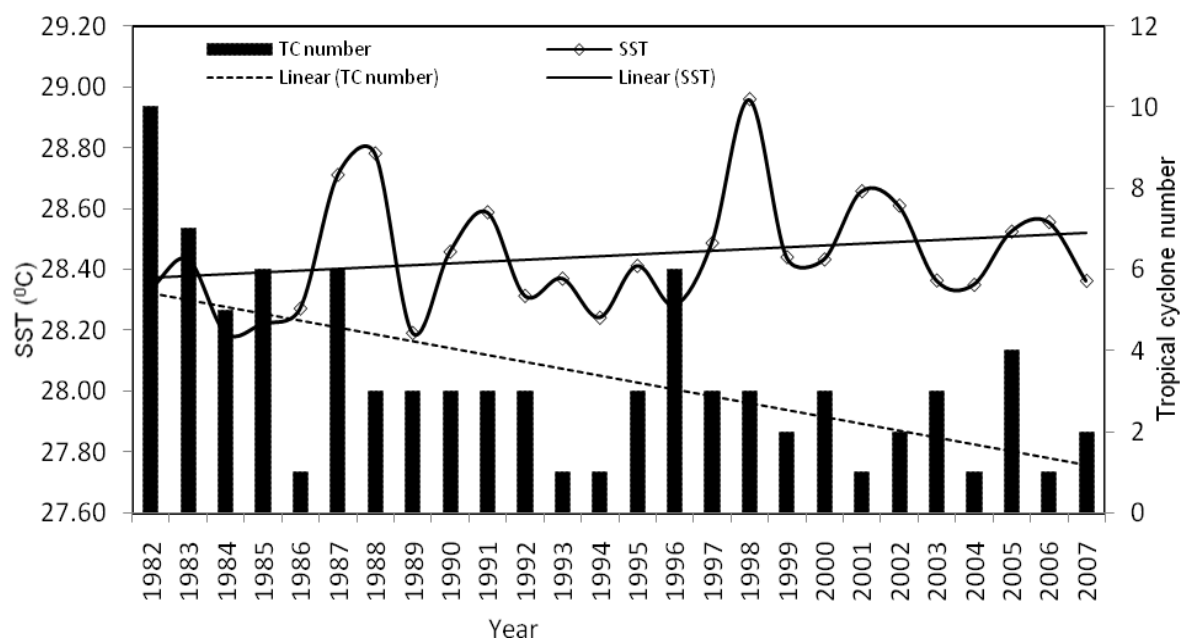


Fig.4.9. Yearly trends of tropical cyclone frequency and SST from 1981-2007.

So the frequency of cyclone showing positive trend in pre-monsoon season and in all other seasons it was showing negative trends.

The decadal variation of SST and cyclone frequency is shown in Figure 4.10. The increasing trend of SST was 0.04°C and decreasing trend of cyclone frequency was 17.5 per decade. In the first decade (1981-1990) the number of total cyclone formation was 49 and the SST was 28.41°C whereas in the second decade (1991-2000) the number of cyclone formation was 28 and the SST was 28.47°C and in the third decade (2001-2007) the number of cyclone formation was 14 and the SST was 28.49°C . It is found that the frequency of tropical cyclone in second decade and in third decade was, respectively, 42% and 150% lower than the first decade.

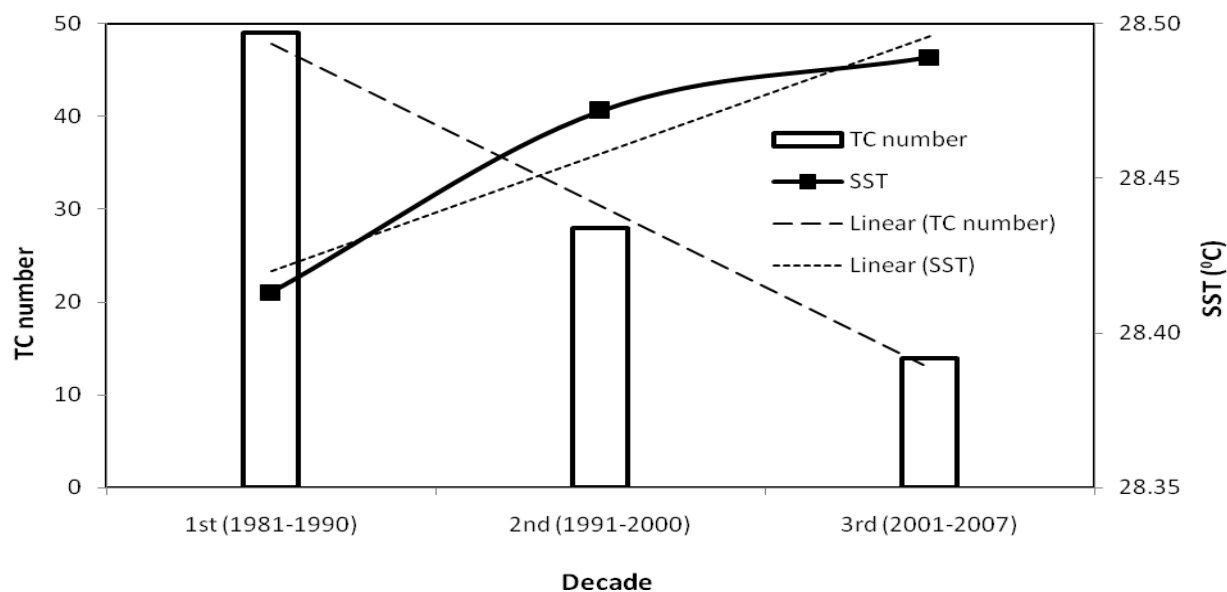


Fig. 4.10: Decadal trends of tropical cyclone frequency and SST from 1981-2007.

4.14 Trends of SST and Tropical Cyclone Duration

The SST shows positive trend in the winter season (Figure 4.11). In each winter season the increment of SST was 0.011°C . The duration of tropical cyclone also shows positive trend (Figure 4.11). In each winter season the increasing rate of cyclone duration was 0.529 h/winter .

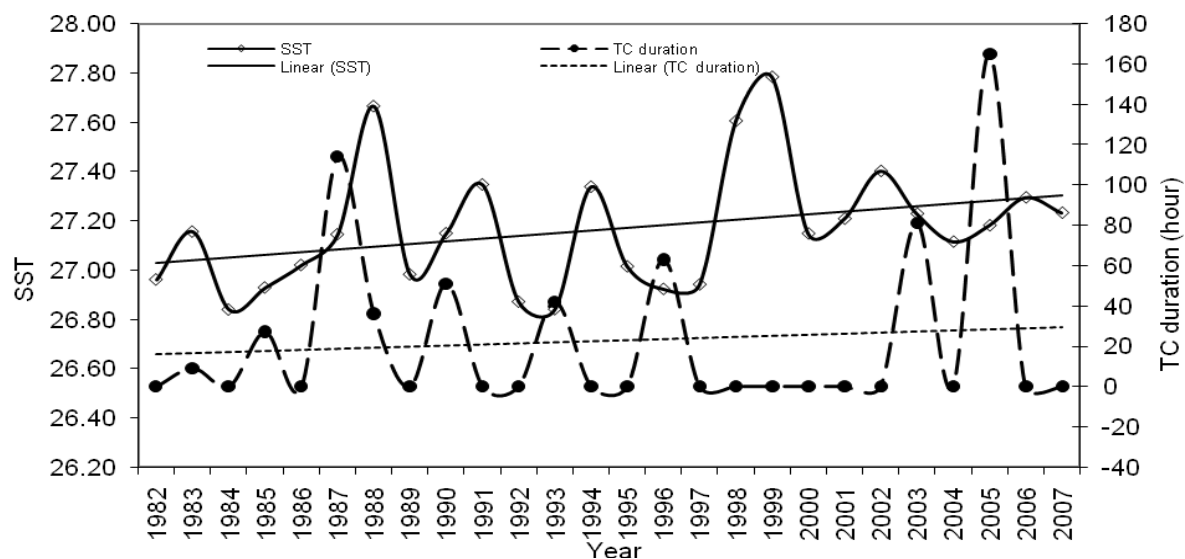


Fig.4.11. Variation of SST and TC duration in winter season during 1982-2007.

The SST shows positive trend in the pre-monsoon season (Figure 4.12). In each pre-monsoon season the increment of SST was 0.003°C . The duration of tropical cyclone also shows positive trend (Figure 4.12). In each pre-monsoon season the increasing rate of cyclone duration was $0.964\text{ h/pre-monsoon}$.

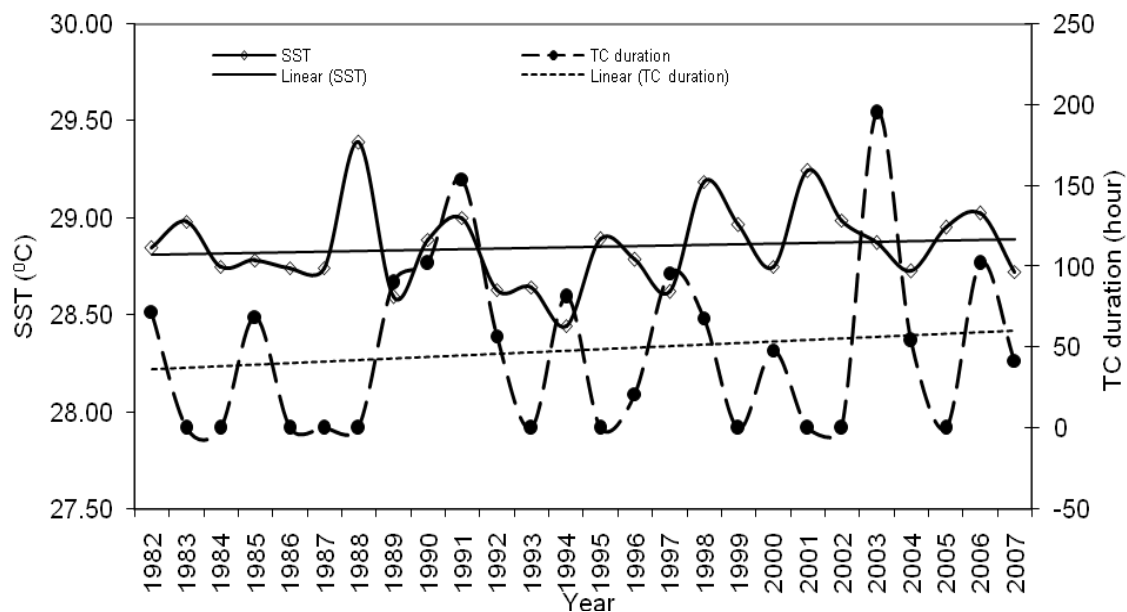


Fig. 4.12. Variation of SST and TC duration in pre-monsoon season during 1982-2007.

The SST shows positive trend in the monsoon season (Figure 4.13). In each monsoon season the increment of SST was 0.003°C . The duration of tropical cyclone shows negative trend (Figure 4.13). In each monsoon season the decreasing rate of cyclone duration was 2.557 h/monsoon .

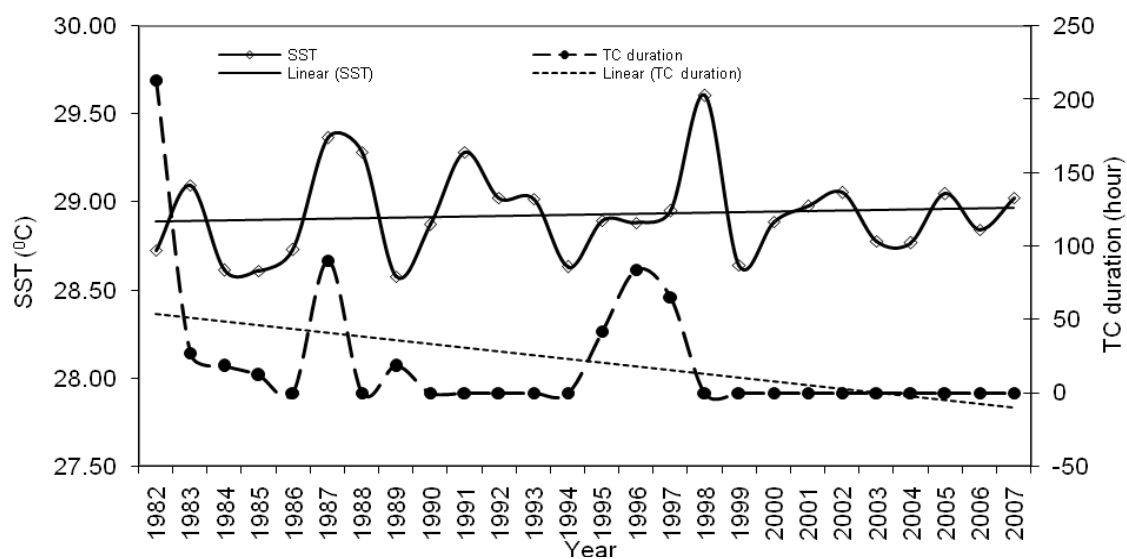


Fig. 4.13. Variation of SST and TC duration in monsoon season during 1982-2007.

The SST shows positive trend in the post-monsoon season (Figure 4.14). In each post-monsoon season the increment of SST was 0.011°C . The duration of tropical cyclone shows negative trend (Figure 4.14). In each post-monsoon season the decreasing rate of cyclone duration was $2.831\text{ h/post-monsoon}$.

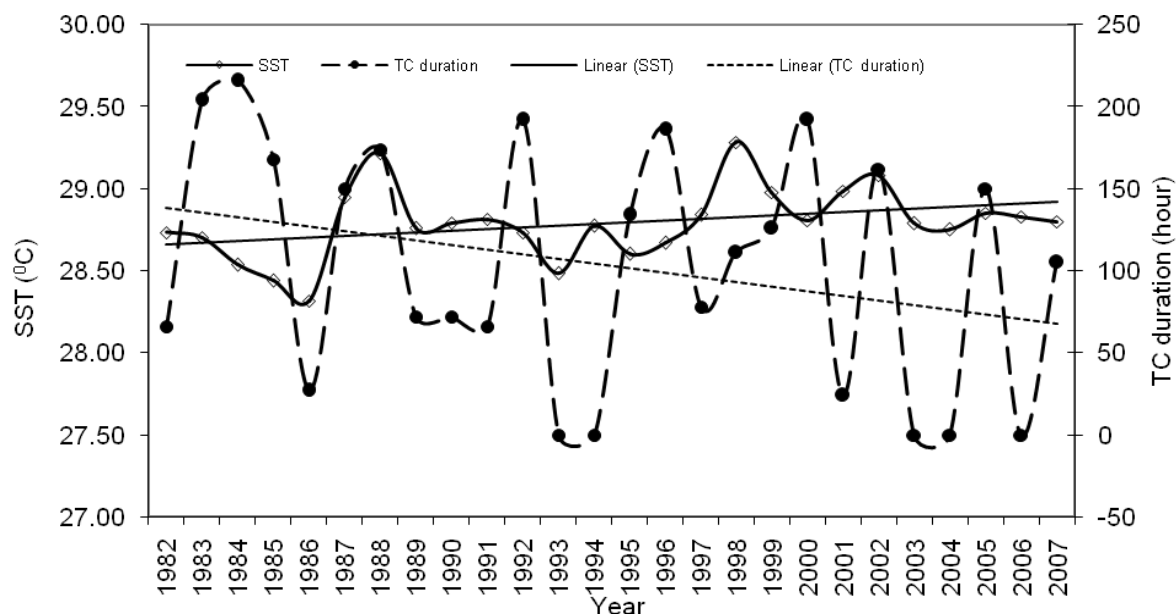


Fig. 4.14. Variation of SST and TC duration in post-monsoon season during 1982-2007.

Figure 4.15 shows yearly trend of SST which was positive through out the study period. The yearly increment of SST was 0.008°C . The duration of tropical cyclone shows negative trend. The decreasing rate of cyclone duration per year was 3.895 h/year .

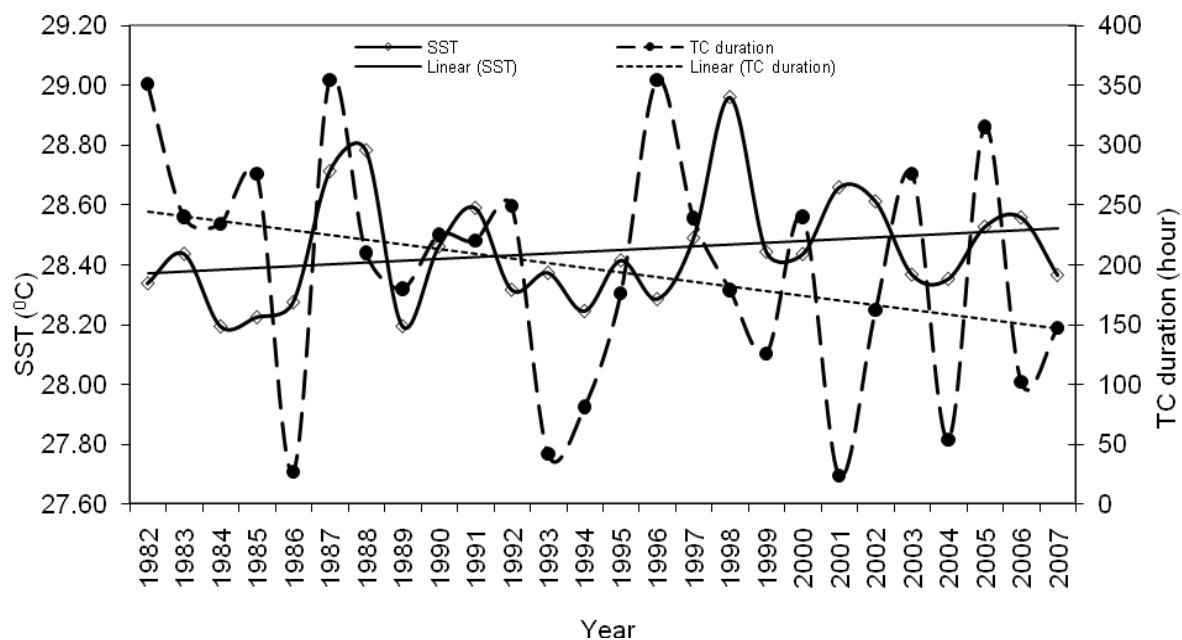


Fig. 4.15. Yearly variation of SST and TC during 1981-2007.

So the duration of cyclone showing positive trends in winter and in pre-monsoon seasons; in monsoon and post-monsoon seasons it was showing negative trends.

4.15 SST and Tropical Cyclone Intensity

Scatter plots are compiled by matching the year, month, week and position of each cyclone first attained its maximum intensity with the corresponding SST. In this study the relationship between SST and intensity of cyclone is not straightforward, similar results also shown in a study of Patrick et al. (2006). But in studies of Evans (1990), Baik and Peak (1998) showed that the peak in intensity occurring below the maximum SST of the cyclones formed in the North Atlantic Ocean. It was found from the Figure 4.16 that there was no VSCS below the SST of 27.44°C and after the SST of 30.34°C .

Figure 4.16 shows that the cent percent of the cyclones got their highest wind speed within the temperature range 28.00°C to 29.50°C. There were 7 tropical cyclones with maximum wind speed ≥ 200 km/h; 86% (6 out of 7) of them attained uppermost wind speed within the temperature range from 28.00°C to 29.50°C. After 29.50°C the intensity of the maximum wind speed depicted decreasing trend, except one cyclone got its maximum wind speed, 240 km/h, at 30.22°C. There were 20 cyclones within the temperature range 30.5°C \leq temperature < 29.5 °C. 50% (10 out of 20) of those cyclones got the maximum wind speed ≥ 100 km/h, 40% (8 out of 20) cyclones were within the speed range 150km/h \leq wind speed > 100 km/h and only 10% (2 out of 20) cyclones crossed 150km/h at its maximum wind speed. This suggests the existence of a temperature dependency but not a continuous positive relationship between maximum storm intensity and SST.

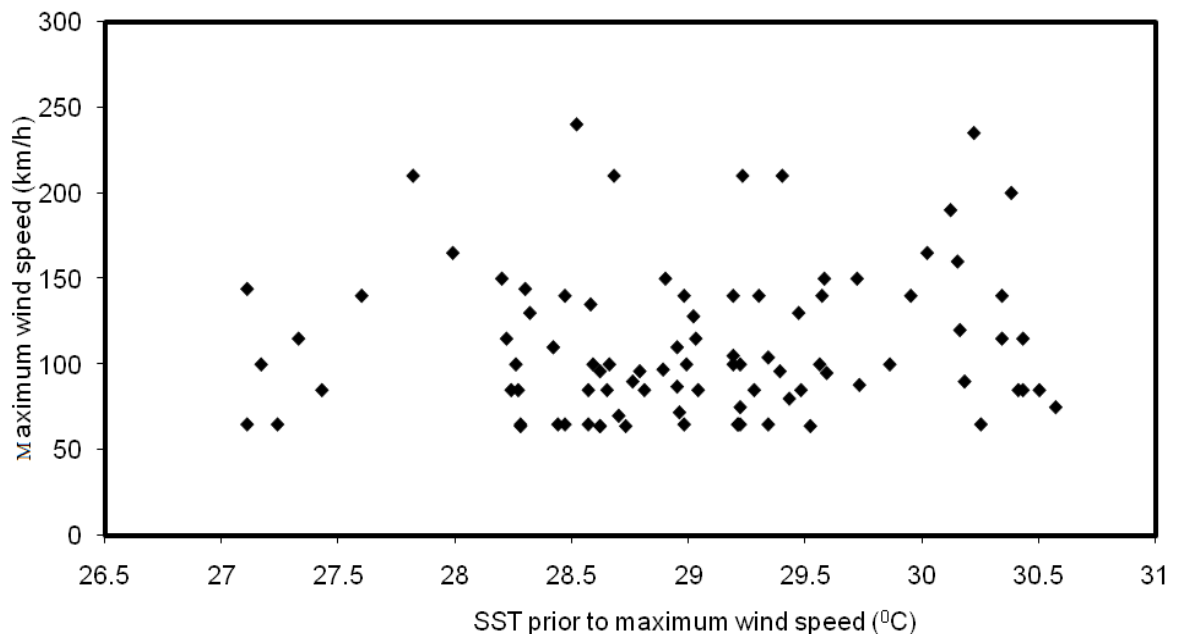


Fig. 4.16. The relationship between maximum wind speed and SST encountered prior to reaching the maximum wind speed.

The initial SST of 91 cyclones formed in the study period is plotted with maximum wind speed in the Figure 4.17. It is found that the wind speed increases with SST upto 28.5 °C then the speed showing to decrease till 30 °C after that the speed increases until 30.3 °C and it is showing decreasing trends.

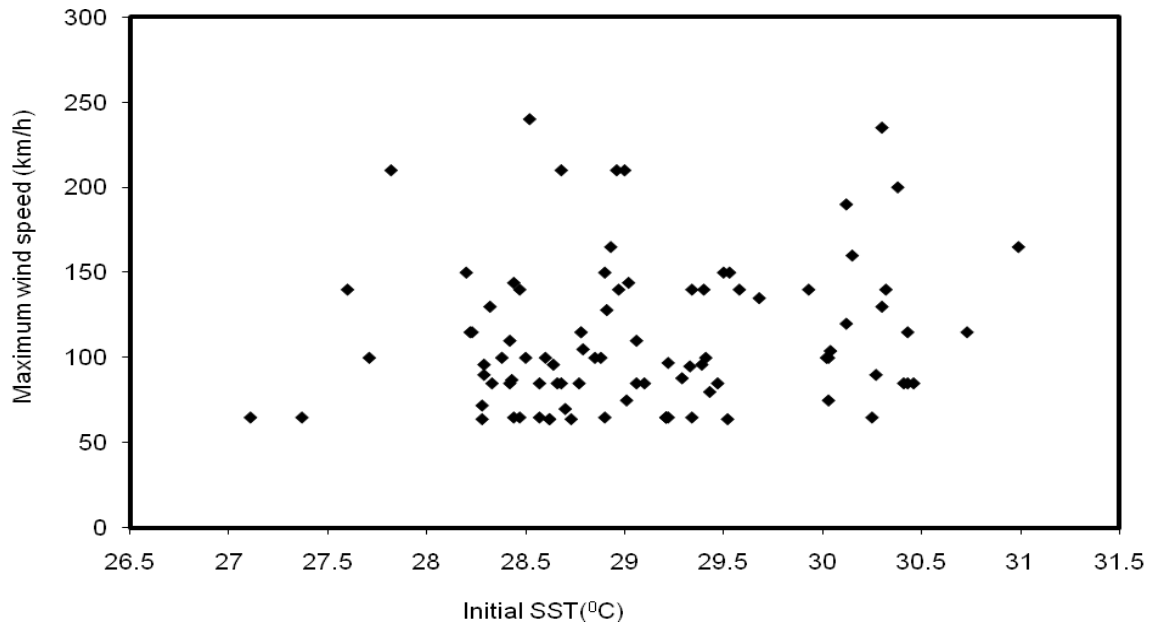


Fig. 4.17. Maximum wind speed and SST at the initial formation locations of 91 tropical cyclones.

From Table 4.11 it is clear that the formation of VSCS and SCS started after SST of 27.50°C and increased with SST. The formation of VSCS decreased for SST from 29.00°C to 29.50°C after that increased with SST. So it revealed that the intensity of cyclone has a step-like, rather than continuous relationship with SST.

Table 4.11. Comparison among the number of various types of cyclones at 0.5 °C temperature bins (starting from 26°C) with the total number of weeks remaining within that temperature bin.

Temperature bin(°C)	No. of total week	CS	% of CS	SCS	% of SCS	VSCS	% of VSCS
26<T• 26.5	14	0	0.0	0	0.0	0	0.0
26.5<T• 27	152	0	0.0	0	0.0	0	0.0
27<T• 27.5	132	2	1.5	0	0.0	0	0.0
27.5<T• 28	105	0	0.0	1	1.0	2	1.9
28<T• 28.5	196	9	4.6	6	3.1	4	2.0
28.5<T• 29	344	10	2.9	6	1.7	8	2.3
29<T• 29.5	247	11	4.5	4	1.6	4	1.6
29.5<T• 30	128	1	0.8	0	0.0	4	3.1
30<T• 30.5	42	5	11.9	5	11.9	7	16.7
30.5<T• 31	5	0	0.0	1	20.0	1	20.0

4.16. SST Profile in the Study Area

The temporal average SST within the study period is shown in Figure 4.18; the proportional circles showing the variation of temporal average SST, the largest circle indicates the highest temporal average SST which is 29.02°C and the smallest circle indicates the lowest temporal average SST which is 27.20°C. The SST remained nearly constant along longitude but decreased towards the higher latitude.

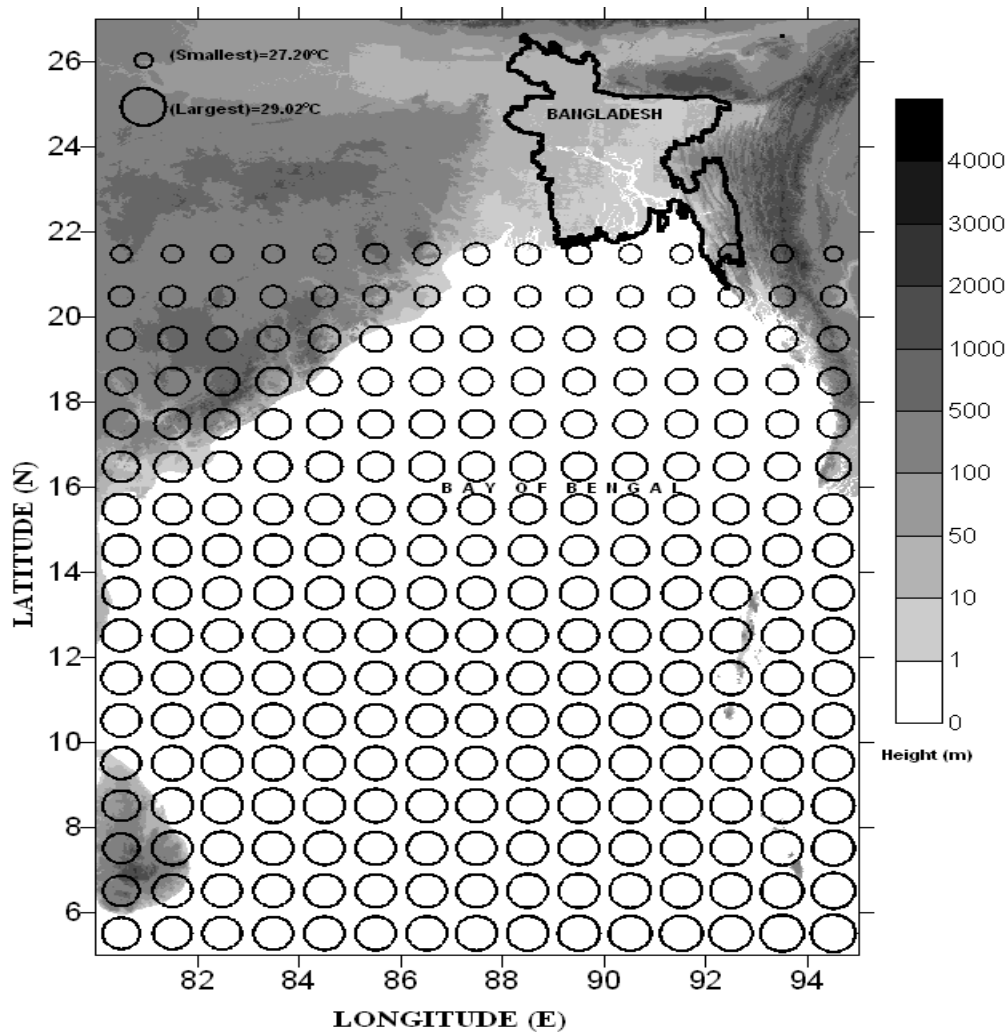


Fig. 4.18. Temporal average sea surface temperature of 272 observation points (17 latitude points for each longitude points, i.e. $17 \times 16 = 272$). Gray shade indicates the topography in meter.

To see the decadal SST variation in the Bay of Bengal, twelve points are taken at 84.5,7.5; 89.5,7.5; 94.5,7.5; 84.5,11.5; 89.5,11.5; 94.5,11.5; 84.5,15.5; 89.5,15.5; 94.5,15.5; 87.5,20.5; 89.5,20.5 and 91.5,20.5 longitude and latitude, these points are mentioned by a,b,c,d,e,f,g,h,i,j,k and l, respectively, in the Figure 4.19 .

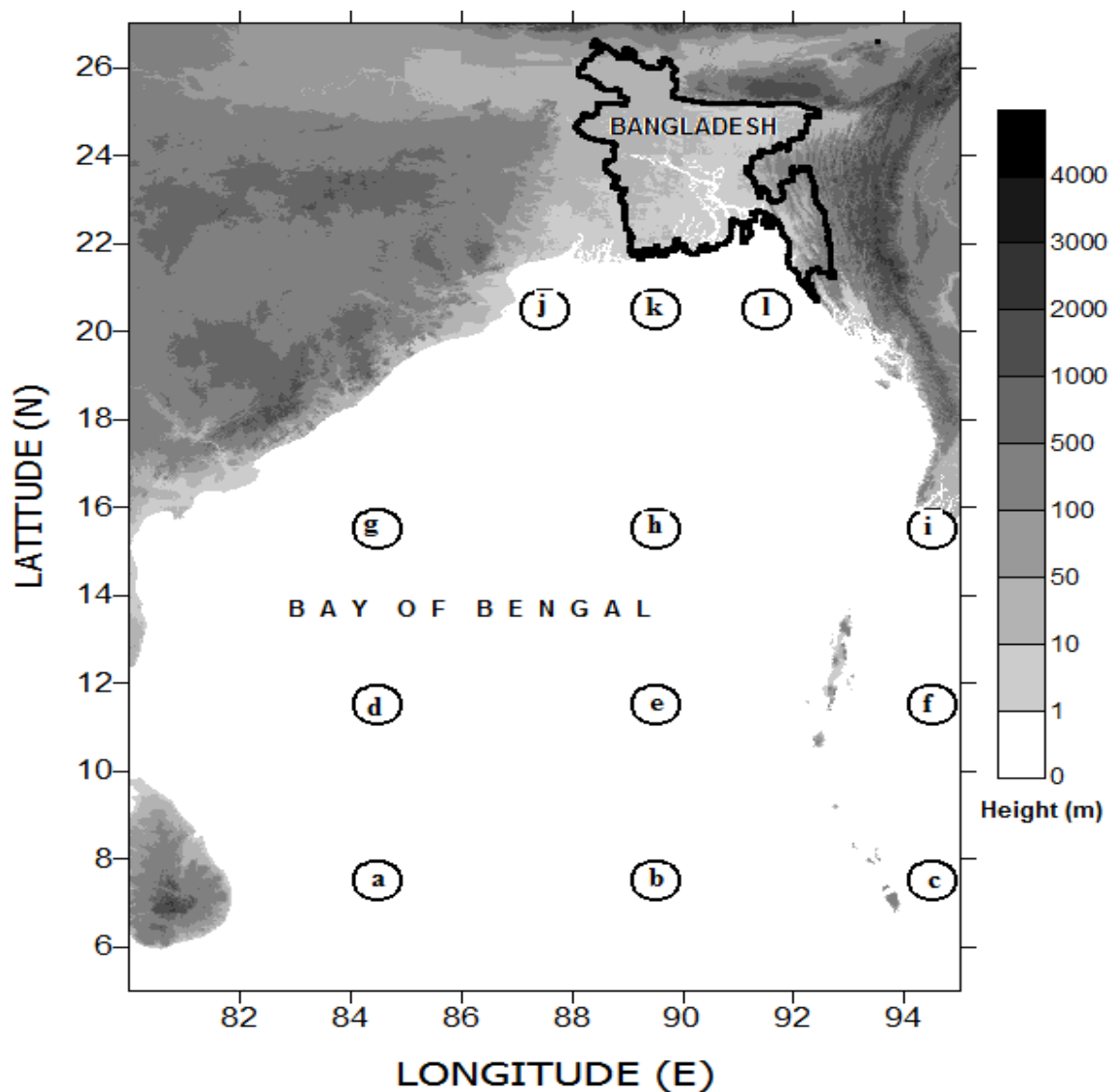


Fig. 4.19. Position of twelve points (a to l) taken in the Bay of Bengal to study the SST variation.

It is found from Figure 4.20 that the SST is fluctuating yearly. Maximum increase of SST at all points observed in 1998. At points j, k, and l, the SST gradually decreases after 1998.

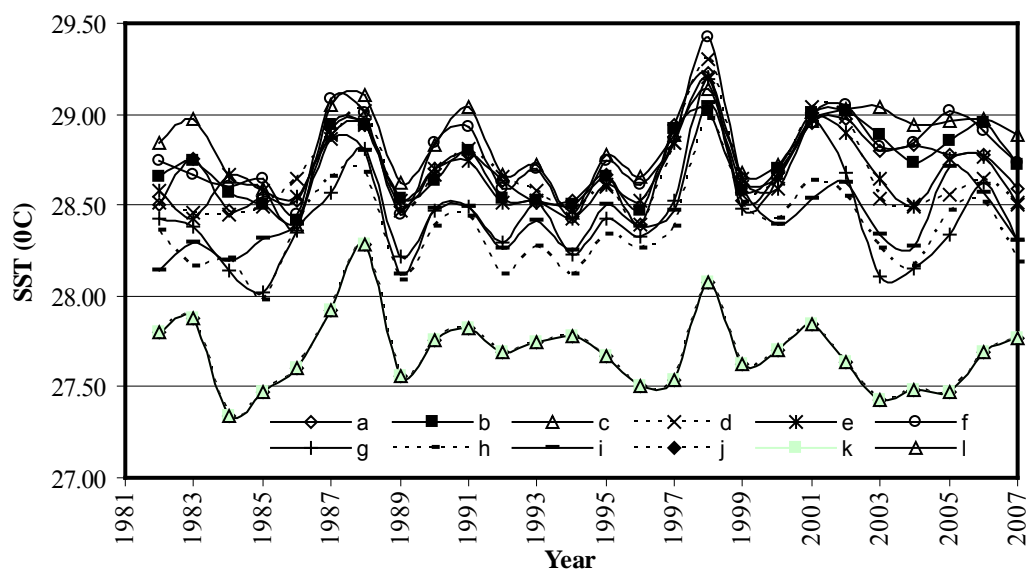


Fig. 4.20 Yearly SST variation at twelve selected points in the Bay of Bengal.

Decadal variation of SST in the Bay of Bengal at twelve points is shown in Figure 4.21. It is found that at points a (84.5, 7.5); b (89.5, 7.5); c (94.5, 7.5); d (84.5, 11.5); e (89.5, 11.5) and f (94.5, 11.5) SST gradually increases, normally very severe cyclonic storm start to form adjacent this area, at points c and f around Andaman and Nicobar Islands, the SST increased 0.19°C , which is the highest increment of SST, in third decade (2001-2007) compared to first decade (1981-1990), but at other six points g (84.5, 15.5); h (89.5, 15.5); i (94.5, 15.5); j (87.5, 20.5); k (89.5, 20.5); l (91.5, 20.5) the SST decreases. The points j (87.5, 20.5), k (89.5, 20.5) and l (91.5, 20.5) which are near the coastal area of Bangladesh, showing the SST decreased 0.11°C , which is the highest decrement of SST, in third decade (2001-2007) compared to first decade (1981-1990).

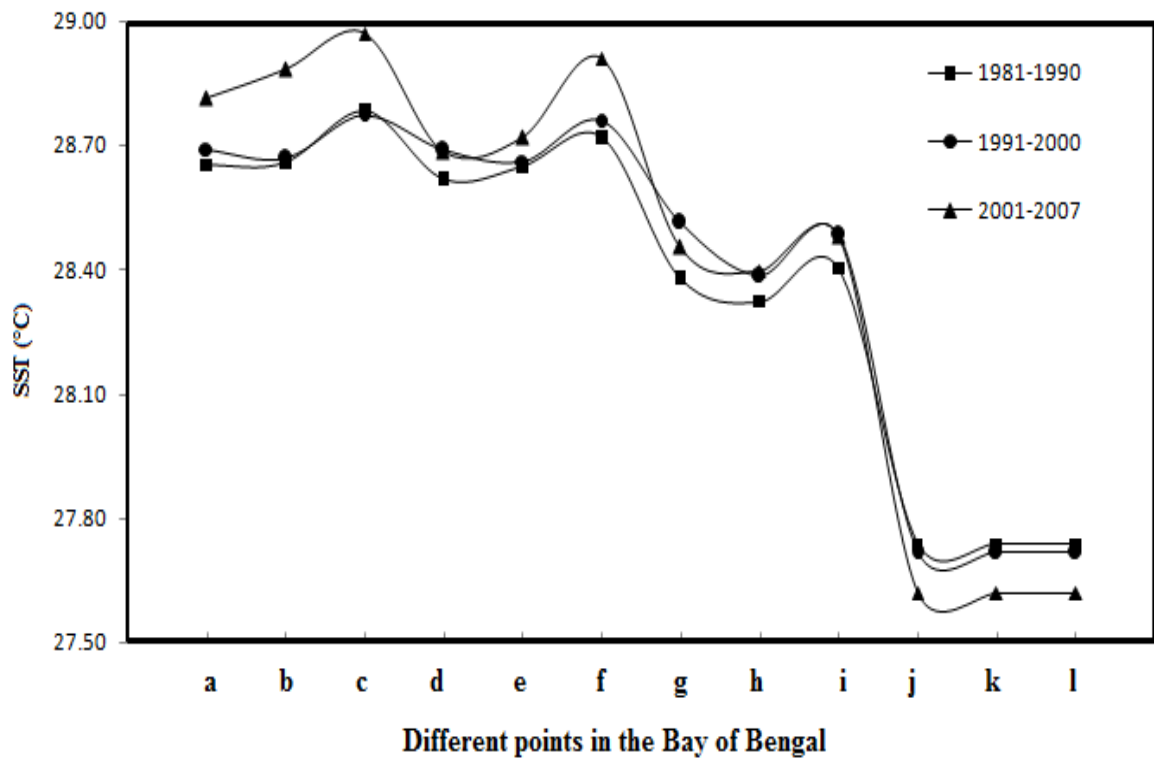


Fig. 4.21. Decadal variation of SST at twelve points (a to l) in the Bay of Bengal.

4.17 Comparison of Temporal SST and Contemporaneous SST

Figure 4.22 shows the comparison of average temporal SST with the contemporaneous SST at the formation location of CS, SCS and VSCS and SC.

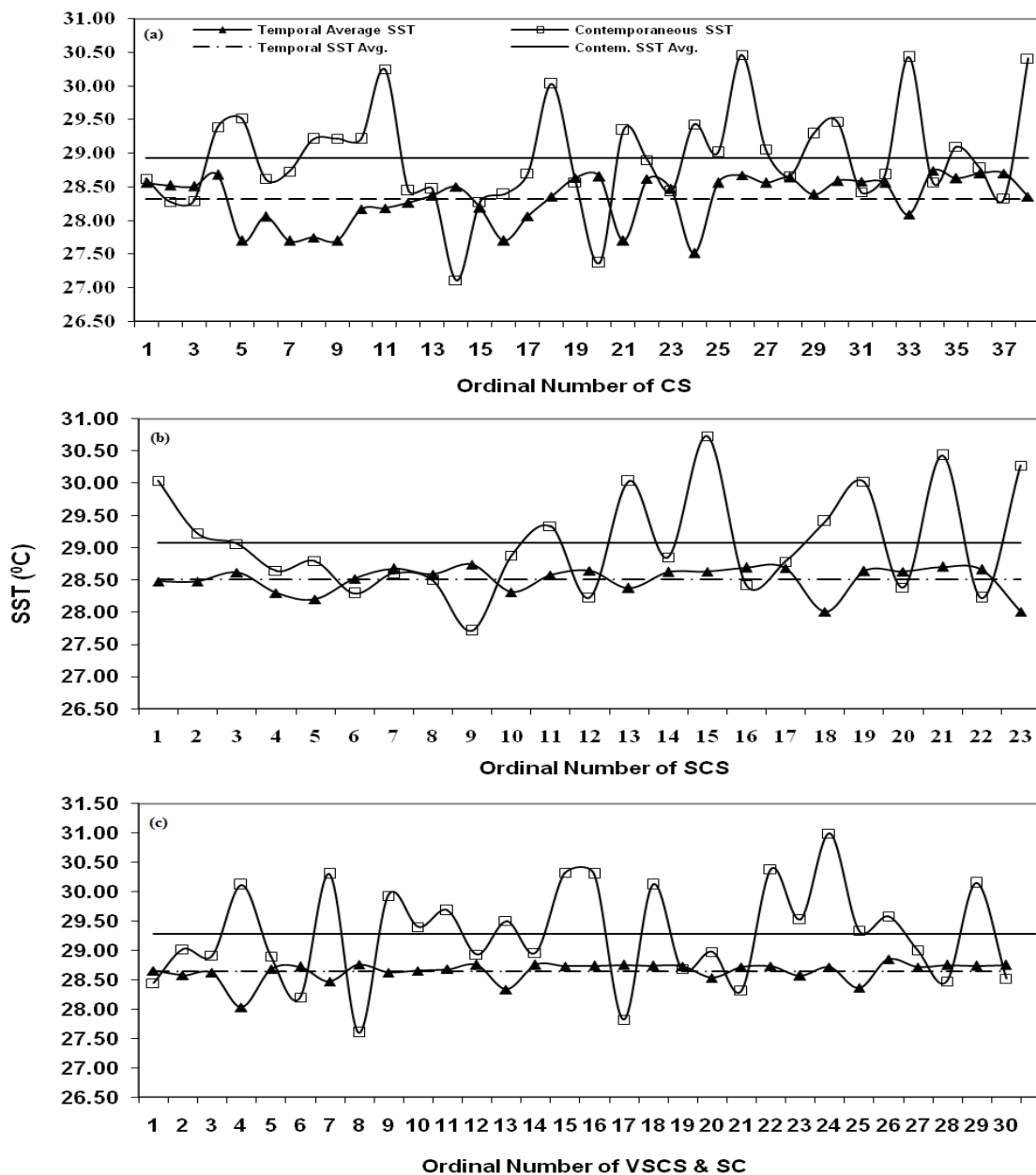


Fig.4.22. Comparison of temporal average SST and contemporaneous average SST at the (a) Cyclonic Storm (CS) (b) Severe Cyclonic Storm (SCS) and (c) Very Severe Cyclonic Storm (VSCS) and Super Cyclone (SC) formation location.

It is found that the average of the temporal average SST was 28.32°C with standard deviation 0.36°C at the formation location of CS. The average of the contemporaneous SST at the formation time of CS, SCS, VSCS and SC was 28.93°C , 29.08°C , 29.27°C and 29.41°C , respectively. It is observed that the overall increase of SST during tropical cyclones was 0.60°C . At the time of CS formation the SST increased 0.61°C from the temporal average value of SST and at the time of SCS formation the increment of SST was 0.57°C . Highest contemporaneous average SST, 29.28°C , was found at the time of formation of VSCS and SC which are most powerful cyclones. At this time the increment of SST was 0.63°C from the temporal average SST

4.18 Observation of Weekly SST during Cyclone Formation

Figure 4.23 showing the weekly SST distribution of 3 weeks before and after the formation of a CS. The duration of the CS was 118 hours. The SST started to rise about 2 weeks before the formation of the CS. It is found that the SST was highest (29.83°C) at the formation time of the CS. The increment (declination) of SST in the week of CS formation was 0.62°C (0.74°C) from the SST of 2 weeks before (after) the CS formation.

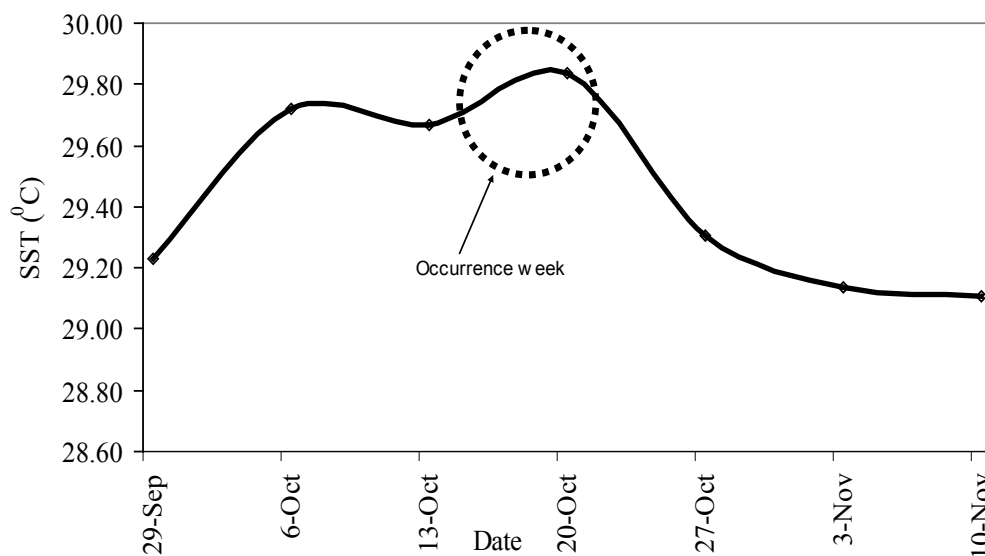


Fig.4.23. Weekly SST distribution at the time of a CS formation on 14/10/2000.

Figure 4.24 showing the weekly SST distribution of 4 weeks before and 2 weeks after the formation of a SCS. The duration of the SCS was 180 hours and it was the highest duration of all the cyclones (91) within the study period. The SST started to increase 4 weeks before the formation of the SCS and the highest SST was 30.54°C in the week of the SCS formation.

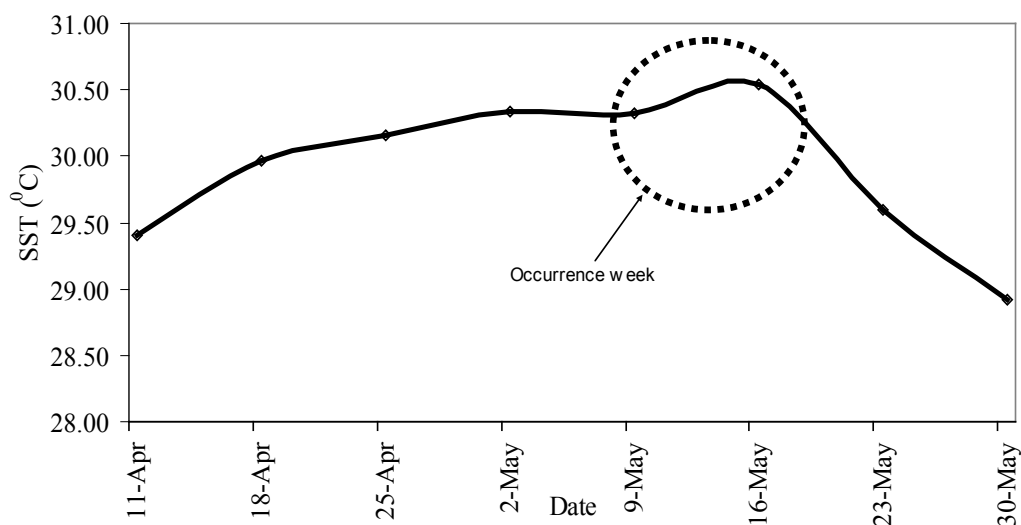


Fig.4.24. Weekly SST distribution at the time of a SCS formation on 10/5/2003.

Figure 4.25 showing the weekly SST distribution of 4 weeks before and 4 weeks after the formation of a VSCS. The duration of the SCS was 90 hours. The SST started to rise 4 weeks before the formation of the VSCS. It is found that the SST was highest (29.86°C) at the formation time of the VSCS. The increment (declination) of SST in the week of the VSCS formation was 0.80 (1.7°C) from the SST of 4 weeks before (after) the VSCS formation.

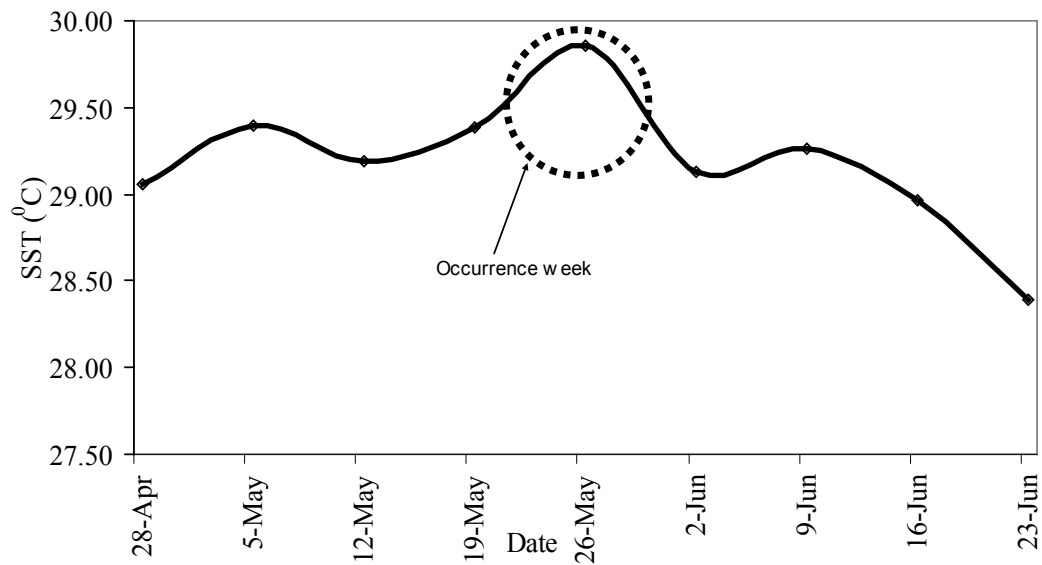


Fig.4.25. Weekly SST distribution at the time of a VSCS formation on 23/5/1989.

Figure 4.26. depicts the weekly SST distribution of 3 weeks before and 3 weeks after the formation of a SC. The duration of the SC was 115 hours. The SST started to rise 2 weeks before the formation of the SC. It is found that the SST was highest (30.00°C) in the formation week of the SC. The increment of SST in the week of SC formation was 1.13°C from the SST of 2 weeks before and the declivity of SST was 1.69°C immediate week after the SC landfall.

So it is seen that the SST increased two to four weeks prior the formation of a tropical cyclone. It is also seen that the highest increment (1.13) of SST was at the time of the highest intensive (super cyclone) cyclone formation.

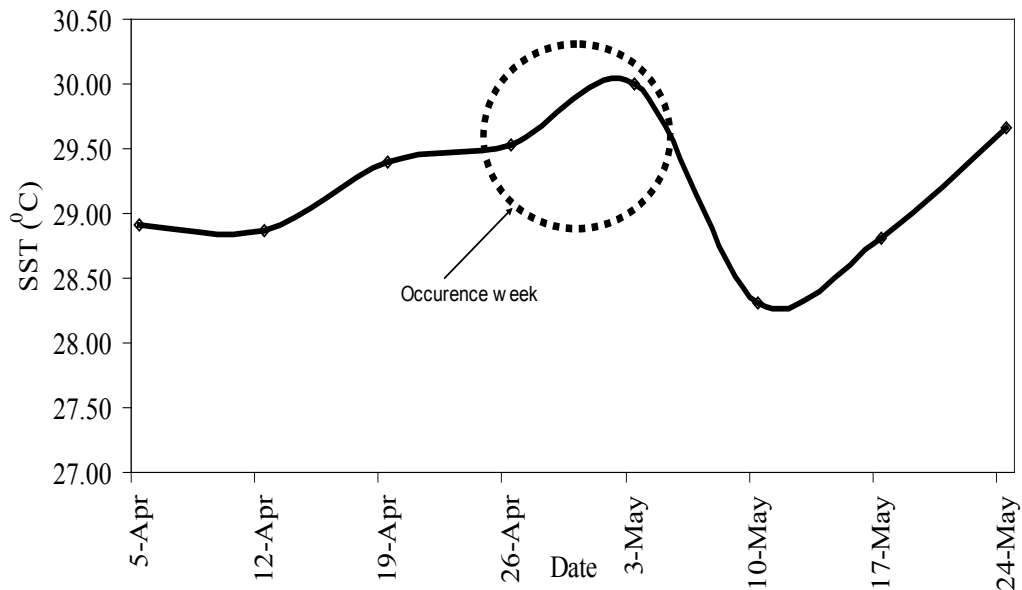


Fig.4.26. Weekly SST distribution at the time of an SC formation on 25/4/1991.

4.19 Probability of Intensification of disturbance and SST

The probability of intensification of D into VSCS and SC is shown in Figure 4.27 along with SST in three decades. In the first decade (from 1981-1990) in (a) the total number of disturbances was 62 and 15 (24%) of them had converted into VSCS and SC. Only one depression formed in the month of February and it had converted into VSCS. The percentages of intensification probabilities of D to VSCS and SC were 67% (4 out of 6) and 44% (7 out of 16) in the months of May and November, respectively.

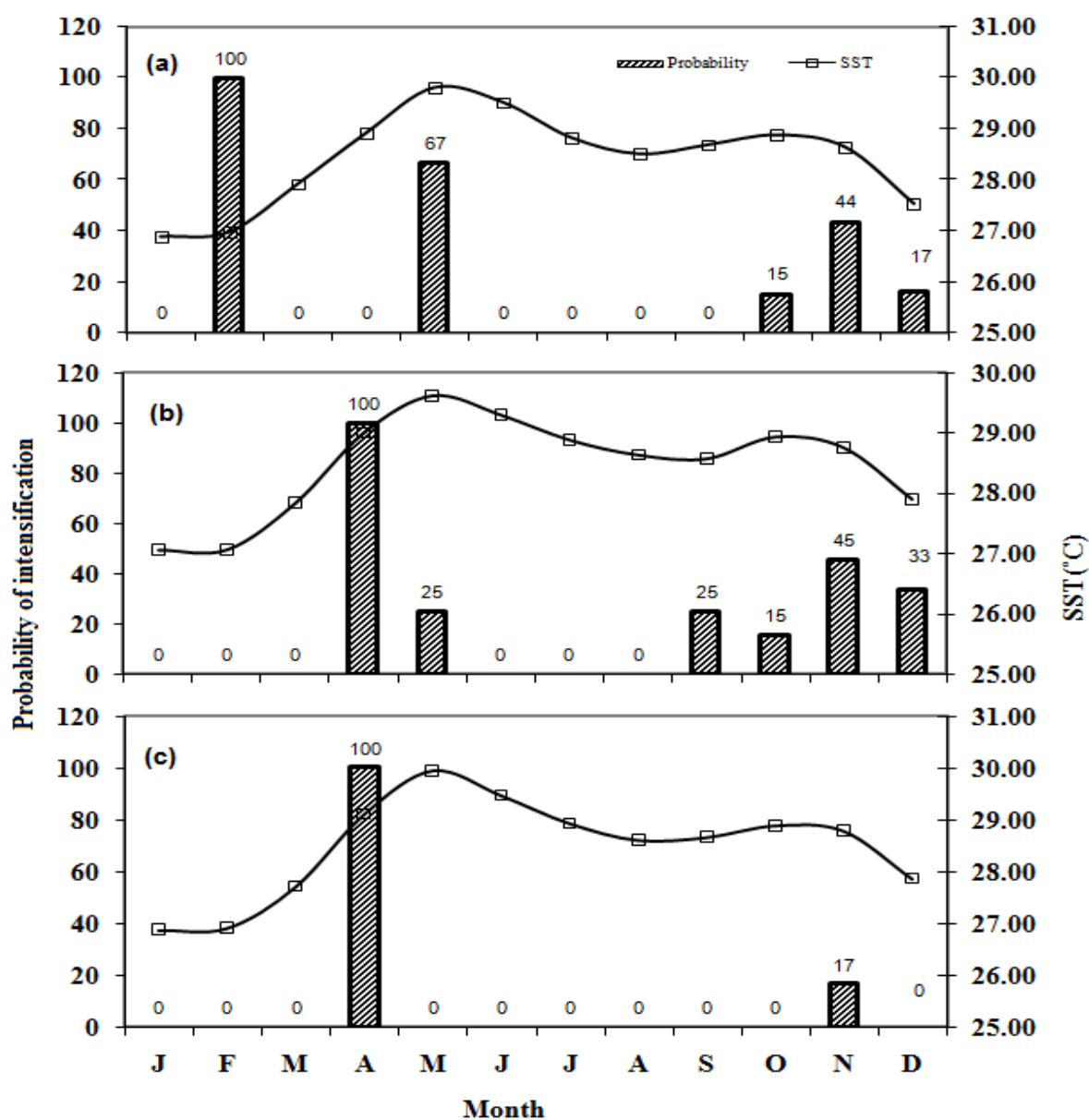


Fig. 4.27. Probability of intensification of D into VSCS and SC during (a) first decade (1981-1990) (b) second decade (1991-2000) and (c) third decade (2001-2007).

In the second decade (from 1990-2000) in (b) the total number of disturbances was 59 and 13 (22%) of them had converted into VSCS and SC. Two depressions formed in the month of April and converted into VSCS. The percentages of intensification probabilities of D to VSCS and SC were 25% (2 out of 8), 45% (5 out of 11) and 33% (1 out of 3) in the months of May, November and December, respectively.

In the third decade (from 2001-2007) in (c) the total number of disturbances was 41 and 2 (5%) of them had converted into VSCS and SC. One depression formed in the month of April and converted into VSCS. The percentage of intensification probability of D to VSCS and SC was 17% (1 out of 6) in the month November.

Overall it is found that the intensification probability from D to VSCS and SC were fluctuating except in April, at the time of increasing SST, the depressions which were formed in this month 100% of them intensified into VSCS and SC.

The probability of intensification of CS into SCS is shown in Figure 4.28 along with SST in three decades. In the first decade (from 1981-1990) in (a) the total number of CS was 49 and 12 (20%) of them had converted into SCS. The percentages of intensification probabilities of CS to SCS were 20% (1 out of 5), 70% (7 out of 10), 13% (2 out of 15) and 33% (2 out of 6) in the months of June, October, November and December, respectively.

In the second decade (from 1991-2000) in (b) the total number of CS was 28 and 8 (29%) of them had converted into SCS. The percentages of intensification probabilities of CS to SCS were 60% (3 out of 5), 50% (1 out of 2), 27% (3 out of 11) and 50% (1 out of 2) in the months of May, June, November and December, respectively.

In the third decade (from 2001-2007) in (c) the total number of CS was 14 and 3 (21%) of them had converted into SCS. The percentages of intensification probabilities of CS to SCS were 50% (2 out of 4) and 50% (1 out of 2) in the months of May and December, respectively.

Overall it is found that the intensification probability from CS to SCS were changeable.

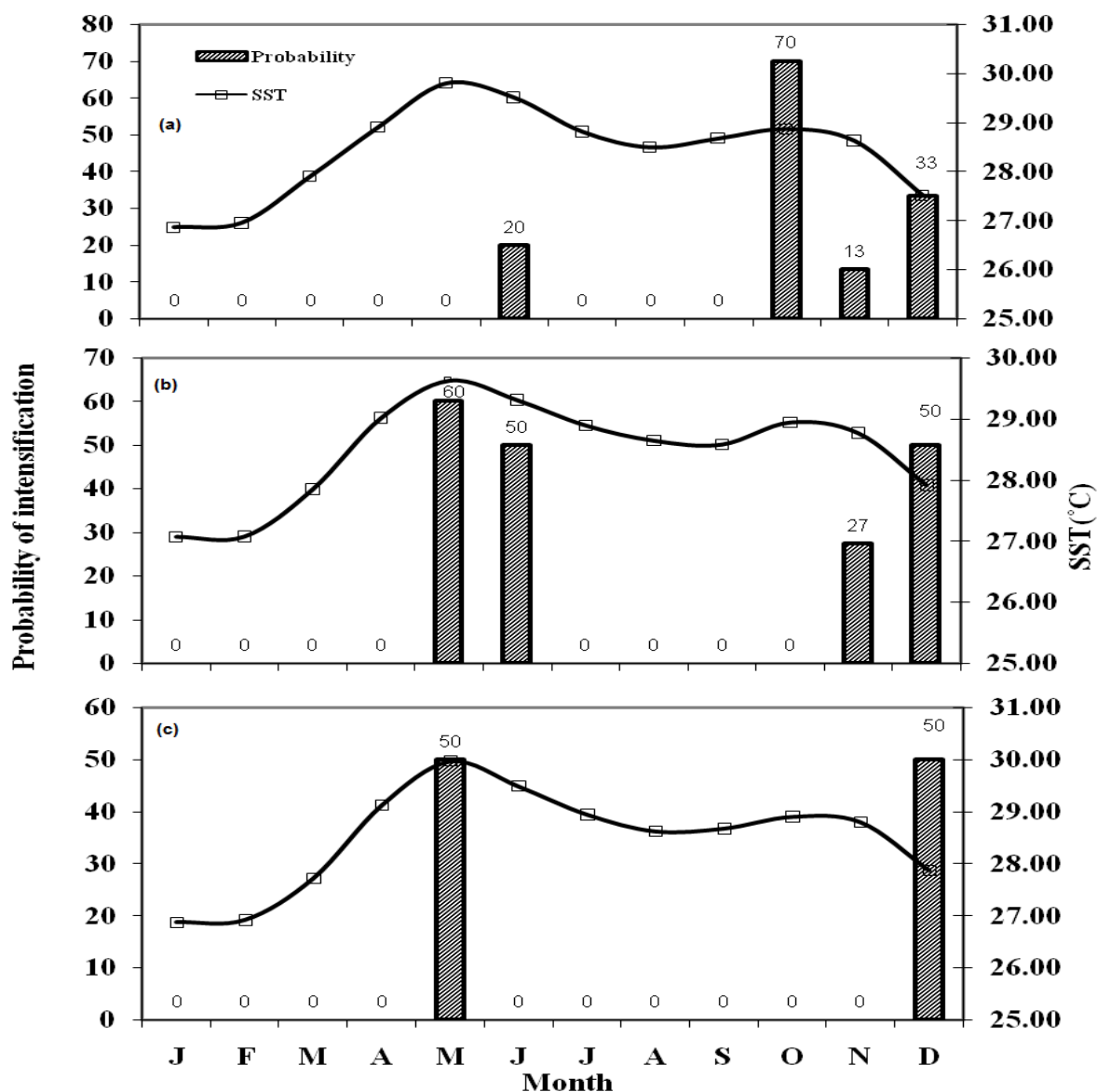


Fig.4.28. Probability of intensification of CS into SCS during (a) first decade (1981-1990), (b) second decade (1991-2000) and (c) third decade (2001-2007).

The probability of intensification of CS into VSCS and SC is shown in Figure 4.29 along with SST in three decades. In the first decade (from 1981-1990) in (a) the total number of CS was 49 and 15 (31%) of them had converted into VSCS and SC. One CS formed in the month of February and converted into VSCS. The percentages of

intensification probabilities of CS to VSCS and SC were 100% (4 out of 4) and 47% (7 out of 15) in the months of May and November, respectively.

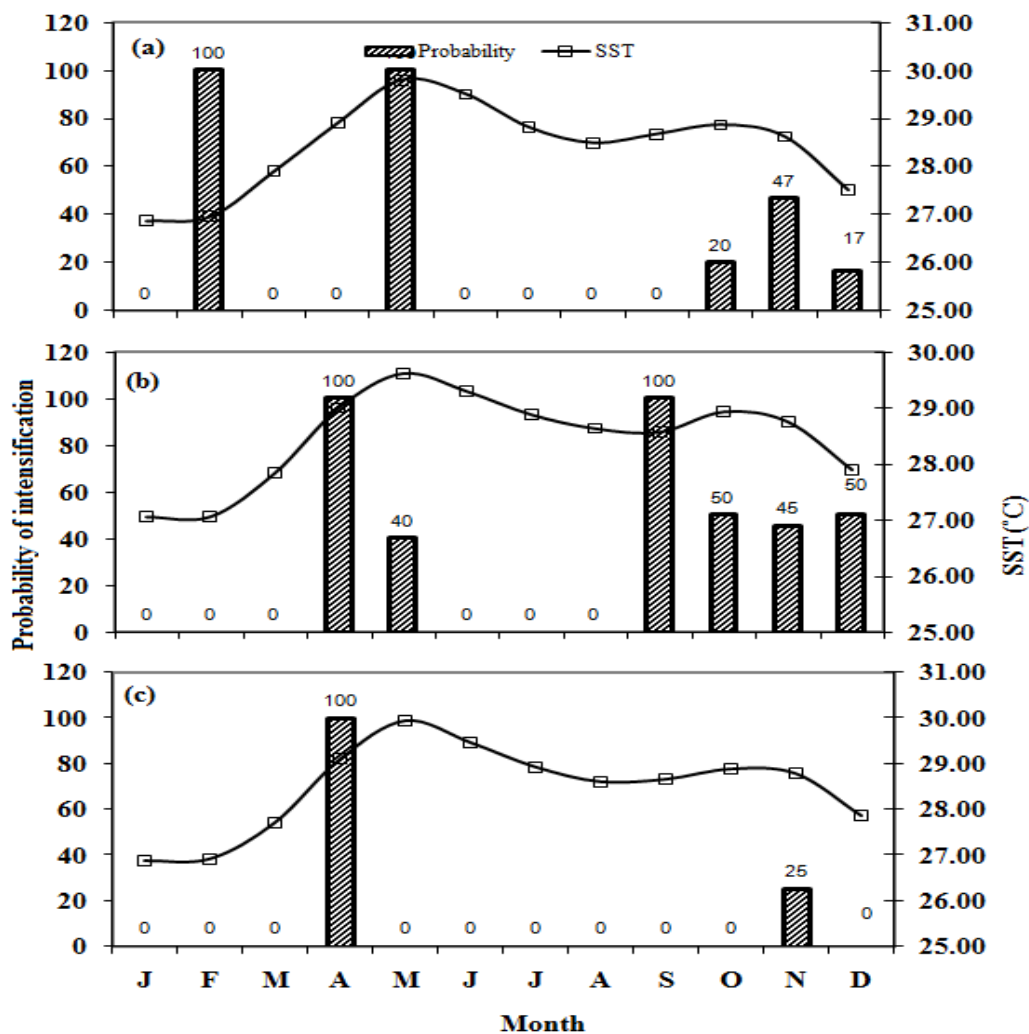


Fig.4.29. Probability of intensification of CS into VSCS during (a) first decade (1981-1990), (b) second decade (1991-2000) and (c) third decade (2001-2007).

In the second decade (from 1991-2000) in (b) the total number of CS was 28 and 13 (46%) of them had converted into VSCS and SC. The CS which was formed in the months of April (2 CS formed) and September (1 CS formed) all of them had converted into VSCS and SC. The percentages of intensification probabilities of CS to VSCS and

SC were 40% (2 out of 5), 50% (2 out of 4), 45% (5 out of 11) and 50% (1 out of 5) in the months of May, October, November and December, respectively.

In the third decade (from 2001-2007) in (c) the total number of CS was 14 and 2 (14%) of them had converted into VSCS and SC. One CS formed in the month of April and converted into VSCS. The percentage of intensification probability of CS to VSCS and SC was 25% (1 out of 4) in the month of November.

Overall it is found that the intensification probability from CS to VSCS and SC were irregular except in April, at the time of increasing SST, the CS which were formed in this month 100% of them intensified into VSCS and SC.

4.20 Area of Powerful Cyclone Formation

In the lower latitudinal area-3 ($7.5^{\circ}\text{N} < \text{latitude} < 13.5^{\circ}\text{N}$) 72% (21 out of 29) VSCS were found (Figure 4.30). On the other hand 14% (6 out of 44) depressions were formed within the same region. The disturbances which were formed within the area-3 had much probability to convert into VSCS. Above the area-3, 86% (38 out of 44) depressions were formed.

The disturbances which were formed above the area-3 had less probability to convert into VSCS. So it is found that the formation of VSCS was higher in area-3 where the SST was higher and the formation of VSCS decreased along the direction of higher latitude where the SST comparatively lower.

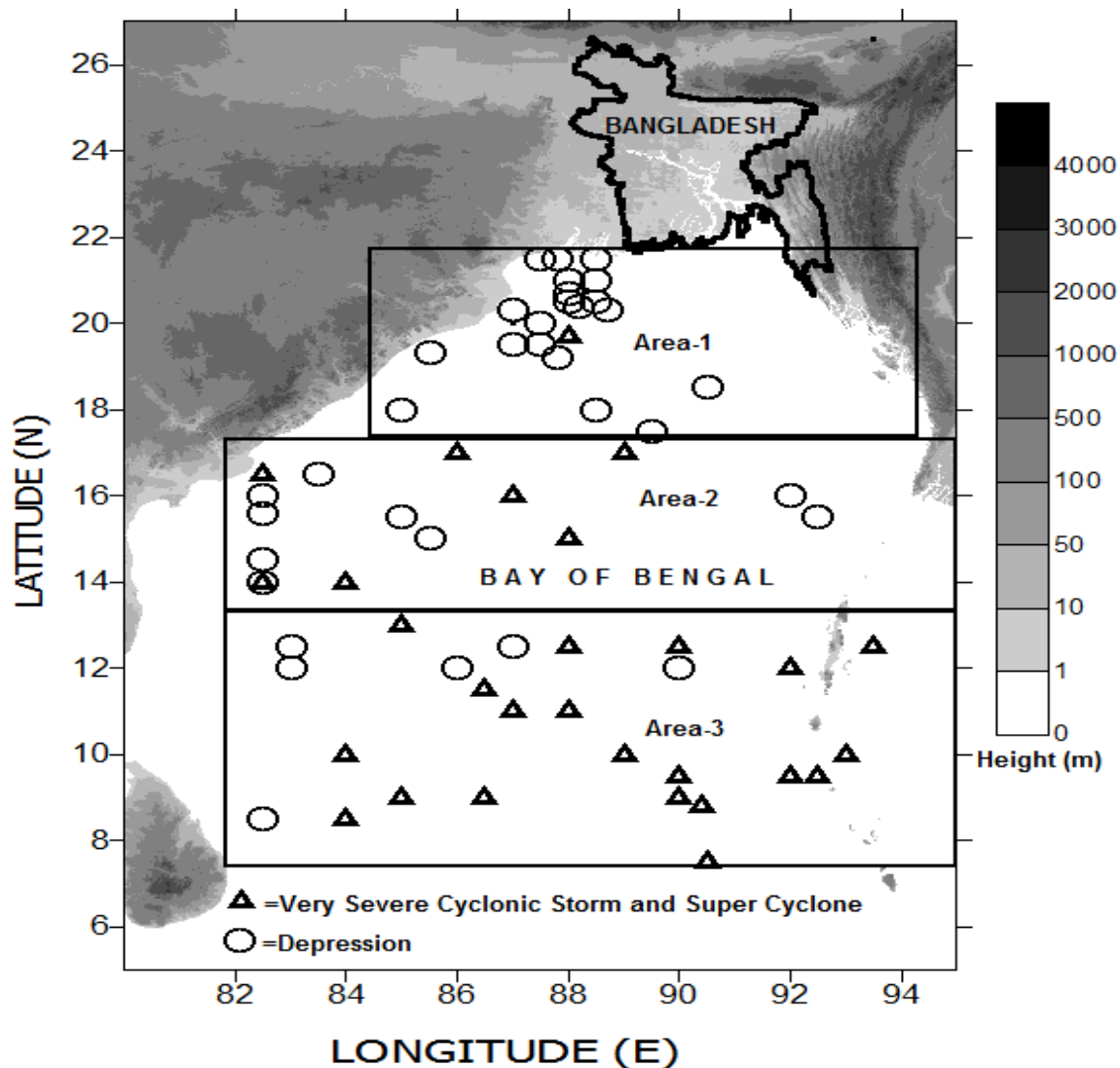


Fig. 4.30. Initial location of very severe cyclonic storm (triangle) and depression (circle). Gray shade indicates the topography in meter.

Figure 4.31 shows the changing behavior of SST with respect to latitude. It is illustrated that from higher to lower latitude, which is toward the direction of the equator, the SST increased. Within area-3 the average temporal SST remains nearly constant around the value of 28.70°C during the study period. It is found that (Figure 4.30) there was no formation of VSCS and SC before 7.5°N latitude; even though the SST was higher but may be due to the lack of Coriolis force there was no VSCS and SC. Moreover it is found that 45% (13 out of 29) VSCS and SC formed within $7.5\text{-}10.5^{\circ}\text{N}$ of area-3 and only 2% (1 out of 44) depressions formed in this region. After 12.5°N , the

decreasing trend of SST was higher with respect to the higher value of latitude. Within area-2 there were 24% (7 out of 29) VSCS and SC and the percentage of formation of depressions were 23% (10 out of 44). Within area-1 only one VSCS (3%) was formed, on the other hand the formations of depression were 64% (28 out of 44). Hence area-1 with average temporal SST 27.75°C was favorable for the formation of depressions and the formation of VSCS and SC within the area-3 around the average temporal SST 28.70°C was favorable.

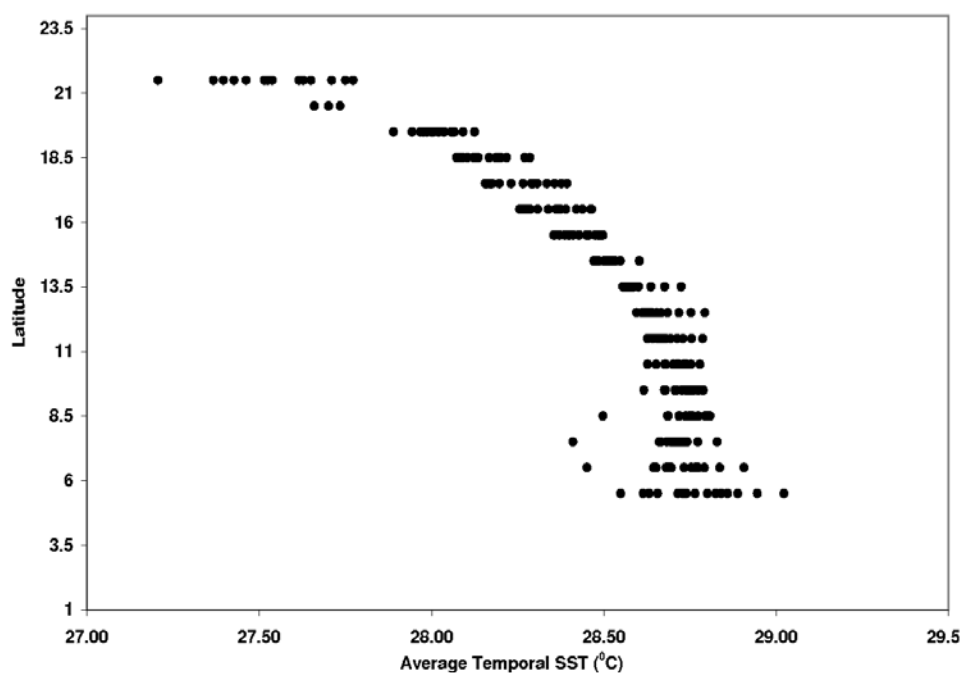


Fig. 4.31. Variation of average temporal SST with respect to the latitude.

4.21 Area of Longest Residence Time of Cyclones

Within the study period there were 13 disturbances, whose duration was more than 100 hours shown in Table 4.12. The total duration of the above mentioned 13 disturbances was 1589 hours, these disturbances spent 50% (801 h) of their lifetime within the area-3, where the rate of change of temperature was nearly constant ($0.01^{\circ}\text{C}/\text{latitude}$) with respect to increasing latitude. 42% (666 h) of their lifetime of the disturbances used up within area-2, where the declination of temperature with respect to increasing latitude was remarkably more, $0.22^{\circ}\text{C}/\text{latitude}$, than the area-3. Only 8% (122 h) of their lifetime

consumed within area-1, the declivity of SST was the highest, $0.36^{\circ}\text{C}/\text{latitude}$, inside this area. When the disturbance remained in area-3 it received nearly constant heat supply. When the cyclone forwarded toward the area-2 and area-1 the decreasing rate of temperature gradually increased.

Table 4.12. Starting point, landfall or die out point and retention time in hour of the disturbances, whose duration was more than 100 hours, in three different regions.

Starting		Disturbance duration (hours)	Duration in area-3 (hours)	Duration in area-2 (hours)	Duration in area-1 (hours)	Just before Landfall/Die out	
Lat($^{\circ}\text{N}$)	Lon($^{\circ}\text{E}$)					Lat($^{\circ}\text{N}$)	Lon($^{\circ}\text{E}$)
8.5	85.0	186	150	36	0	17.0	91.0
15.0	89.0	118	--	118	0	15.0	82.0
13.0	87.0	129	--	129	0	17.2	91.5
10.0	90.0	102	102	0	0	12.7	82.5
11.0	87.0	132	54	42	36	21.2	89.0
7.0	89.0	180	75	105	0	15.0	84.0
9.0	86.5	102	72	30	0	15.0	80.3
10.0	93.0	111	72	27	12	20.5	89.0
10.0	84.0	102	63	39	0	15.8	80.5
10.0	89.0	115	51	36	28	22.3	91.8
9.5	92.5	105	36	38	31	21.5	92.5
9.5	90.0	102	66	36	0	16.5	92.8
9.5	92.0	105	60	30	15	21.0	89.3

It is found from Figure. 4.32 that 59% (17 out of 29) of VSCS and SC got highest wind speed in area-1. Within area-2, 28% (8 out of 29) of the VSCS and SC reached highest speed. Only 4 out of 29 (14%) achieved their highest wind speed within 11 - 12.5 $^{\circ}\text{N}$ latitude of area-3. So area-3 was the region where the SST remained highest and nearly constant. The formation of VSCS and SC and the retention time (Table 4.12) of the disturbances were also highest within this area. At the initial stage the speed of the disturbance remains less, so the consumption of heat energy from the reservoir, of nearly constant and higher SST, remains lower. As the heat acts as fuel for cyclone, may be due

to adequate heat energy the cyclone survives more time when it stays in area-3. As the disturbance moves to the higher latitudinal direction the speed gradually increases (Figure 4.32) but the SST declines (Figure 4.30). As the SST dwindles the heat energy also wanes. It may be due to the augmentation of wind speed the supplied energy does not cope up with the burning up of the heat energy, for this reason highest numbers of cyclones die out within area-1.

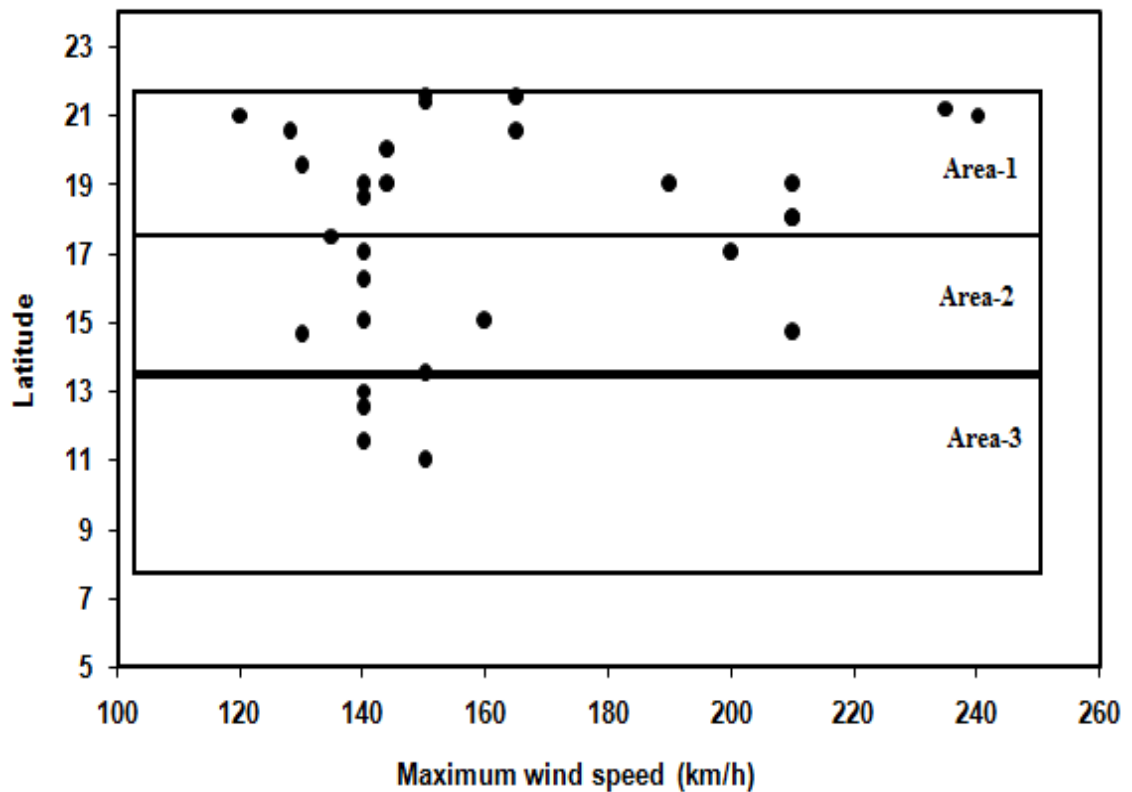


Fig. 4.32. Variation of maximum wind speed of VSCS and SC with respect to latitude.

Chapter Five

Conclusions

The influence of sea surface temperature (SST) on tropical cyclone formed in the Bay of Bengal was examined, using 314 months (November 1981-December 2007) of National Oceanic and Atmospheric Administration (NOAA) Optimum Interpolation version 2 weekly mean SST data and historical cyclone data obtained from Bangladesh Meteorological Department. The study area was from 5.5-21.5°N to 80.5-95.5°E; from that area total 272 grid points for SST at 1° × 1° grid spans were found. During the study period, 91 cyclones were formed over the Bay of Bengal, among these cyclones 38 cyclonic storms (CS), 23 were severe cyclonic storms (SCS), 28 were very severe cyclonic storms (VSCS) and 2 were super cyclones (SC). The SSTs were 27.17°C, 28.85°C, 28.93°C and 28.79°C in winter, pre-monsoon, monsoon and post-monsoon, respectively. It is found that the total cyclonic hours during the period 1981-2007 was 5449. The seasonal durations of tropical cyclones were 720 hours, 1251 hours, 569 hours and 2909 hours in winter, pre-monsoon, monsoon and post-monsoon, respectively. In the winter period the SST was the lowest (27.17°C) and the formation of powerful cyclones was also lowest (2). Even though the SST was the highest (28.93°C) in the monsoon period, formation of tropical cyclones were less. The positive SST anomalies were in the months from April to November. On the other hand, negative SST anomalies were in the months from December to March. In the highest negative SST anomaly month which was in January, the number of cyclones formation was 1% (1 out of 91) of the total cyclones. The SST shows increasing trends all the four seasons. The frequency of cyclone shows positive trends in pre-monsoon period and negative trends all other seasons. The trends of duration of tropical cyclone were positive in winter and pre-monsoon periods, in the monsoon and post-monsoon periods the tropical cyclone duration shows negative trends. At the formation location of CS, SCS, VSCS and SC the averages of the temporal average SSTs were 28.32°C, 28.51°C, 28.64°C and 28.74°C (showing increasing trends), respectively. During the time of formation of CS, SCS, VSCS and SC the averages of the contemporaneous SSTs were 28.93°C, 29.08°C,

29.27°C and 29.41°C, respectively. The formation of SCS, VSCS and SC started after 27.50°C and increased with SST but discontinuously. The intensity of cyclone has a step-like, rather than continuous relationship with SST. The area-3 (within 7.5°N • latitude < 13.5°N) with the average temporal SST 28.70°C was the favorable atmosphere for the formation of VSCS and SC. On the other hand the average temporal SST 27.75°C within the area-1 (within 17.5°N • latitude < 21.5°N) was the salutary environment for the formation of depression (D). It is seen that the SST increased two to four weeks prior the formation of a tropical cyclone. The intensification probability from D to VSCS and SC were fluctuating except in April, the depressions which were formed in this month 100% of them intensified into VSCS and SC. The retention time of the disturbances was also highest within the area-3. Results showed that, although SST was the highest in the monsoon period, tropical cyclones generally were less observed. This is due to the fact that the monsoon trough is generally located to the north over land during summer. Hence, the required dynamical conditions, relative vorticity and vertical wind shear, for tropical cyclone formation are not satisfied. So, the SST is not found to be the only prevailing factor in determining the maximum storm intensity and there are other possible influences. The full reasons behind the observed changes remain an area of active scientific inquiry. So it is urged a precautionous approach to assigning an underlying cause in this complex system by using SST data with improved time resolution because the use of weekly SST data here may have veiled an association between the formation of severe tropical cyclone and the actual SST over which the storm exists.

References

- Bahulayan N, Shaji C. 1996: Diagnostic model of 3-D circulation in the Arabian Sea and western equatorial Indian Ocean: simulation results of sea surface topography. Proc. Ind. Nat. Sci. Acad. (Physical Sciences) **62**, A, 4, 325–347.
- Baik JJ, Paek JS. 1998: A climatology of sea surface temperature and the maximum intensity of western North Pacific tropical cyclones. J. Meteorol. Soc. Jpn. **76**: 129–137.
- Bengtsson L, Botzet M, Esch M 1996. : Will greenhouse gas-induced warming over the next 50 years lead to higher frequency and greater intensity of hurricanes? Tellus **48A**: 57–73.
- Broccoli A J, Manabe S. 1990: Can existing climate models be used to study anthropogenic changes in tropical cyclone climate? Geophys. Res. Lett. **17**: 1917–1920.
- Camargo S J, Sobel A H. 2005: Western North Pacific tropical cyclone intensity and ENSO. J. Climate. **18**: 2996–3006.
- Chan JCL. 1985: Tropical cyclone activity in the Northwest Pacific in relation to the El Nino/Southern Oscillation phenomenon. Mon. Wea. Rev. **113**: 599–606.
- Chan JCL. 2000: TC activity over the western North Pacific associated with El Nino and La Nina events. J. Climate. **13**: 2960–2972.
- Chan J CL. 2006: Comment on ‘ ‘change in tropical cyclone number, duration, and intensity in a warming environment’’. Science **311**: 1713–1714.
- Chan H C, Shi L J. 1996: Long-term trends and interannual variability in the tropical cyclone activity over the western North Pacific. Geophys. Res. Lett. **23**: 2765–2767.
- Chauvin F, Royer J-F, De'que' M. 2006: Response of hurricane-type vortices to global warming as simulated by ARPEGE-Climat at high resolution. Clim. Dyn. **27**: 377–399.
- Chen SS, Frank WM. 1993: A numerical study of the genesis of extratropical convective mesovortices. Part I: Evolution and dynamics, J. Atmos. Sci. **50**: 2401–2426.

- Chen T S, Weng P, Yamazaki N, Kiehl S. 1998: Interannual variation in the TC formation over the western North Pacific. *Mon. Wea. Rev.* **126**: 1080–1090.
- Chia HH, Ropelewski CF. 2002: The interannual variability in the genesis location of TCs in the Northwestern Pacific. *J. Clim.* **15**: 2934–2944.
- Cox MD. 1970: A mathematical model of the Indian Ocean. *Deep-Sea Res.* **17**: 47–75.
- Cox MD. 1976: Equatorially trapped waves and the generation of the Somali Current. *Deep-Sea Res.* **23**: 1139–1152.
- Cox MD. 1979: A numerical study of Somali Current eddies. *J. Phys. Oceanogr.* **9**: 311–326.
- Cutler AN and Swallow JC. 1984: Surface currents in Indian Ocean (to 25°S, 100°E). Tech Rep **187**: 8, Institute of Oceanogr., Wormley, England.
- Dash SK, Jenamani RK, Shekhar S. 2004: On the decreasing frequency of monsoon depressions over the Indian region. *Curr. Sci.* **86**(10): 1406–1411.
- Dong K. 1988: El Niño and tropical cyclone frequency in the Australian region and the northwest Pacific. *Aust. Meteorol. Mag.* **36**: 219–255.
- Donlon C J. 2002: GHRSSST-PP Data Product Specifications v2.0. Technical report, GODEA Height Resolution Sea Surface Temperature Pilot Project, GHRSSST-PP Reference Document GHRSSST/10, <http://ghrsst-pp.org>.
- Elsner JB, Liu KB. 2003: Examining the ENSO-typhoon hypothesis. *Clim. Res.* **25**: 43–54.
- Emanuel KA. 1987: The dependency of hurricane intensity on climate. *Nature* **326**: 483–485.
- Emanuel K A. 1993: "The physics of tropical cyclogenesis over the Eastern Pacific. Tropical Cyclone Disasters J. Lighthill, Z. Zheming, G. J. Holland, K. Emanuel (Eds.), Peking University Press, Beijing, 136-142.
- Emanuel KA. 2000: A statistical analysis of tropical cyclone intensity. *Mon. Wea. Rev.* **128**: 1139-1152.
- Emanuel K A. 2005: Increasing destructiveness of tropical cyclones over the past 30 years. *Nature* **436**: 686–688.

- Evans J L. 1990: Envisaged impacts of enhanced greenhouse warming on tropical cyclones in the Australian region. CSIRO Division of Atmospheric Research Tech. Paper No 20 pp 31 [Available from CSIRO/DAR, Private Bag No. 1, Mordialloc, 3195, Australia.].
- Frank WM. 1987: Tropical cyclone formation. A Global View of Tropical Cyclone. R. L. Elsberry Ed U.S. Office of Naval Research, Marine Meteorology Program 53-90.
- Godfrey JS and Golding TJ. 1981: The Sverdrup relation in the Indian Ocean, and the effect of the Pacific-Indian throughflow on Indian Ocean circulation and on East Australian current. *J. Phys. Oceanogr.* **11**: 771–779.
- Gray WM. 1968: "A global view of the origin of tropical disturbances and storms" *Mon. Wea. Rev.* **96**: 669-700.
- Gray W M (1975) Tropical cyclone genesis. Dept. of Atmos. Sci. Paper No. 234, Colorado State University, Ft. Collins, CO, USA, 121 pp.
- Gray WM. 1979: "Hurricanes: Their formation, structure and likely role in the tropical circulation" *Meteorology Over Tropical Oceans*. D. B. Shaw (Ed.), Roy. Meteor. Soc., James Glaisher House, Grenville Place, Bracknell, Berkshire, RG12 1BX, pp 155-218.
- Gualdi S, Scoccimarro E, Navarra A. 2008: Changes in tropical cyclone activity due to global warming: results from a highresolution coupled general circulation model. *J. Clim.* **21**: 5204–5228.
- Hastenrath S, Lamb PJ. 1979: *Climatic Atlas of the Indian Ocean, I, The Ocean Heat Budget*. University of Wisconsin Press, Madison, 110 pp.
- Hurlburt HE, Thompson JD. 1976: A numerical model of the Somali Current. *J. Phys. Oceanogr.* **6**: 646–664.
- Iizuka S, Matsuura T. 2008: ENSO and western North Pacific tropical cyclone simulated in a CGCM. *Clim. Dyn.* **30**: 815–830.
- Jensen TG. 1990: A numerical study of the seasonal variability of the Somali Current. Ph.D. Dissertation, Florida State Univ., Tallahassee, 118 pp.

- Jadhav SK. 2002: Summer monsoon low pressure systems over the Indian region and their relationship with the sub-divisional rainfall. *Mausam* **53**(2): 177–186.
- Jadhav S K, Munot A A. 2004: Statistical study of the low pressure systems during summer monsoon season over the Indian Region. *Mausam* **56**(1): 17–25.
- Joseph P V. 1981: Ocean atmosphere interaction on a seasonal scale over the north Indian Ocean and Indian monsoon rainfall and cyclonic tracks: a preliminary study. *Mausam* **32**: 237–246.
- Kindle KC and Thompson JD. 1989: The 26 and 50 day oscillation in the western Indian Ocean, model results. *J. Geophys. Res.* **94**: 4721–4736.
- Knutson T R and Tuleya R E. 2004: Impact of CO₂-induced warming on simulated hurricane intensity and precipitation: sensitivity to the choice of climate model and convective parameterization. *J. Clim.* **17**: 3477–3495.
- Koteswaram P, George CA. 1958: On the formation of monsoon depressions in the Bay of Bengal. *Ind. J. Meteorol. Geophys.* **9**: 9–22.
- Lander M A. 1993: Comments on ‘ ‘a GCM simulation of the relationship between tropical storm formation and ENSO’’. *Mon. Wea. Rev.* **121**: 2137–2143.
- Lander MA. 1994: An exploratory analysis of the relationship between tropical storm formation in the western North Pacific and ENSO. *Mon. Wea. Rev.* **122**: 636–651.
- Landsea CW, Harper BA, Hoarau K, Knaff JA. 2006: Can we detect trends in extreme tropical cyclones? *Science* **313**: 452-454.
- Luther ME, O'Brien JJ. 1985: A model of the seasonal circulation in the Arabian Sea forced by observed winds. *Prog. Oceanogr.* **14**: 353–385.
- Mandal GS. 1991: Tropical cyclones and their forecasting and warning systems in the North Indian Ocean, WMO/TDNO. 430, Tropical Cyclones Program, Report No. TCP-28, WMO, Geneva.
- Mandake S K, Bhide U V. 2003: A study of decreasing storm frequency over Bay of Bengal. *J. Ind. Geophys. Union* **7**(2): 53–58.
- Mark A Saunders, Adam S Lea. 2008: Large contribution of sea surface warming to recent increase in Atlantic hurricane activity. *Nature* **451**: 557-560.

- McCreary JP, Kundu PK. 1986: On the dynamics of the throughflow from the Pacific to the Indian Ocean. *J. Phys. Oceanogr.* **16**: 2191–2198.
- McDonald R E, Bleaken D G, Cresswell D R, Pope V D, Senior C A. 2005: Tropical storms: representation and diagnosis in climate models and the impacts of climate change. *Clim. Dyn.* **25**: 19–36.
- Merrill RT. 1988 : Environmental influences on hurricane intensification. *J. Atmos. Sci.* **45**: 1678–1687.
- Mooley DA, Shukla J. 1987: Characteristic of the west-moving summer monsoon low pressure systems over the Indian region and their relationship with the monsoon rainfall. Centre for Ocean-Land-Atmosphere Interactions, University of Maryland, College Park, MD, USA.
- Oouchi K, Yoshimura J, Yoshimura H, Mizuta R, Kusunoki S, Noda A. 2006: Tropical cyclone climatology in a global-warming climate as simulated in a 20 km-mesh global atmospheric model: frequency and wind intensity analyses. *J. Meteorol. Soc. Jpn.* **84**: 259–276.
- Palmen EH. 1948: On the formation and structure of tropical cyclones. *Geophysica* **3**: 26-38.
- Pan YH. 1982: The effect of the thermal state of equatorial eastern Pacific on the frequency of typhoon over the western Pacific (in Chinese with English abstract). *Acta. Meteorol. Sin.* **40**: 24–34.
- Patwardhan SK and Bhalme HN. 2001: A study of cyclonic disturbances over India and the adjacent ocean. *Int. J. Climatol.* **21**: 527–534.
- Pilke R et al. 2006: Reply to ‘‘Hurricanes and global warming- Potential linkages and consequences’’. *Bull. Am. Meteorol. Soc.* **87**: 628–631.
- Potemra JT, Luther ME, O’Brien JJ. 1991: The seasonal circulation of the upper ocean in the Bay of Bengal. *J. Geophys. Res.* **96**: 12667–12683.
- Patrick J Michaels, Paul C Knappenberger, Robert E Davis. 2006: Sea-surface temperatures and tropical cyclones in the Atlantic basin. *Geophysical Research Letters* **33** L09708.

- Rajeevan M, Khole M, De US. 2000a: Variability of sea surface temperature and tropical storms in the Indian Ocean in the recent years, Proc. of TROPMET-2000, National Symposium on Tropical Meteorology, Cochin, India, 1–4 February 2000, pp 234–237.
- Rajeevan M, De US, Prasad RK. 2000b: Decadal variation of sea surface temperatures, cloudiness and monsoon depressions in the north Indian Ocean. *Curr. Sci.* **79**(3): 283–285.
- Ramage CS, Hori AM. 1981: Meteorological aspects of E I N i ñ o. *Mon Wea Rev* **109**:1827–1835 Smith TM, Reynolds RW (2004) Improved extended reconstruction of SST (1854–1997). *J. Climate.* **17**: 2466–2477.
- Rao RR, Molinari RL, Festa JF. 1989: Evolution of the climatological near-surface thermal structure of the tropical Indian Ocean, 1, Description of mean monthly mixed-layer depth and sea surface temperature, surface current, and surface meteorological fields. *J. Geophys. Res.* **94**: 10801–10815.
- Rao KN, Jayaraman S. 1958: A statistical study of frequency of depressions and cyclones in the Bay of Bengal. *Ind. J. Meteorol. Geophys.* **9**: 233–250.
- Saha KR, Sanders F, Shukla J. 1981: Westward propagating predecessors of monsoon depressions. *Mon. Weather. Rev.* **109**: 330–343.
- Schott F. 1983: Monsoon response of the Somali Current and associated upwelling. *Prog. Oceanogr.* **12**: 357–382.
- Schott F, Fieux M, Kindle J, Swallow J, Zantopp R. 1988: The boundary currents east and north of Madagascar, 2, Direct measurements and model comparisons. *J. Geophys. Res.* **93**: 4963–4974.
- Shaji C, Bahulayan N, Dube SK, Rao AD. 1999: A multi-level adaptation model of circulation for the western Indian Ocean. *Interna. Jour. Numer. Method. Fluids.* **31**: 1221–1264.
- Shaji C, Rao AD, Dube SK, Bahulayan N. 2000: On the semi-diagnostic computation of climatological circulation in the western tropical Indian Ocean. *Mausam* **51**: 329–348.

- Shaji C, Iizuka S, Matsuura T. 2003: Seasonal variability of near-surface heat budget of selected oceanic areas in the North Tropical Indian Ocean *Journal of Oceanography*, Vol. **59**: 87–103.
- Sikka DR. 1977: Some aspects of the life history, structure and movement of monsoon depressions. *Pure Appl. Geophys.* **115**: 1501–1529.
- Sikka DR. 2006: A study on the monsoon low pressure systems over the Indian region and their relationship with drought and excess monsoon seasonal rainfall, Centre for Ocean-Land-Atmosphere Studies, Center for the Application of Research on the Environment, Calverton, MD, USA.
- Singh OP. 2001: Long term trends in the frequency of monsoonal cyclonic disturbances over the north Indian ocean. *Mausam* **52**: 655–658.
- Sugi M, Noda A, Sato N. 2002: Influence of the global warming on tropical cyclone climatology: an experiment with the JMA global model. *J. Meteor. Soc. Jpn.* **80**: 249–272.
- Swallow JC, Molinari RL, Bruce JG, Brown OB, Evans RH. 1983: Development of near-surface low P patterns and water mass distribution in the Somali Basin in response to the southwest monsoon of 1979. *J. Phys. Oceanogr.* **13**: 1398–1415.
- Tsutsui J. 2002: Implications of anthropogenic climate change for tropical cyclone activity: a case study with the NCAR CCM2. *J. Meteorol. Soc. Jpn.* **80**: 46–65.
- Tahmeed MA I-Hussaini, Arjumand Habib, Akram Hossain M. 2005: Multi-hazard disaster reduction in the coastal region of Bangladesh. International Symposium Disaster Reduction on Coasts Scientific-Sustainable-Holistic-Accessible 14 – 16 November Monash University Melbourne Australia.
- UNESCO. 1971: Discharge of Selected Rivers of the World Vol. **2**. Paris, 194 pp.
- Velasco, I., and J. M. Fritsch (1987), Mesoscale convective complexes in the Americas, *J. Geophys. Res.* **92**: 9591–9613.
- Vinayachandran PN, Yamagata T. 1998: Monsoon response of the sea around Sri Lanka: Generation of thermal domes and anticyclonic vortices. *J. Phys. Oceanogr.* **28**: 1946–1960.

- Vinayachandran P N, Saji NH, Yamagata T. 1999: Response of the equatorial Indian Ocean to an unusual Wind event during 1994. *Geophys. Res. Lett.* **26**: 1613–1616.
- Wacongne S, Pacanowski R. 1996: Seasonal heat transport in a primitive equations model of the tropical Indian Ocean. *J. Phys. Oceanogr.* **26**: 2666–2699.
- Wang B, Chan JCL. 2002: How strong ENSO events affect tropical storm activity over the western North Pacific. *J. Clim.* **15**:3252–3265.
- Webster P J, Holland G J, Curry J A, Chang H R. 2005: Changes in tropical cyclone number, duration and intensity in a warming environment. *Science* **309**: 1844-1846.
- Wick GA. 2002: Infrared and microwave remote sensing of sea surface temperature. Seminar at the University of Colorado at Boulder “Remote Sensing Seminar” graduate course.
- Woodbury KE, Luther ME, O’Brien JJ. 1989: The wind-driven seasonal circulation in the southern tropical Indian Ocean. *J. Geophys. Res.* **94**(C12): 17985–18002.
- Wu G, Lau N-C. 1992: A GCM simulation of the relationship between tropical-storm formation and ENSO. *Mon. Wea. Rev.* **120**: 958–977.
- Wyrtki K. 1971: *Oceanographic Atlas of the International Indian Ocean Expedition*. National Science Foundation, Washington, D.C., 531 pp.
- Xavier PK, Joseph PV. 2000: Vertical wind shear in relation to frequency of monsoon depressions and tropical cyclones of Indian Seas, *Proc. of TROPMET-2000*, National Symposium on Tropical Meteorology, 1–4 February 2000, Cochin, India, pp 242–245.
- Zehr RM. 1992: "Tropical cyclogenesis in the western North Pacific. NOAA Technical Report NESDIS 61, U. S. Department of Commerce, Washington, DC 20233, 181 pp.

List of Published/Submitted Papers

Md. Rezaul Karim Khan, M. Nazrul Islam and M. Rafiuddin, "The influence of sea surface temperature on tropical cyclone formed in the Bay of Bengal", Proceedings in the International Conference on Recent Advance in Physics (RAP-2010), 27-29 March 2010, Dhaka, Bangladesh.

R. K. Khan, M. Rafiuddin, M. Nazrul Islam. 2010: The relationship between sea surface temperature and formation of tropical cyclone in the Bay of Bengal. Natural Hazards (Submitted).

R. K. Khan, M. Rafiuddin, M. Nazrul Islam. 2010: Interseasonal variation of sea surface temperature and frequency of cyclones in the Bay of Bengal. Bangladesh Journal of Physics (Submitted).